Behavioral and Physiological On- and Offline Effects of Transcranial Alternating Current Stimulation (tACS)

Von der Fakulät für Medizin und Gesundheitswissenschaften der Carl von Ossietzky Universität Oldenburg zur Erlangung des Grades und Titels eines

Doktor rerum naturalium, Dr. rer. nat.

angenommene

Dissertation

von Herrn Florian H. Kasten

Geboren am 06.06.1990 in Twistringen

Erstgutachter:	Prof. Dr. Christoph S. Herrmann
Weitere Gutachter:	Prof. Dr. Stefan Debener
	Prof. Dr. Michael Nitsche
Weiteres Mitglied der Prüfungskommission:	Prof. Dr. Daniel Strüber
Tag der Disputation:	13.11.2018

Contents

List of Figures

List of Tables

List of Abbreviations

AM	Amplitude modulated
(rm)ANOVA	(repeated measurement) Analysis of Variance
BOLD	Blood oxygen level dependent
DAC	Digital-analog converter
EEG	Electroencephalogram
EOG	Electrooculogram
ERD/ERS	Event-related (de-)synchronization
ERP	Event-related Potential
f_c	Carrier frequency
FFT	Fast Fourier Transformation
f_m	Modulation frequency
IAF	Individual alpha frequency
IC(A)	Independend component (analysis)
LCMV	Linearly constrained minimum variance
MEG	Magnetoencephalogramm
MR	Mental rotation
(f)MRI	functional Magnetic resonance imaging
MSR	Magnetically shielded room
(f)NIRS	(functional) near-infrared spectroscopy
NFT	Neurofeedback training
PCA	Principal component analysis
RT	Reaction time
SEM	Standard error of the mean
STP	Spike-timing dependent plasticity
(t)SSS	(spatiotemporal) Signal Space Separation

tACS	Transcranial alternating current stimulation
tDCS	Transcranial direct current stimulation
tES	Transcranial electrical stimulation
TF	Transfer function
TFR	Time frequency representation
TI	Temporal interference
(r)TMS	(repetitive) Transcranial magnetic stimulation

Abstract

Non-invasive tools to modulate brain activity are increasingly popular in neuroscience. One of these methods, transcranial alternating current stimulation (tACS) is used to interfere with brain oscillations within specific frequency ranges by applying sinusoidal, alternating currents through the scalp.

The first two experiments in this dissertation focused on aftereffects of tACS on alpha activity in resting state EEG (study 1) and during a more complex mental rotation task (study 2). In Study 3 online effects of tACS on event-related alpha oscillations during mental rotation were investigated during mental rotation. To this end, an artifact reduction approach based on spatial filtering was applied to MEG data. Study 4 characterizes artifacts in M/EEG signals, which arise during amplitude modulated tACS (AM-tACS), a new stimulation approach, designed to avoid the spectral overlap between the brain signal of interest and the electromagnetic artifact of the stimulation.

Study 1, showed that tACS can increase the power of intrinsic brain oscillations in the alpha band for up to 70 minutes. This aftereffect also showed up during a more complex cognitive task and fostered event-related alpha desynchronization, as well as task performance (study 2). Study 3 demonstrated that effects of tACS on event-related modulations of alpha oscillation can be recovered after application of a spatial filter, despite the presence of residual artifacts. TACS facilitated the pre-existent, task-induced modulation of oscillations in the alpha range, rather than overwriting it. Study 4 revealed that small non-linearities of hardware used for stimulation and data acquisition during AM-tACS can lead to low-frequency artifacts in M/EEG recordings.

In summary, tACS exhibited effects on both spontaneous and event-related oscillations. An analysis framework is proposed that allows to investigate event-related oscillations during tACS, that can obtain robust effects even in the presence of residual artifacts. In addition, recommendations for concurrent tACS-M/EEG are discussed.

Zusammenfassung

Nicht-invasive Methoden zur Modulation von Hirnaktivität finden immer häufiger Anwendung in den Neurowissenschaften. Eine dieser Methoden, die transkranielle Wechselstromstimulation (tACS), wird genutzt um Hirnoszillationen innerhalb bestimmter Frequenzbereiche, durch die Applikation sinusoidaler Ströme durch die Kopfoberfläche, zu beeinflussen.

Die ersten beiden Experimente dieser Dissertation beschäftigen sich mit Nacheffekten von tACS auf Alphaaktivität im Ruhe-EEG (Studie 1) und während einer komplexeren mentalen Rotationsaufgabe (Studie 2). In Studie 3, wurden online Effekte von tACS auf ereigniskorellierte Alphaoszillationen während mentaler Rotation untersucht. Hierzu wurde ein räumlicher Filter zur Artefaktreduktion auf MEG Daten angewandt. Studie 4 charakterisiert Artefakte in M/EEG Signalen, welche bei amplitudenmodulierter Wechselstromstimulation (AM-tACS), einer neuen Stimulationsmethode, welche Überlappungen zwischen der untersuchten Hirnoszillation und dem starken, elektromagnetischen Artefakt der Stimulation vermeiden soll, entstehen.

Studie 1 zeigte, dass tACS die Power von intrinsischen Hirnoszillationen im Alphaband für bis zu 70 minuten erhöhen kann. Dieser Nacheffekt zeigte sich auch während einer komplexeren, kognitiven Aufgabe und verbesserte die ereigniskorrelierte Desynchronization von Alphaoszillationen, sowie die Aufgabenleistung (Studie 2). Studie 3 zeigte, dass Effekte von tACS auf die ereigniskorrelierte Modulation von Alphaoszillationen, nach der Anwendung eines räumlichen Filters, trotz verbleibender Residualartefakte wiederhergestellt werden können. TACS verstärkte die bereits vorhandene, aufgabeninduzierte Modulation von Alphaoszillationen, anstatt diese zu überschreiben. Studie 4 zeigte, dass geringe Nicht-Linearitäten von Hardware zur Stimulation und Datenaufnahme bei AM-tACS zu niederfrequenten Artefakten in M/EEG Aufnahmen führen.

Zusammenfassend zeigten sich Effekte von tACS sowohl auf spontane, als auch ereigniskorrelierte Hirnoszillationen. Ein Analysevorgehen zur Untersuchung von ereigniskorrelierten Oszillationen wärend tACS wird vorgeschlagen, welches auch in Gegenwart von Restartefakten, robuste Effekte finden kann. Empfehlungen für die Messung von M/EEG während tACS werden diskutiert.

Outline

Neural oscillations are ubiquitous phenomena in the brain that have been linked to numerous domains of cognitive functioning. Traditional imaging approaches have strongly broadened our understanding of these relationships, however, the insights they can provide remains limited to correlational evidence. In order to demonstrate that brain oscillations have causal influence on cognitive functioning, and are not mere epiphenomena of the underlying brain activity, methods to non-invasively modulate these oscillations are increasingly used.

Chapter 1 will provide a brief introduction to neural oscillations and their relation to cognitive functions, as well as to the underlying mechanisms of transcranial alternating current stimulation and some related approaches.

Chapters 2 - 5 cover four experimental studies that were published in peer-reviewed journals. The first tracked the commonly reported outlasting effect of tACS for a sustained period of 90 minutes and found the effect to decay approximately after 70 minutes. The second study found prolonged effects of tACS in the alpha band on performance in a mental roation task, as well as increased spontaneous and event-related activity in the stimulated frequency band. For the third study, the experiment was repeated in an MEG scanner. While the aftereffects of study 2 could not be replicated, a substantial online effect was observed. In the realm of the study, control analyses were developed to rule out that tACS online effects were driven by residual stimulation artifacts. Study 4 demonstrates the influence of hardware properties of stimulation and recording devices, in the generation of low-frequency artifacts during a new tACS method that works with an amplitude modulated stimulation waveform.

In chapter 6 implications of the current work for tACS effects on spontaneous and event-related oscillations as well as for the investigation of tACS online effects in M/EEG signals are discussed.

Chapter 1

General Introduction

1.1 Neural Oscillations and Cognitive Functions

Neural oscillations are a common feature of brain activity that can be observed across different brain structures and species (Buzsáki, 2006). In humans, these oscillations are a subject of investigation for almost a century. Since the discovery of the alpha rhythm in the late 1920's (Berger, 1929), five major frequency bands have been identified in the human electroencephalogram (EEG). These frequency bands have been labeled in the order of their discovery as the alpha ($\sim$8 Hz - 12 Hz), beta ($\sim$12 Hz - 30 Hz), gamma ($\sim$30 Hz - 80 Hz), delta ($<$4 Hz) and theta ($\sim$4 Hz - 8 Hz) frequency bands. During the past decades, properties of this rhythmic activity such as amplitude, frequency and phase, as well as cross-frequency interactions have been associated with numerous domains of cognitive functions (Basar, Basar-Eroglu, Karakas, and Schürmann, 2000; Buzsáki, 2006; Klimesch, 1999; Klimesch, Hanslmayr, Sauseng, Gruber, and Doppelmayr, 2007). In addition, dysfunction of oscillatory activity in the brain has been linked to psychiatric and neurological disorders, such as ADHD, Parkinson's Desease, Epilepsy and Schizophrenia (Herrmann and Demiralp, 2005; Uhlhaas and Singer, 2006, 2012). This section will give a brief introduction to different types of oscillatory activity in the brain and the five major frequency bands with their associated cognitive functions and disorders.

Generally, one can observe two distinct types of oscillatory activity in the brain. The first are spontaneous oscillations that occur in the ongoing EEG signal and are not correlated with the onset of a specific event (e.g. a task or a stimulus), but that can nevertheless correlate with cognitive functioning. The second type are event-related oscillations. This type of oscillatory activity is correlated with the onset of an event, which imposes changes to the oscillation. Here, again two subtypes can be differentiated. Induced oscillations change in amplitude with onset of the event, but are not perfectly time- and phase locked to its onset. Evoked oscillations can exhibit similar changes in amplitude in response to the event, but in addition phase-reset with its onset (Herrmann, Grigutsch, and Busch, 2004).

The alpha rhythm was the first frequency band that has been discovered in the EEG during the late 1920's by the German neurologist Hans Berger (Berger, 1929). The alpha band is usually defined between $\sim$8 Hz to $\sim$12 Hz, although some authors also use slighly different frequency ranges (e.g. 7 Hz - 13 Hz). Oscillations in this frequency range are strongest over occipito-parietal sites and have been associated with basic visual perception (Busch, Dubois, and VanRullen, 2009; Hanslmayr et al., 2007; Mathewson, Gratton, Fabiani, Beck, and Ro, 2009; van Dijk, Schoffelen, Oostenveld, and Jensen, 2008), attention (Händel, Haarmeier, and Jensen, 2011; Okazaki, De Weerd, Haegens, and

Jensen, 2014) and cognitive performance, especially in visual-spatial tasks (Doppelmayr, Klimesch, Stadler, Pöllhuber, and Heine, 2002; Klimesch, 1999; Klimesch, Sauseng, and Gerloff, 2003). In these domains, alpha oscillations are hypothesized to reflect states of cortical inhibition, serving to facilitate information processing by suppressing task irrelevant (e.g. unattended) information (Jensen and Mazaheri, 2010). Further, increase of spontaneous alpha activity is observed in states of reduced vigilance and mental fatigue (Boksem, Meijman, and Lorist, 2005; Cajochen, Brunner, Krauchi, Graw, and Wirz-Justice, 1995; Daniel, 1967; Simon et al., 2011). While EEG recordings are usually dominated by alpha oscillations over posterior sites, rhythmic activity in the 8 Hz to 12 Hz range can also be observed in the auditory (Weisz, Hartmann, Müller, Lorenz, and Obleser, 2011), as well as in the somatosensory system. The latter has a distinct shape and is often referred to as the Rholandic alpha or mu rhythm (Arroyo et al., 1993; Cole and Voytek, 2017; Salmelin and Hari, 1994). Similar to the visual domain, alpha oscillations in these systems are hypothesized to serve as an inhibitory rhythm (Haegens, Handel, and Jensen, 2011; Weisz et al., 2011). Dysfunctional patterns of alpha band activity were observed in patients with ADHD (ter Huurne et al., 2013).

Oscillations in the beta range have frequencies of $\sim$12 Hz - 30 Hz and have been related to motor functions. More specifically, a suppression of beta oscillations is observed during movement execution, which is followed by a rebound effect approximately one second after the movement (Arroyo et al., 1993). A similar pattern of beta suppression and rebound can be observed during involuntary movements, elicited by electric stimulation (Salmelin and Hari, 1994), or imaginary movements (McFarland, Miner, Vaughan, and Wolpaw, 2000; Pfurtscheller, Neuper, Brunner, and Lopes Da Silva, 2005; Pfurtscheller and Neuper, 1997). In line with these findings, alterations in beta band activity have been observed in movement disorders such as Parkinson's Disease (Hammond, Bergman, and Brown, 2007; McCarthy et al., 2011).

The gamma band refers to fast neural oscillations with frequencies beyond 30 Hz. Gamma band activity is mostly analyzed in the range between 30 Hz and 100 Hz. However, some authors also investigated fast gamma activity up to 600 Hz, which is assumed to be the theoretical boundary for activity in the EEG due to the duration of action potentials (Buzsáki and Lopes Da Silva, 2012). Whereas alpha oscillations have been characterized as an inhibitory rhythm of sensory systems, gamma oscillations are thought to reflect active information processing in the brain and serve as a counterpart of alpha activity (Jensen and Mazaheri, 2010). Indeed, several studies found antagonistic relationships between alpha and gamma oscillations that manifested in increased gamma activity during periods of suppressed alpha and vise versa (Boyle and Frohlich, 2013; Jensen and Mazaheri, 2010). Event-related gamma responses have been linked to early sensory processing in different

domains as well as higher cognitive processes such as attention and memory (Fries, Nikolić, and Singer, 2007; Herrmann, Fründ, and Lenz, 2010). Gamma band oscillations have been suggested to organize information flow of local brain networks (Fries et al., 2007) and to provide a mechnism to bind sensory features, which are processed in distributed areas in the brain, through synchronization of the involved regions (Gray, König, Engel, and Singer, 1989; Herrmann et al., 2010). Dysfunctional gamma band activity is observed in numerous brain pathologies. Those include ADHD, Schizophrenia, Alzheimer's Disease, Autism, Migrane and Epilepsy (Herrmann and Demiralp, 2005).

Slow oscillations in the delta range ($<$ 4 Hz) can be observed during sleep (Amzica and Steriade, 1998), where they have been linked to memory consolidation (Marshall, Helgadóttir, Mölle, and Born, 2006). In the awake brain, delta oscillations can be observed during early childhood (Clarke, Barry, McCarthy, and Selikowitz, 2001), but have long been assumed to be absent in healthy adults. The presence of pronounced delta activity in the awake adult brain is considered a sign of brain lesions (Butz et al., 2004; Gloor, Ball, and Schaul, 1977) or tumor (Oshino et al., 2007). In recent years, however, numerous studies emphasized a role of delta band activity in the awake brain for mental tasks involving calculation or semantic processing, attention and working memory (Harmony, 2013). The most elaborated theory on the functional role of delta oscillations has been proposed by Knyazev (2012). According to that, delta oscillations reflect evolutionary early processes. In humans, these oscillations are overshadowed by higher frequency oscillations, associated with more advanced, evolutionary younger processes that dominate information processing during wakefulness. However, when the dominance of these processes is reduced, for example during sleep or in early developmental stages, more pronounced activity in the delta range can be observed (Knyazev, 2012).

Activity in the theta frequency band ranges between $\sim$4 Hz - 8 Hz. Theta oscillations have been linked to cognitive processing and especially memory performance (Klimesch, 1999). Again, an antagonistic relationship with oscillations in the alpha range has been documented. While power in the alpha range decreases during cognitive performance, activity in the theta range increases (Klimesch, 1999). This event-related power increase has been linked particularly to the encoding of episodic memory. In addition, phase-amplitude coupling between theta and gamma oscillations has been linked to working/short-term memory capacity. Specifically, the number of gamma oscillations that fit into one theta cycle are assumed to determine the number items that can be uphold in working memory (Lisman and Idiart, 1995; Lisman and Jensen, 2013; Vosskuhl, Huster, and Herrmann, 2015). Dysfunctional oscillations in the theta range can be observed in patients with memory disorders such as Alzheimer's disease (Goutagny et al., 2013; Montez et al., 2009).

1.2 Non-invasive Brain Stimulation to Investigate Brain Oscillations and Their Role for Cognition

Measurements of oscillatory activity using methods like EEG and MEG can provide important insights to link brain oscillations to cognitive functions. However, as these methods only allow to monitor activity during different task conditions (e.g. high vs. low task performance), the evidence they provide remains correlational (Herrmann, Strüber, Helfrich, and Engel, 2016). In order to establish causal relationships between brain oscillations and behavior, one needs to modulate the oscillation under investigation and monitor the resulting behavioral changes (Bergmann, Karabanov, Hartwigsen, Thielscher, and Siebner, 2016; Herrmann, Strüber, et al., 2016). Such experimental designs can be realized with pharmacological interventions, optogenetics or intracranial stimulation. However, all these methods are highly invasive and their applicabillity is either very resticted in humans or completely limited to animal models. Non-invasive brain stimulation, using repetitive transcranial magnetic stimulation (rTMS) or transcranial alternating current stimulation (tACS), offers new opportunities to safely and tolerably modulate brain oscillations of healthy human participants in everyday experimental practice (Antal et al., 2017; Chaieb et al., 2014; Fertonani, Ferrari, and Miniussi, 2015; Rossi et al., 2009). Both methods are assumed to entrain (synchronize) oscillations in the brain to an external driving force (Thut, Schyns, and Gross, 2011). In the following, an introduction to basic mechanisms and approaches to monitor stimulation effects will be given. The section will focus mainly on tACS. However, since tDCS and rTMS are methodologically closely related in several aspects, these techniques will be briefly introduced as well.

1.2.1 Basic Mechanisms

TMS works via the transcranial application of strong, transient magnetic pulses, applied via a coil, placed in the proximity of the scalp over the to-be stimulated brain region. The magnetic pulses induce electric currents in the brain, sufficiently large to depolarize cell membranes and initiate firing of action potentials (Barker, Jalinous, and Freeston, 1985; Ilmoniemi and Kičić, 2010). Transcranial electrical stimulation approaches (e.g. tDCS and tACS), in contrast, induce much more subtle changes on the cellular level. In tES, current intensities in the range of 0.5 mA - 2 mA are commonly applied through the scalp via two or more electrically conductive rubber, or saline soaked sponge electrodes. Some systems also make use Ag/AgCl electrodes, as used in most EEG systems. Due to the high resistance of the scull, a large proportion of the applied current is directly shunted through

the scalp. However, simulations of current flow, as well as results from intracranial recordings indicate that small amounts of the current reach the underlying brain structures (Miranda, Lomarev, and Hallett, 2006; Neuling, Wagner, Wolters, Zaehle, and Herrmann, 2012; Opitz et al., 2016). Figure 1.1A depicts the electric field distribution for an exemplary subject. Although the resulting field strength in the brain is too weak to directly trigger neural fireing, they are sufficiently large to modulate the polarisation of the cell membrane of stimulated neurons. Thereby, tES methods can modulate neuronal excitability, thus changing the likelihood of a neuron to fire in response to incomming exitatory postsynaptic potentials. In case of tDCS, a constant current in the range of $\sim$1 mA is applied between an anodal and a cathodal electrode. Early work on animal models has demonstrated increased neuronal excitability during anodal and decreased neuronal excitability during cathodal DC stimulation (Figure 1.1B; Bikson et al., 2004; Bindman, Lippold, and Redfearn, 1964; Creutzfeldt, Fromm, and Kapp, 1962; Jefferys, 1981). Later, a similar pattern has been observed on motor evoked potentials measured during and after tDCS (Nitsche and Paulus, 2001; Nitsche, Nitsche, et al., 2003; Nitsche and Paulus, 2000). In case of tACS, an alternating current, usually with a sinusoidal shape, is applied through the scalp. Here, neurons in the stimulated brain regions are rhythmically hyper- and depolarized with the phase of the alternating current. The application of weak alternating currents in-vivo and in-vitro has been demonstrated to align spike-timing to the phase of the applied current (Figure 1.1C; Fröhlich and McCormick, 2010; Ozen et al., 2010; Reato, Rahman, Bikson, and Parra, 2010). The current intensities necessary to induce these effects falls roughly into the range of the current strength reaching the brain during tACS (Antal and Herrmann, 2016; Opitz et al., 2016).

While the effects of rTMS and tACS on the neuronal level are different, the basic mechanism of entrainment/synchronization of an oscillation to an external driving force is common to both approaches. In fact, oscillators and their synchronization are ubiquitous phenomena, which are not restricted to the brain, but can be observed everywhere in nature as well as in human-made, artificial systems (Pikovsky, Rosenblum, and Kurths, 2003). While there is a large diversity in the systems exhibiting oscillations and synchronization, from pendulum clocks and electric circuits over chirping crickets to the beating of the human heart and activity in the brain, the general framework describing these phenomena is universal (Pikovsky et al., 2003). For synchronization to occur, the presence of a so-called self-sustained oscillator is required. Such oscillators are characterized by an internal source of energy that is transformed into rhythmic activity at a preferred frequency (eigenfrequency), which persists until the energy source is exhausted (Pikovsky et al., 2003). A key feature of these oscillators is that they synchronize in frequency and phase, if weakly coupled to another oscillator or an external driving force with a similar eigenfrequency (Pikovsky et al., 2003). The more the frequency

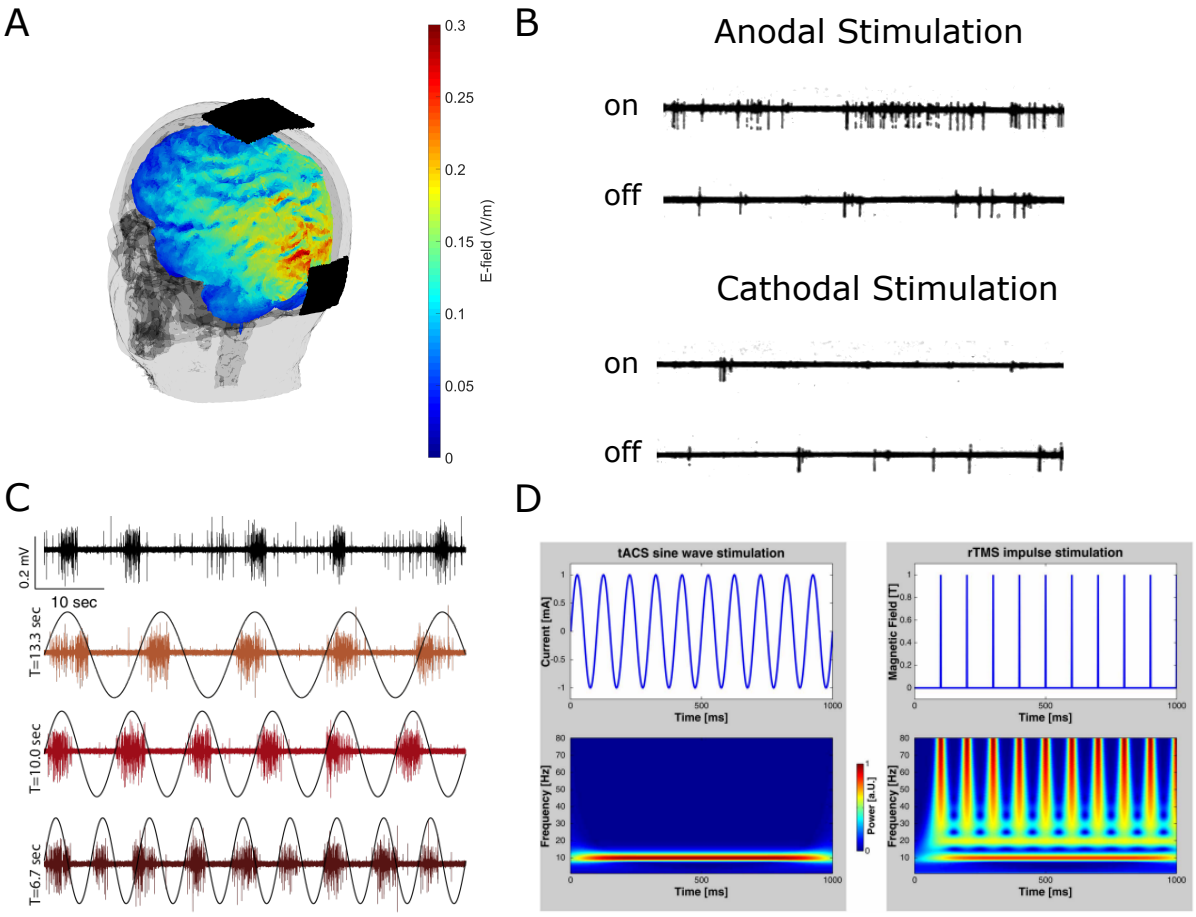

Figure 1.1: Mechanisms of non-invasive brain stimulation. (A) Simulated electric field of a Cz - Oz montage in an exemplary subject (the author). Simulation was performed using the ROAST toolbox (Huang, Datta, Bikson, and Parra, 2017) **(B)** Effect of anodal vs. cathodal stimulation on spontaneous firing recorded from rat cerebral cortex in vivo. Top traces show spontaneous activity during stimulation, bottom traces in absence of stimulation (adapted from Bindman, Lippold, and Redfearn, 1964). **(C)** Application of alternating currents synchronizes neural activity in vitro. Top trace shows the spontaneous rhythmic activity recorded without stimulation. Bottom traces show the temporal alignment of the spontaneous activity to the external stimulation at different frequencies (adapted from Fröhlich and McCormick, 2010). **D** Time-domain (top) and time-frequency (bottom) representations of stimulation waveforms used during tACS (left) and rTMS (right). While the sinusoidal waveform of tACS results in a sharp peak at the applied frequency, the transient pulses applied during rTMS have a widespread frequency content (adapted from Herrmann, Rach, Neuling, and Strüber, 2013)

of an external driving force differs from the preferred frequency of the to-be synchronized oscillator, the more energy is needed to entrain the oscillation. In the human brain, such synchronization can be observed between brain regions (Buzsáki, 2006) or even individuals (Zhou, Bourguignon, Parkkonen, and Hari, 2016), as well as to external driving forces such as rhythmic light stimulation (Notbohm and Herrmann, 2016; Notbohm, Kurths, and Herrmann, 2016) or rhythmic magnetic pulses via rTMS (Thut, Veniero, et al., 2011). Evidence from computational and animal models suggest that the application of alternating currents can entrain neural oscillations in a similar manner (Ali, Sellers, and Frohlich, 2013; Fröhlich and McCormick, 2010; Negahbani, Kasten, Herrmann, and Frohlich, 2018; Ozen et al., 2010; Reato et al., 2010). Figure 1.1C shows an example for entrainment of sponta-

neous neural firing to an externally applied alternating current in vitro. Unfortunately, direct evidence for online entrainment of brain oscillations in humans to tACS is largely missing at this point. In comparison to tACS, where relatively large areas are affected by the generated electric fields (Figure 1.1A), rTMS allows for focal stimulation of specific areas in the brain. However, the rhythmic application of transient pulses spans a wide range of frequencies and may thus not solely affect the targeted brain oscillation (Figure 1.1D; Herrmann, Rach, Neuling, and Strüber, 2013). Further, TMS is accompanied by strong visual and somatic sensations, which complicate the design of appropriate control conditions and blinding when conducting experiments.

The mechanisms reviewed so far provide the basic framework underlying effects observed during stimulation. Apart from these so-called online effects, it is commonly observed that the changes introduced to behavioral or physiological outcome measures outlast the duration of the stimulation (Nitsche, Nitsche, et al., 2003; Veniero, Vossen, Gross, and Thut, 2015). Although the sustained alterations of such outcome variables may appear similar during and after stimulation, distinct mechanisms may underlie the observed effects during the two periods. Such distinct processes have been well documented for tDCS. It has been demonstrated that pharmacological blocking of NMDA receptors abolishes aftereffects of both anodal and cathodal tDCS on motor evoked potentials, while not affecting tDCS induced changes on MEP size during stimulation (Nitsche, Fricke, et al., 2003). In contrast, blockage of sodium or calcium channels, abolished or reduced both on- and offline effects of anodal but not cathodal tDCS (Nitsche, Fricke, et al., 2003). These results indicate that offline effects of tDCS depend on NMDA receptor mediated plasticity, while the online effects are related to cell membrane polarization. In addition, the induction of an online effect seems to be necessary to elicit the offline effect (Nitsche, Fricke, et al., 2003). As presented already, online effects of tACS and rTMS are usually assumed to be caused by entrainment of intrinsic oscillations in the brain to the external driving force. For offline effects it has been debated whether they reflect entrainment echos, a state of sustained synchronization of the targeted oscillation after switching off the external driving force, or processes of spike-timing dependent plasticity (STP; Vossen, Gross, and Thut, 2015; Zaehle, Rach, and Herrmann, 2010). STP generally depends on the timing between the input and output activity of a synapse. If a pre-synaptic potential repeatedly precedes a post-synaptic potential, long term potentiation (LTP) occurs and the synapse is strengthened. Contrary, if the pre-synaptic potential repeatedly arrives after the post-synaptic potential, the synaptic connection is weakened, which is referred to as long-term depression (LTD). In a neural circuit that oscillates, spiking activity requires specific time to run through the circuit, which determines the frequency of its oscillation. Accordingly, the spiking activity arrives at the synapse at specific times. If a periodic stimulation

that matches the frequency of the circuit is applied, synaptic activity can be strengthened, because the external current arrives temporally aligned with the spiking activity. In circuits oscillating at other frequencies, the stimulation arrives at random times relative to the spiking activity and the synaptic strength remains unaffected (Zaehle et al., 2010). While entrainment echos may exist in the range of few oscillatory cycles after tACS offset, the STP model seems more appropriate to explain the long lasting aftereffects of tACS, which have been observed to last for at least several minutes and commonly exceed the duration of post-stimulation measurements (Veniero et al., 2015).

1.2.2 Neuroimaging of Brain Stimulation effects

One of the major challenges in tES is to monitor the induced alterations in brain activity. The application of electric currents with tES introduces massive distortions to EEG and MEG recordings. The artifact caused by tACS is especially problematic due to the spectral overlap with the targeted brain oscillation. Many studies circumvented the artifact by focusing on the analysis of M/EEG effects outlasting the stimulation (Neuling, Rach, and Herrmann, 2013; Veniero et al., 2015; Vossen et al., 2015; Wach et al., 2013a; Zaehle et al., 2010), effects on behavioral measures (Brignani, Ruzzoli, Mauri, and Miniussi, 2013) or by using other imaging modalities such as functional magnetic resonance imaging (fMRI; Cabral-Calderin, Williams, Opitz, Dechent, and Wilke, 2016; Violante et al., 2017; Vosskuhl, Huster, and Herrmann, 2016; Weinrich et al., 2017). The application of tES causes comparably small distortions to fMRI signals (Antal et al., 2014). In case of tACS, the alternating current flow cancels out in the net signal allowing to measure changes in brain activity in absence of distortions (Antal et al., 2014). A major disadvantage, however, is that fMRI relies on measurements of blood-oxygenation (blood-oxygen level dependent response; BOLD response), which is an indirect indicator of brain activity, especially for neural oscillations. In order to fully understand effects of tACS and its mechanisms, it is inevitable to concurrently record M/EEG while stimulating and to recover the artifact contaminated brain signals. In recent years, different approaches to achieve this goal have been tested on EEG and MEG data.

For EEG data, some authors tackled the tACS artifact by creating a template of the artifact waveform and subtract it from the EEG recording (Dowsett and Herrmann, 2016; Helfrich, Schneider, et al., 2014; Kohli and Casson, 2015; Voss et al., 2014). This approach assumes that the shape of the waveform originating from the stimulation is relatively stable over time, while signals reflecting brain activity underlie strong fluctuations. Thus, if a template is created from averages of EEG segments, which are all time-locked to the same phase of the artifact waveform (e.g. the crossing of the zero

line), the brain activity averages out, while retaining the artifact shape. The subtraction of the template should then remove the artifact from the signal while the superimposed brain signals remain intact. As this approach turned out to leave residual artifacts in the data, some authors subsequently applyed principal component analysis (PCA) to remove residual artifacts that remained in the signal after the template subtraction (Helfrich, Schneider, et al., 2014).

In the MEG, the application of spatial filtering by means of synthetic aperture magnetometry (Soekadar et al., 2013) or linearly constraint minimum variance (LCMV) beamforming (Neuling et al., 2015) has been suggested to suppress artifacts arising during tACS and tDCS. Beamformers separate signals originating from different directions and have widespread applications in radar and sonar technologies (Van Veen and Buckley, 1988). In neuroimaging, beamformers are used to localize sources of brain signals recorded from EEG or MEG sensors and can be devided into time-domain beamformers such as LCMV (Van Veen, Van Drongelen, Yuchtman, and Suzuki, 1997) as well as frequency-domain beamformers such as DICS (Dynamic Imaging of Coherent Sources; Gross et al., 2001). In principle, these spatial filters are designed to pass signals originating from a specific location in the brain, while attenuating activity from all other locations (Van Veen et al., 1997). By constructing multiple filters with different pass-bands for a pre-defined grid of possible source locations, a spatial map of brain activation can be obtained (Van Veen et al., 1997). An important feature of the LCMV beamformer in the context of concurrent tACS-MEG, is its insensitivity to highly correlated sources (Neuling et al., 2015). The spatial filter at each source location is constructed to minimize the variance of the filter output (which gives the LCMV beamformer its name). In the presence of two or more distinct, highly correlating sources, the filter optimizes this variance minimization by canceling the correlating proportion of the signals (Van Veen et al., 1997). While high correlations between spatially separated sources are unlikely to occur naturally in the brain, and the LCMV beamformer is relatively robust to moderate correlations between sources (Van Veen et al., 1997), the strong artifact arising during tACS propagates to virtually all sensors with high consistency (Neuling et al., 2015). This way, LCMV beamforming can cancel out large proportions of the tACS artifact. However, as a consequence the artifact suppression capabilities of the method are also limited by the degree to which the recorded artifact signal is correlated (or uncorrelated) over sensors (Mäkelä, Sarvas, and Ilmoniemi, 2017).

Recently, physiological processes have been identified that can compromise the tACS artifact suppression capabilities of template subtraction (plus PCA) and beamformer approaches (Noury, Hipp, and Siegel, 2016; Noury and Siegel, 2018). In fact, basic physiological processes such as heart beat or respiration can lead to small changes in body impedance that can change the size of the tACS

artifact in EEG sensors. In the MEG, the subtle body movements that accompany these processes, change the distance of stimulation electrodes (and cables) to the sensor array, resulting in similar systematic modulations of the recorded tACS artifact, which manifest in an amplitude modulation of the sinusoidal tACS waveform (Noury et al., 2016). These amplitude modulations of the tACS artifact led to side-bands around the main artifact frequency that survived the correction procedures (Noury et al., 2016, also see Neuling, Ruhnau, Weisz, Herrmann, and Demarchi, 2017; Noury and Siegel, 2017). In addition, these processes may impair suppression of the artifact directly. The variation of the tACS artifact over time cannot be incorporated in the construction of a template, which relies on the assumption of a time-invariant artifact signal. Consequently, any variation of the artifact from its average strength remains in the data as a residual artifact, which needs additional correction. Similarly, the variability of artifact strength might reduce the correlation of the artifact signal over sensors, which is the foundation of the artifact suppression process in LCMV beamforming (Mäkelä et al., 2017; Van Veen et al., 1997). In spite of the aforementioned problems, template subtraction and LCMV beamforming offer powerful suppression of the tACS artifact that allows at least some insights to tACS online effects, if carefully accounting for the imperfection of artifact suppression approaches. It has been argued that contrasting two conditions within the same tACS condition (e.g. pre- and post-interval of a sensory stimulus) can correct for residual artifacts in the data, by canceling each other out (Neuling et al., 2017; Noury and Siegel, 2017). This approach has been tested in study 3 of this dissertation (chapter 4).

As another solution to reduce/avoid residual tACS artifacts, the use of alternative waveforms such as saw-tooth waves (Dowsett and Herrmann, 2016) or amplitude modulated tACS (AM-tACS; Witkowski et al., 2016) has recently been proposed. Saw-tooth waves offer the advantage of a unique shape that is distinct from the more sinusoidal EEG signals. In the frequency domain, such signals introduce strong harmonics which makes residual artifacts easier to detect and allows for post-hoc rejection of trials with sub-optimal artifact suppression (Dowsett and Herrmann, 2016). AM-tACS relies on the modulation of a high frequency carrier-oscillation (e.g. 200 Hz) by a lower frequency modulating oscillation, tuned to the to-be stimulated brain oscillation (e.g. 10 Hz). Amplitude modulated signals contain spectral power at the frequency of the carrier oscillation (and two side-bands at carrier frequency $\pm$ modulation frequency), but no power at the frequency of the modulating oscillation. This way, the spectral overlap between brain signal of interest and tACS artifact is avoided (Witkowski et al., 2016). A recent computer simulation was able to demonstrate that an oscillating cortical network can be entrained to the modulating oscillations of an amplitude modulated stimulation waveform, although to a weaker extend as compared to conventional sine-wave stimulation (Negahbani et al.,

2018). However, in another recent study low-frequency distortions during concurrent AM-tACS-MEG were reported, questioning whether this type of waveform is completely artifact-free in the range of the modulation frequency (Minami and Amano, 2017).

1.3 Introduction to Papers

This dissertation has two main foci. The first is concerned with aftereffects of tACS especially in the alpha band and their potential to alter cognitive function. The second focus of the dissertation is on online effects of tACS with a special emphasis on the electromagnetic artifact that has to be dealt with in M/EEG signals.

Due to the strong electromagnetic artifact contaminating M/EEG signals during stimulation, early research on tACS effects focussed on aftereffects outlasting the stimulation (Neuling et al., 2013; Wach et al., 2013a; Zaehle et al., 2010). These aftereffects have been reported in multiple studies, utilizing different stimulation montages and frequencies (Veniero et al., 2015). However, thus far the majority of these studies monitored aftereffects for several minutes up to 30 minutes after tACS application, with the common observation that the effect outlasted the duration of the experiments (Neuling et al., 2013; Vossen et al., 2015; Wach et al., 2013a). The objective of the first experiment, reported in chapter 2, was to track the duration of the aftereffect on resting EEG activity for a sustained period of 90 minutes after stimulation. This duration is comparable with effects observed on motor evoked potentials after application of tDCS over the motor cortex (Nitsche, Fricke, et al., 2003; Nitsche and Paulus, 2001; Nitsche, Nitsche, et al., 2003). The article was published in *Frontiers in Human Neuroscience*.

While several studies so far reported outlasting effects of tACS on EEG activity during rather simple resting-state or detection task paradigms (Neuling et al., 2013; Vossen et al., 2015; Zaehle et al., 2010), tACS studies utilizing behavioral measures usually monitor effects during stimulation (online). The goal of the second study, presented in chapter 3, was to monitor aftereffects of tACS during the performance of a cognitive task that involves task induced modulations of the targeted alpha oscillations. In particular, the study focused on whether tACS does not only modulate spontaneous alpha activity, but also event-related oscillatory activity. A further aim was to investigate whether tACS induced alterations in oscillatory activity also result in altered task performance. The data leading to this article were collected in the scope of my master's thesis. A detailed reanalysis was performed on the EEG data that was extended to additional in-depth analysis of the event-related EEG data, and additional measures of the tACS aftereffect that added substantial new results to the article which

was published in *Frontiers in Human Neuroscience*.

Investigations of tACS aftereffects, like those presented in chapter 2 and 3, can provide important insights to tACS effects. Especially for clinical applications, long lasting effects of the stimulation are desireable in order to achieve sustainable treatment effects. In the context of research on brain oscillations, behavioral effects are typically measured during tACS application. The exposition to sensory stimuli as well as the performance of cognitive tasks typically involves event-related modulations of oscillatory activity in the brain (Pfurtscheller and Lopes Da Silva, 1999). How the continuous application of tACS during such tasks influences these event-related oscillations remains elusive so far. Several studies demonstrated state dependent effects of tACS (Feurra et al., 2013; Neuling et al., 2013; Ruhnau, Keitel, Lithari, Weisz, and Neuling, 2016). Depending on whether tACS merely affects oscillations during the pre- or post-stimulus interval (or both) of a task, tACS may alter event-related oscillations in various directions or leave them unaffected. The goal of the third study, presented in chapter 4, was to elucidate effects of continuous tACS on event-related oscillations. To this end, the experiment presented in chapter 3 was repeated inside an MEG scanner. The application of spatial filtering to MEG recordings during tES has been shown to strongly attenuate the massive tACS artifact in the sensors (Neuling et al., 2015; Soekadar et al., 2013). Data for this experiment were collected during an internship for my Master studies at the MEG site of the Max Planck Institute for Human Cognitive and Brain Sciences in Leipzig in collaboration with Dr. Burkhard Maess. The analysis of the data was entirely performed within the scope of this dissertation. The results were published in the open access journal of the Society for Neuroscience *eNeuro*.

Removing the massive electromagnetic artifact from concurrent tACS-M/EEG recordings is among the most (if not the single most) challenging task in tACS research. Nevertheless, investigating online effects of the stimulation is inevitable to fully understand the basic mechanisms underlying tACS effects on the brain. Several studies utilized artifact cleaning approaches like template subtraction (Helfrich, Schneider, et al., 2014; Voss et al., 2014) or beamforming (Neuling et al., 2015; Ruhnau et al., 2016) to recover M/EEG signals during tACS. However, it has been shown that these approaches have imperfect artifact suppression capabilities, such that a residual tACS artifact remains present in the data (Mäkelä et al., 2017; Noury et al., 2016; Noury and Siegel, 2017, 2018). As a solution, alternative tACS waveforms such as sawtooth waves (Dowsett and Herrmann, 2016)) or amplitude modulated tACS (Witkowski et al., 2016) have been proposed. The latter is especially interesting, as a high frequency signal, which is modulated in amplitude by a lower frequency sine wave shifts the resulting spectral power into higher frequencies, avoiding spectral overlap between the brain oscillation of interest and the tACS artifact. The fourth study (chapter 5), is devoted to

non-linear processes in stimulation and recording hardware that can reintroduce artifacts at the modulations frequency. The paper has been published in *NeuroImage*.

Chapter 2

Study I: Sustained Aftereffect of α-tACS Lasts Up to 70 min after Stimulation

Published as:

Kasten, FH., Dowsett,J.,Herrmann, CS., (2016) Sustained Aftereffect of α-tACS Lasts Up to 70 min after Stimulation. *Frontiers in Human Neuroscience*., 10:245.

Author Contributions:

Designed research: FHK, JD, CSH

Perfomed Research: FHK

Analyzed Data: FHK, JD

Wrote paper: FHK, JD, CSH

2.1 Abstract

Transcranial alternating current stimulation (tACS) has been repeatedly demonstrated to increase power of endogenous brain oscillations in the range of the stimulated frequency after stimulation. In the alpha band this aftereffect has been shown to persist for at least 30 min. However, in most experiments the aftereffect exceeded the duration of the measurement. Thus, it remains unclear how the effect develops beyond these 30 min and when it decays. The current study aimed to extend existing findings by monitoring the physiological aftereffect of tACS in the alpha range for an extended period of 90 min post-stimulation. To this end participants received either 20 min of tACS or sham stimulation with intensities below their individual sensation threshold at the individual alpha frequency (IAF). Electroencephalogram (EEG) was acquired during 3 min before and 90 min after stimulation. Subjects performed a visual vigilance task during the whole measurement. While the enhanced power in the individual alpha band did not return back to pre-stimulation baseline in the stimulation group, the difference between stimulation and sham diminishes after 70 min due to a natural alpha increase of the sham group.

2.2 Introduction

During the past decade transcranial alternating current stimulation (tACS) has emerged as a promising new method for non-invasive brain stimulation; several findings from human and animal research as well as neural network simulations provide evidence for its capability to entrain intrinsic brain oscillations via the application of sinusoidal currents on the scalp (i.e. Ali et al., 2013; Fröhlich and McCormick, 2010; Helfrich, Schneider, et al., 2014; Neuling et al., 2013; Vossen et al., 2015; Zaehle et al., 2010, for a recent overview of human and animal findings see Herrmann et al., 2013; Reato, Rahman, Bikson, and Parra, 2013). This feature makes tACS a promising technology to investigate causal relationships between neural oscillations and behavior or perception (Herrmann et al., 2013; Herrmann, Strüber, et al., 2016) as well as for the treatment of several neurological and psychiatric disorders in which dysfunctional neural oscillations are involved, such as Epilepsy, ADHD, Parkinson's disease, Schizophrenia or Alzheimer's disease (Brittain, Probert-Smith, Aziz, and Brown, 2013; Herrmann and Demiralp, 2005; Uhlhaas and Singer, 2006, 2012).

Besides behavioral (Antal et al., 2008; Brignani et al., 2013; Hoy et al., 2015; Laczó, Antal, Niebergall, Treue, and Paulus, 2012; Sela, Kilim, and Lavidor, 2012; Strüber, Rach, Trautmann-Lengsfeld, Engel, and Herrmann, 2014; Vosskuhl et al., 2015) and physiological online effects of which the lat-

ter remain difficult to investigate (at least in humans) due to the massive artifact introduced to the signal (Helfrich, Schneider, et al., 2014; Neuling et al., 2015; Witkowski et al., 2016) numerous studies demonstrated different types of physiological aftereffects following tACS application in various frequency bands and using different stimulation protocols (for a recent overview, see Veniero et al., 2015). For example Helfrich, Knepper, et al. (2014) observed increased gamma-band coherence lasting for up to 20 min after applying either 20 min of in-phase or anti-phase gamma tACS targeting left and right extra-striate visual cortex. Wach et al. (2013a) found a decrease in cortico-muscular coherence during isometric contraction in the gamma-band after tACS in the alpha band to persist for at least 38 min. Other studies demonstrated increased amplitudes of endogenous brain oscillations within the range of the stimulation frequency after tACS (Neuling et al., 2013; Vossen et al., 2015; Zaehle et al., 2010). However, Neuling et al. (2013) found this amplitude increase to be dependent on the current brain state during which tACS is administered; while an aftereffect was successfully produced during eyes-open (corresponding to low baseline alpha power), no increase in alpha power was observed under eyes-closed condition (accompanied by high baseline alpha power). A common finding of all these experiments was that the duration of the aftereffect exceeded the duration of the post stimulation measurement (up to 30 min). Thus, the development and duration of the tACS aftereffect beyond this point remains unclear. The current study aimed to extend existing findings on the time course of the tACS aftereffect. To this end the development of the aftereffect at the stimulated and neighboring frequency bands was monitored for a duration of 90 min following the application of 20 min tACS at participants' individual alpha frequency (IAF). We hypothesized that power in the individual alpha band would increase in the stimulation group compared to both a control group receiving sham stimulation and to pre-stimulation baseline, at least during the first 30 min after tACS which would replicate previous findings (Neuling et al., 2013). However, during the following 60 min we expected the aftereffect to decay such that alpha power in the stimulation group no longer differs from sham or baseline alpha power.

2.3 Materials and Methods

For comparability with previous findings the experimental procedures and data analysis in the current study follow the approaches of Zaehle et al. (2010) and Neuling et al. (2013) except for slight changes. The study was approved by the Ethics Committee of the University of Oldenburg and conducted in accordance with the Declaration of Helsinki.

2.3.1 Participants

Twenty-two subjects participated in the experiment. All were students at the University of Oldenburg and received monetary compensation for participation and a performance dependent bonus (see "Paradigm" Section). Participants gave written informed consent prior to the experiment. They were medication-free at the day of the experiment and none of them reported presence or history of neurological or psychiatric disorders. All subjects were right-handed according to the Edinburgh handedness-scale (Oldfield, 1971). In a single-blind design participants were randomly assigned to one of the experimental groups (stimulation or sham) with the groups being counterbalanced for participants' sex and time of measurement (sessions started either at 9 am or 2 pm). Subjects were debriefed immediately after the experiment. Due to technical issues the experiment had to be aborted for two subjects. A recent study reported tACS to be only effective with low baseline power in the targeted frequency band (Neuling et al., 2013). To avoid non-responsiveness to the stimulation due to such ceiling effects absolute baseline IAF power was z-transformed. Three participants exhibited z-scores exceeding 1.65 (corresponding to an α-level $<$ 0.05, one-tailed) and were excluded from further analysis. Thus, 17 participants (stimulation group: 9, sham group: 8, age: 22.0 $\mp$ 2.24 years, 8 females) remained for analysis. An a priori power analysis based on the findings of Neuling et al. (2013) was conducted to estimate the required sample sizes. Results suggest sufficient power ($1 - \beta$ = 0.83) at a total sample size of 16 (eight per group). Therefore the obtained sample should be sufficient to detect effects of similar size. Furthermore, we provide effect sizes for all results as an additional measure independent of sample size.

2.3.2 EEG

The Experiment was conducted in a dimly lit room with participants seated in a recliner in front of a computer screen at a distance of approximately 100 cm. The electroencephalogram (EEG) was measured from 10 sintered Ag-AgCl electrodes mounted in an elastic cap (EasyCap GmbH, Herrsching, Germany) placed at five frontal and five parietal positions around Fz and Pz following the international 10–20 system layout. An electrode attached to the nose served as reference. The ground electrode was positioned at Fpz. Additionally a vertical Electrooculogram (EOG) was recorded underneath the right eye to monitor eye-movements during the experiment. All impedances were kept below 10 kΩ. EEG was recorded using a BrainAmp (Brain Products GmbH, Gilching, Germany) amplifier and the BrainVision Recorder Software (Brain Products GmbH, Gilching, Germany). Data were sampled at a rate of 250 Hz and a resolution of 0.5 μV to increase the voltage range of the amplifier avoiding clip-

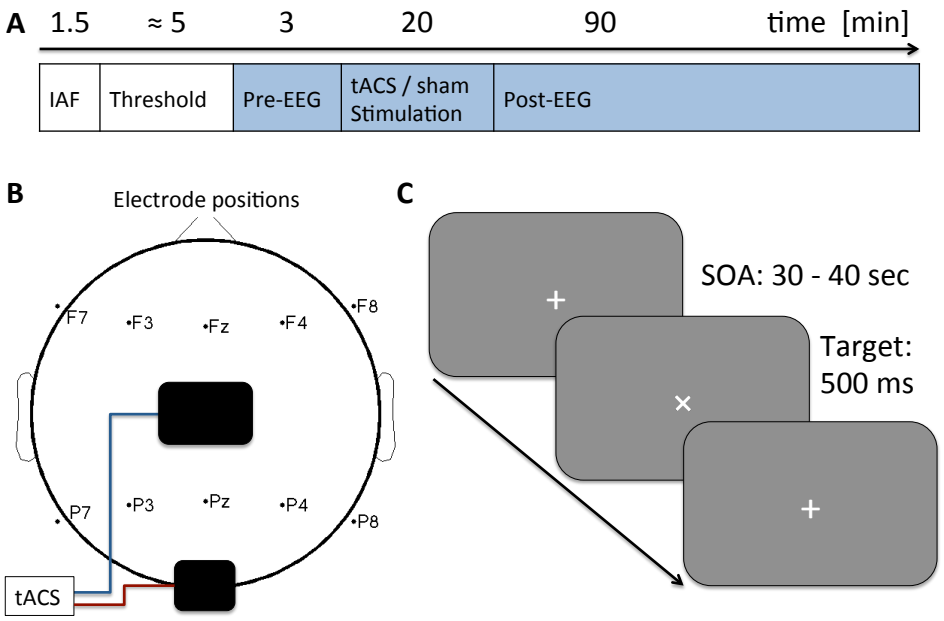

Figure 2.1: Experimental procedure. (A) Time course of the current experiment. First 90 s of eyes-closed EEG were acquired to determine participants' individual alpha frequency (IAF) which was used as stimulation frequency in the subsequent steps. Next, stimulation intensity was adjusted to the individual sensation threshold. During the following 113 min participants performed a visual vigilance task (indicated in blue) while 3 min of baseline EEG was measured followed by 20 min of tACS or sham stimulation and 90 min post-stimulation EEG. **(B)** Electrode setup. Stimulation electrodes were placed above Cz (5 $\times$ 7 cm) and Oz (4 $\times$ 4 cm) following the international 10-20 system. Additionally 10 EEG electrodes were positioned over five frontal and five parietal sides. **(C)** Visual vigilance task. Participants fixated a white cross at the center of a computer screen. Every 30-40 s the cross was rotated by 45 $^\circ$ for a duration of 500 ms. Participants were given 2 s to manually respond to the rotation and received 0.05 € for each detected target. A total of 191 targets were presented during the experiment.

ping effects during tACS application. A DC reset was applied when the amplifier ran into saturation.

Prior to the main experiment participants IAF was determined by 90 s of eyes-closed resting EEG. The obtained EEG data were segmented into 1 s epochs. Subsequently a Fast Fourier Transform (FFT) was applied to each epoch to compute power spectra. The first 50 artifact free spectra were averaged and the power peak in the 8–12 Hz range at electrode Pz was visually identified and used as stimulation frequency for the main experiment. If no clear peak was evident the procedure was repeated.

EEG was recorded during the whole course of the main experiment. In the beginning 3 min of baseline EEG were obtained, followed by 20 min of tACS or sham stimulation. Subsequently another 90 min of post-tACS EEG were acquired (for an overview of the time course of the experiment, see Figure 2.1A).

2.3.3 Electrical Stimulation

Stimulation was administered by two surface conductive rubber electrodes attached to participants' scalp. One was positioned centered above Cz (5 $\times$ 7 cm), the other above Oz (4 $\times$ 4 cm) using an

adhesive, electrically conductive paste (ten20 conductive paste, Weaver and Co., USA). In a recent modeling study this montage has been shown to produce highest current densities in posterior brain regions (Neuling, Wagner, et al., 2012). A smaller electrode over Oz was used to further increase current density in occipital areas below the electrode. An overview of the EEG and tACS montage is given in Figure 2.1B. Electrodes were connected to a battery-operated stimulator system (DC Stimulator Plus, Neuroconn, Ilmenau, Germany). The stimulation signal was digitally sampled at 100 kHz using Matlab 2012a (The MathWorks Inc., Natick, MA, USA) and sent in chunks of 1 s segments to a digital to analog converter (Ni USB 6229, National Instruments, Austin, Texas, USA) converting the digital sinusoidal signal into an analog output for the stimulator. Electrode impedance was kept below 10 kΩ. Participants were stimulated at their IAF. Intensity of the stimulation was adjusted to subjects' individual sensation threshold which was defined as the highest intensity at which participants did not notice the stimulation (no phosphene or skin sensation). To determine the threshold participants were stimulated with an initial intensity of 1000 μA (peak-to-peak). If participants noticed the stimulation, intensity was decreased in steps of 100 μA until they did not notice the stimulation anymore. In case participants did not notice the initial stimulation, intensity was increased in steps of 100 μA until they noticed the stimulation. Each of the steps was applied for 20 s, without fade-in or fade-out. The obtained intensity was used as the stimulation intensity during the experiment. On average stimulation intensity was 1200 μA ($\pm$ 440 μA, min: 400 μA, max: 1800 μA) peak-to-peak with an average frequency of 10 Hz ($\pm$1.12 Hz). Student's two-sample t-test revealed no significant difference in intensities ($t_{15} = -0.22, p = 0.83, d = 0.1$) or stimulation frequencies ($t_{15} = -0.42 p = 0.68, d = 0.2$) between experimental groups. After 3 min of baseline EEG the experimental group received 20 min of tACS with 10 s fade-in and fade-out at the beginning and the end of the stimulation period (intensity was increased/decreased every second by 1/10 of the final stimulation intensity). While all other stimulation parameters were kept the same as in the experimental group the sham group received only 30 s of stimulation (including 10 s fade-in and fade-out) in the beginning of the 20 min period.

2.3.4 Paradigm

To ensure participants being awake and attentive they performed a visual vigilance task during the whole course of the main experiment (baseline, tACS, post-tACS measurement). Visual stimuli were delivered simultaneously with the tACS signal generation using Matlab and the Psychtoolbox 3. Stimuli were displayed on a computer screen (Samsung SyncMaster P2470H, 1920 $\times$ 1080 pixels, 60 Hz refresh rate) at a distance of approximately 100 cm. Subjects were instructed to fixate a white cross

(diameter 1.58 °) at the center of the screen which was rotated by 45° for 500 ms every 30–40 s. Participants had to manually respond to each of the rotations within 2 s after stimulus onset (see Figure 2.1C). To maintain subjects motivation they received a bonus of 0.05 € for each hit. A total of 191 targets were presented during the 113 min of the experiment.

2.3.5 Debriefing

After finishing the experiment participants were asked to fill out a translated version of an adverse effects questionnaire introduced by Brunoni et al. (2011). The questionnaire assesses the 10 most commonly reported adverse effects during transcranial electric stimulation (headache, neck pain, scalp pain, tingling, itching, burning sensation, skin redness, sleepiness, trouble concentrating and acute mood change). Subjects had to rate the intensity of each adverse effect (1 – none, 2 – mild, 3 – moderate, 4 – severe) and how strongly they attributed them to tACS (1 – none, 2 – remote, 3 – probable, 4 – definite). To confirm participants' blindness towards their experimental condition they were finally asked to guess whether they had been stimulated or not. Immediately afterwards they were informed about their true experimental condition and the aims of the study.

2.3.6 Data Analysis

Data analysis was performed using Matlab 2012b and the Fieldtrip toolbox (Oostenveld, Fries, Maris, and Schoffelen, 2011). For statistical analysis statistical software R 3.2.3 (R Foundation for Statistical Computing, Vienna, Austria) was used.

EEG data were high-pass filtered at 0.3 Hz, low-pass filtered at 100 Hz and subsequently segmented into 3 min blocks resulting in one baseline block prior to and 30 blocks after tACS. EEG data acquired during tACS application were not further analyzed. Each block was subsequently divided into 180 non-overlapping 1 s epochs. Segments containing visual stimulation or manual responses were removed as well as epochs containing artifacts. FFT spectra (Hanning window, 2 s zero-padding) were computed and averaged for the first 120 artifact free epochs in each 3 min block. From these spectra, power in the individual alpha band (IAF $\pm$ 2 Hz) was obtained and averaged for each block. To account for inter-individual differences, IAF band power in the post stimulation blocks was normalized with respect to pre-stimulation baseline. Data for three subsequent 30 min time periods were analyzed separately using three rmANOVAs to ensure comparability with the results of Neuling et al. (2013) and to preserve the opportunity of assumption testing which is only possible with more observations than levels of measurement. Each rmANOVA was conducted with the

within subject factor time (10 levels) and the between subject factor group (two levels, stimulation vs. sham). Please note that due to the previous normalization only post stimulation data were analyzed and a stimulation effect would therefore reveal itself as a significant main effect of the factor group. Separate two-sided t-tests for stimulation and sham group against baseline were computed to test for deviations from baseline IAF band power for each of the conditions. All obtained p-values were Bonferroni-corrected to account for multiple comparisons. Greenhouse-Geisser corrected values are reported in case sphericity was violated. Furthermore, power in an upper (IAF + 3 Hz to IAF + 5 Hz) and a lower frequency band (IAF - 5 Hz to IAF - 3 Hz) were analyzed with the same procedure to ensure frequency specificity of the tACS effect. Finally, a set of FDR corrected, one-sided post hoc t-tests on relative IAF band power between stimulation and sham group were calculated for each of the 3 min post-tACS blocks to determine the point in time were the tACS aftereffect vanishes.

Statistical analysis of participants' ratings on adverse effects was performed using Wilcoxon rank sum test for independent samples. To improve chances to detect undesired group differences no p-value correction was applied. Participants guesses about their assigned experimental condition was analyzed using Fisher's exact test for count data.

2.4 Results

2.4.1 Debriefing

The most reported adverse effects (intensities rated higher than 1) after the experiment were sleepiness (82.35%), trouble concentrating (64.70%) and tingling (41.17%). Ratings for intensity of adverse effects were generally relatively low, except for sleepiness ($M = 2.71$) and trouble concentrating ($M = 2.12$). For the ratings on whether subjects attributed the adverse effects to the stimulation only tingling achieved an average score above 2 (remote, $M = 2.18$). Two-sided t-test between experimental groups revealed no significant differences between groups for any of the items (all $p > 0.08$). After filling out the questionnaire 41.2% of subjects indicated that they thought they were stimulated during the experiment (33.3% in the stimulation group 50% in the sham group). Fisher's exact test for count data confirmed that participants were unaware of their experimental condition ($OR = 0.52, p = 0.63$).

2.4.2 Vigilance Task

On average participants detected 96.61% ($\pm$ 6.01%) of all targets. None of them performed worse than 80%, confirming that participants were vigilant and attentive during the experiment. A Students'

two sample t-test revealed no difference between experimental groups ($M_{stim} = 97.61, M_{sham} = 95.48; t_{15} = 0.72, p = 0.48, d = 0.35$).

2.4.3 Electrophysiological Data

For the 17 subjects included in the final analysis the rmANOVA on relative IAF band power for the first 30 min post-tACS revealed a significant main effect of group ($F_{(1,15)} = 11.88, p = 0.011, \eta^2 = 0.3$), but no effect of time ($F_{(9,135)} = 1.75, p = 0.44, \eta^2 = 0.05$) or a group $\times$ time interaction ($F_{(9,135)} = 1.78, p = 0.42, \eta^2 = 0.05$). Subsequent Bonferroni-corrected post hoc t-tests against baseline showed a significant divergence from baseline for the stimulation group ($t_8 = 5.43, p = 0.004, d = 1.8$) but not for sham ($t_7 = 1.86, p = 0.62, d = 0.66$). Results demonstrate that power in the IAF band was increased in the stimulation group compared to sham and to baseline, while power in the sham group remained at baseline level. The rmANOVA for the second 30 min post-tACS shows a similar pattern with a significant main effect of group ($F_{(1,15)} = 10.12, p = 0.019, \eta^2 = 0.26$) but neither an effect of time ($F_{(9,135)} = 0.70, p = 1, \eta^2 = 0.02$) nor a significant group $\times$ time interaction ($F_{(9,135)} = 1.36, p = 0.78, \eta^2 = 0.04$). Post hoc t-test exhibited a significant deviation from baseline for the stimulation group ($t_8 = 5.75, p = 0.003, d = 1.9$) but not for sham ($t_7 = 3.53, p = 0.058, d = 1.2$) suggesting that power in the IAF band remains increased in the stimulation group compared to baseline and to sham. However, for the last 30 min period the rmANOVA revealed neither a significant effect of group ($F_{(1,15)} = 4.75, p = 0.14, \eta^2 = 0.17$) nor an effect of time ($F_{(9,135)} = 1.96, p = 0.32, \eta^2 = 0.04$) or a significant group $\times$ time interaction ($F_{(9,135)} = 0.72, p = 1, \eta^2 = 0.02$). Post hoc t-tests suggest a significant difference from baseline IAF band power for both stimulation ($t_8 = 4.85, p = 0.007, d = 1.61$) and sham ($t_7 = 3.75, p = 0.04, d = 1.2$). Results suggest that the difference in IAF band power between stimulation and sham group vanishes, due to power increase in the IAF band in the sham group (refer to Figure 2.2 for an overview).

Statistical analysis of the upper and lower frequency bands revealed no significant effects. However, the rmANOVA on upper band power during the first 30 min shows a marginal effect of group ($F_{(1,15)} = 6.72, p = 0.06, \eta^2 = 0.18$). Bonferroni-corrected t-tests against baseline confirmed that neither of the groups significantly differed from baseline (stimulation: $t_8 = 1.77, p = 0.69, d = 0.59$; sham: $t_7 = -2.05, p = 0.48, d = 0.72$). A detailed overview on results of upper and lower band power is given in Table 2.1. Time courses of upper and lower band power are illustrated in Figure 2.3.

To further investigate the time course of the tACS aftereffect a set of 30 one-sided FDR-corrected t-tests comparing relative alpha power between stimulation and sham group were calculated for each

Table 2.1: Results for upper and lower alpha band. mANOVA and t-test results for normalized power in the lower (IAF - 3 Hz to IAF - 5 Hz) and upper (IAF + 3 Hz to IAF + 5 Hz) frequency bands. Analysis follows the same procedure as for the normalized IAF data. Left half shows ANOVA results, right half results for the comparisons of each group against baseline. None of the analysis exhibited significant results. Only a trend for the factor group is evident in the upper band during the first 30 min (indicated by upper case T)

rmANOVA	F	p	η^2	**t-test vs. baseline**	T	p	d
Lower first 30 min							
Group	1.30	0.81	0.06	*Stim*	1.06	1.00	0.35
Time	0.68	1.00	0.01				
Group $\times$ *Time*	1.02	1.00	0.02	*Sham*	0.58	1.00	0.21
Lower second 30 min							
Group	3.38	0.26	0.14	*Stim*	0.47	1.00	0.16
Time	1.57	0.58	0.03				
Group $\times$ *Time*	1.16	1.00	0.02	*Sham*	1.75	0.74	0.62
Lower third 30 min							
Group	1.94	0.55	0.09	*Stim*	0.31	1.00	0.10
Time	1.34	0.82	0.02				
Group $\times$ *Time*	1.37	0.80	0.02	*Sham*	1.60	0.93	0.56
Upper first 30 min							
Group	6.72	0.06^T	0.18	*Stim*	1.77	0.69	0.59
Time	0.77	1.00	0.03				
Group $\times$ *Time*	0.45	1.00	0.01	*Sham*	2.05	0.48	0.72
Upper second 30 min							
Group	1.60	0.68	0.05	*Stim*	2.98	0.01	0.99
Time	1.44	0.53	0.05				
Group $\times$ *Time*	1.24	0.84	0.04	*Sham*	1.01	1.00	0.35
Upper third 30 min							
Group	0.45	1.00	0.02	*Stim*	2.50	0.22	0.83
Time	1.49	0.65	0.05				
Group $\times$ *Time*	0.31	1.00	$>$0.01	*Sham*	1.01	1.00	0.35

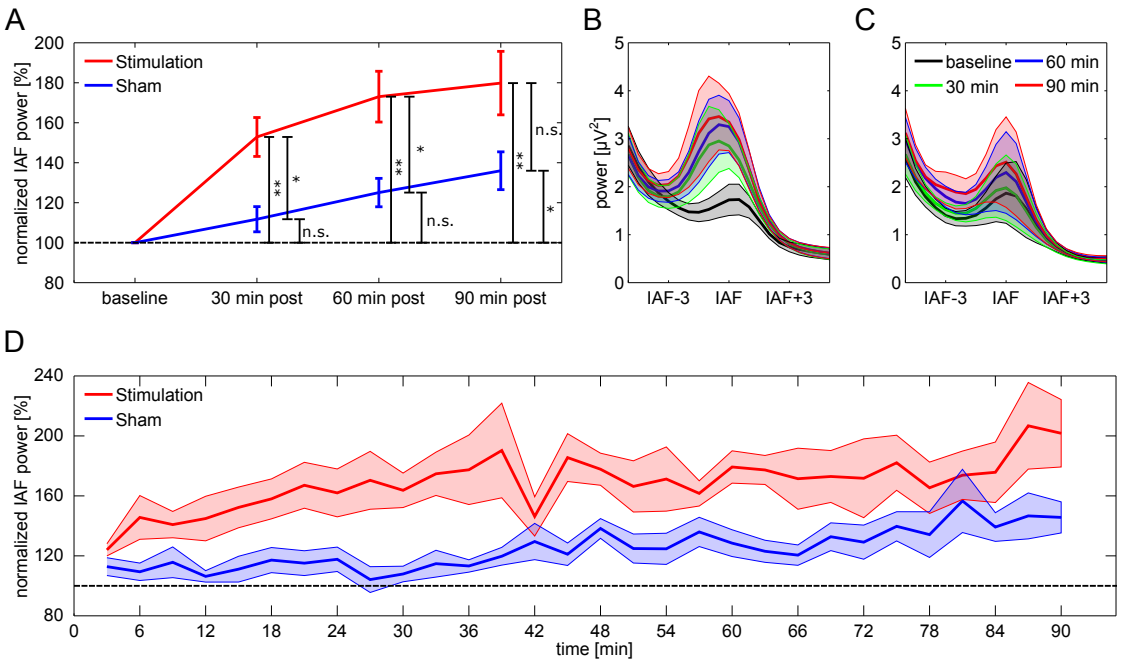

Figure 2.2: Power change in the individual alpha band. **(A)** Post period increase in the individual alpha band. Stars coding for significant differences ($* < 0.05, ** < 0.01$). Error bars reflect standard error of the mean (SEM), the dashed line reflects baseline level. **(B,C)** Spectra for stimulation **(B)** and sham **(C)** group aligned on IAF and averaged over subjects. **(D)** Time course of normalized power in the individual alpha band for stimulation and sham group. Shaded areas around the lines depict SEM, the dashed line reflects baseline level.

of the 3 min blocks. The obtained p-values are illustrated in Figure 2.4A. The corresponding effect sizes (Cohen's d) are shown in Figure 2.4B. Most of the comparisons yielded significant or very close to significant differences between groups, however during the first 20 comparisons time bin 1 (0–3 min post-tACS) and 14 (39–42 min post-tACS) clearly failed to reach significance. After around 70 min several comparisons exhibit non-significant results supporting the corresponding ANOVA results by showing that the aftereffect begins to vanish around this time period.

2.5 Discussion

The current study aimed to elucidate the time course and duration of the tACS aftereffect in the alpha band beyond 30 min after stimulation. Results successfully replicate the aftereffect reported by Neuling et al. (2013) during the first 30 min after tACS and demonstrate the group difference between stimulation and sham group to persist up to 70 min. However, this diminishing group effect is due to a natural alpha rise in the sham group rather than a decrease of alpha power back to baseline level in the stimulation group. The findings are in line with studies investigating electrophysiological correlates of vigilance, time on task and mental fatigue reporting an increase in alpha power over

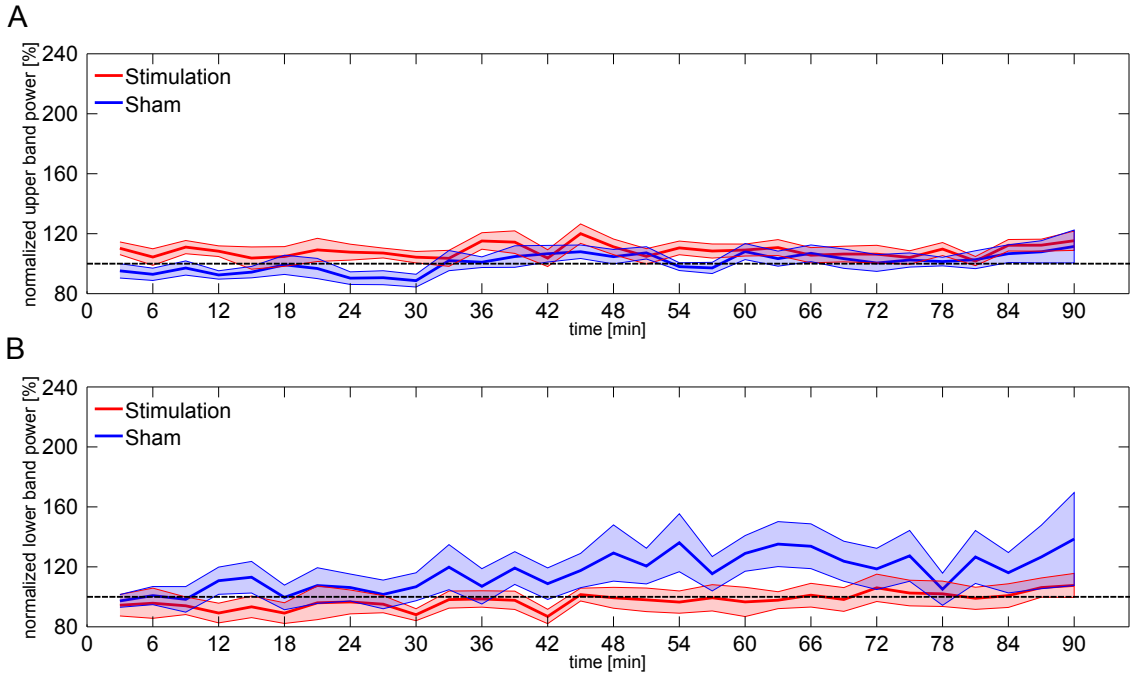

Figure 2.3: Power change in upper and lower frequency bands. (A) Time course of normalized power in the upper frequency band 3–5 Hz above participants IAF. Shaded areas around the lines reflect SEM, dashed line reflects baseline level. **(B)** Time course of normalized power in the lower frequency band 3–5 Hz below participants IAF. Shaded areas around the lines reflect SEM, dashed line reflects baseline level.

time, especially at occipital and parietal electrode sides (Boksem et al., 2005; Cajochen et al., 1995; Daniel, 1967; Oken, Salinsky, and Elsas, 2006). In summary, these results suggest alpha power is unlikely to fall back to baseline for neither stimulation nor sham group during any of the commonly used vigilance paradigms which have been used to investigate the aftereffect in the alpha band (Neuling et al., 2013; Vossen et al., 2015; Zaehle et al., 2010). This emphasizes the importance of carefully chosen criteria for the definition of the aftereffect which can be either compared to its own pre stimulation baseline or to a sham condition. In the case of alpha band stimulation it is more reasonable to define the aftereffect as the difference between stimulation and sham group instead of the difference to a pre-stimulation baseline since the latter does not account for participants' natural alpha increase.

By comparing stimulation and sham group in smaller time bins the current study tried to reveal further insights into the time course of the stimulation aftereffect. The effect appears to build up during the first minutes of the post-tACS measurement and stabilizes afterwards. Espeacially in the first time bin which samples alpha power within the first 3 min after tACS the aftereffect appears to be relatively weak, if present at all (Figures 2.2D, 2.4). A similar pattern can also be found in the data of Neuling et al. (2013) but has neither been analyzed nor described in more detail there since the time course of alpha power in the stimulation group was only tested against baseline and

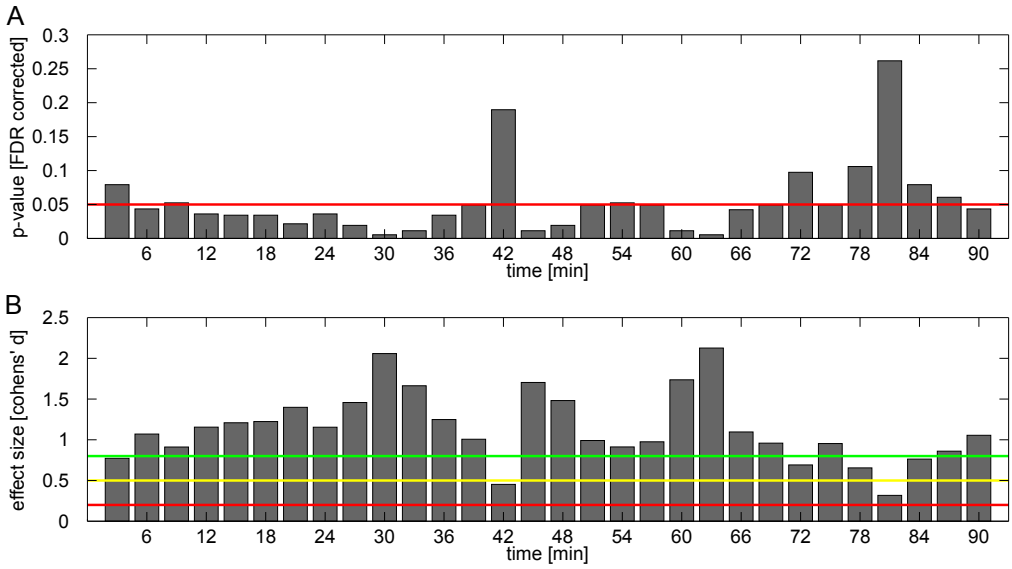

Figure 2.4: Results of post hoc analysis. (A) FDR corrected p-values for the comparison of normalized IAF band power between stimulation and sham group for each time bin. Red line depicts 0.05 significance boundary. **(B)** Corresponding effect sizes (Cohen's d) for each of the comparisons. Colored lines depict suggestions for small (d = 0.2; red line), medium (d = 0.5; yellow line) and large (d = 0.8, green line) effects given by Cohen (1992).

not compared to the corresponding time course of the sham group. This observation provides further support for the idea that on- and offline effects of tACS reflect distinct processes (Veniero et al., 2015; Vossen et al., 2015). While attempts to measure the online effects of tACS in humans and animal data suggest entrainment as the core underlying mechanism during tACS (Fröhlich and McCormick, 2010; Helfrich, Schneider, et al., 2014; Neuling et al., 2015; Witkowski et al., 2016), data from offline measurements and neural-network simulations favor mechanisms of synaptic plasticity, e.g., spike timing dependent placticity, to account for aftereffects (Neuling et al., 2013; Veniero et al., 2015; Vossen et al., 2015; Zaehle et al., 2010). On the other hand, there is some evidence which suggests that online and aftereffects are not completely indepent. For example Helfrich, Knepper, et al. (2014), Helfrich, Schneider, et al. (2014) demonstrated correlations between the strength of online entrainment with aftereffect strength. It seems plausible to assume that an online effect of entrainment is necessary before an offline effect of synaptic plasticity can be observed. Further insights into the underlying physiological procesess during and after tACS could be achieved by adapting the approach of Nitsche, Fricke, et al. (2003). By selectively blocking sodium and calcium channels as well as NMDA receptors by pharmacological treatment they were able to demonstrate the involvement of calcium and sodium channels in the generation of online- and aftereffects of anodal transcranial direct current stimulation (tDCS) but not of cathodal tDCS as well as an additional involvement of NMDA receptors in the generation of both cathodal and anodal tDCS aftereffects. A similar role of

NMDA receptors after tACS application would be particularly interesting because these receptors are involved in procesees of synaptic placticity such as long-term potentiation and long-term depression (Bennett, 2000; Luscher and Malenka, 2012; Nitsche, Fricke, et al., 2003).

Interestingly, within the time bin 39–42 min after stimulation the aftereffect in the current study appears to collapse and immedeately build up again. From the data at hand it remains unclear which mechanism accounts for this phenomenon or whether it is a random effect resulting from participants waxing and waning in alpha power. However, single subject time courses in the stimulation group quite consistently exhibit negative slopes around this time bin. During the subsequent minutes the effect builds up again until it begins to vanish after around 70 min as indicated by several subsequent t-tests failing to reach significance. This duration falls approximately in the same range as aftereffects reported for tDCS evaluated by means of motor-evoked-potentials, which last up to 60 min for cathodal tDCS (Nitsche, Nitsche, et al., 2003) and up to 90 min for anodal tDCS (Nitsche and Paulus, 2001).

The current study provides first evidence for the development and total duration of the tACS aftereffect in the alpha band. However, the results can only provide a first step towards understanding the dynamics and long term effects of tACS. For example, it remains unclear how far stimulation parameters like stimulation duration, intensity and matching between stimulation and individual peak frequency in the targeted frequency band affect duration and amplitude of the aftereffect. Two recent studies pointed out the importance of stimulation duration for the successful production of an aftereffect (Strüber, Rach, Neuling, and Herrmann, 2015; Vossen et al., 2015). Furthermore, one of the studies found correlations between the mismatch between stimulation and individual peak frequency and aftereffect (Vossen et al., 2015). But so far these relationships have not been systematically investigated. For tDCS an almost linear relationship between stimulation duration and aftereffect duration has been demonstrated (Nitsche and Paulus, 2001; Nitsche, Nitsche, et al., 2003) as well as an increase of aftereffect strength with stimulation amplitude (Nitsche and Paulus, 2000). Additionally, some authors emphasized the role of the brain state during which tACS is applied (Kar and Krekelberg, 2014; Kar, 2015; Neuling et al., 2013). According to these authors stimulation is only effective in modulating behavior and physiology when applied during a brain state involving the stimulated frequency band. These aspects are crucial since deviations in stimulation parameters as compared to the ones used in the current study, especially weaker intensities or shorter durations, might lead to weaker and/or shorter aftereffects or, in the worst case, to no effect at all. On the other hand, despite the vanishing difference between stimulation and sham group 70 min after stimulation in the current results, it cannot be ruled out that plastic changes induced by tACS might persist on

even larger scales of hours or even days. Long term measurements including several measurements for example within the course of a week could shed light on this question.

2.6 Acknowledgements

This work was supported by a Grant of the German Research Foundation (DFG, SPP1665) to CSH.

Chapter 3

Study II: Transcranial Alternating Current Stimulation (tACS) Enhances Mental Rotation Performance during and after Stimulation

Published as:

Kasten, FH.,Herrmann, CS., (2017) Transcranial Alternating Current Stimulation (tACS) Enhances Mental Rotation Performance during and after Stimulation. *Frontiers in Human Neuroscience*., 11:2.

Author Contributions:

Designed research: FHK, CSH

Perfomed Research: FHK

Analyzed Data: FHK

Wrote paper: FHK, CSH

3.1 Abstract

Transcranial alternating current stimulation (tACS) has been repeatedly demonstrated to modulate endogenous brain oscillations in a frequency specific manner. Thus, it is a promising tool to uncover causal relationships between brain oscillations and behavior or perception. While tACS has been shown to elicit a physiological aftereffect for up to 70 min, it remains unclear whether the effect can still be elicited if subjects perform a complex task interacting with the stimulated frequency band. In addition, it has not yet been investigated whether the aftereffect is behaviorally relevant. In the current experiment, participants performed a Shepard-like mental rotation task for 80 min. After 10 min of baseline measurement, participants received either 20 min of tACS at their individual alpha frequency (IAF) or sham stimulation (30 s tACS in the beginning of the stimulation period). Afterwards another 50 min of post-stimulation EEG were recorded. Task performance and EEG were acquired during the whole experiment. While there were no effects of tACS on reaction times or event-related-potentials (ERPs), results revealed an increase in mental rotation performance in the stimulation group as compared to sham both during and after stimulation. This was accompanied by increased ongoing alpha power and coherence as well as event-related-desynchronization (ERD) in the alpha band in the stimulation group. The current study demonstrates a behavioral and physiological aftereffect of tACS in parallel. This indicates that it is possible to elicit aftereffects of tACS during tasks interacting with the alpha band. Therefore, the tACS aftereffect is suitable to achieve an experimental manipulation.

3.2 Introduction

Transcranial alternating current stimulation (tACS) is a relatively novel method that has been demonstrated to modulate endogenous brain oscillations in a frequency specific manner (Helfrich, Schneider, et al., 2014; Herrmann et al., 2013; Reato et al., 2013). By applying weak sinusoidal currents on the scalp, tACS is thought to entrain spontaneous brain oscillations in the range of the stimulation frequency, rendering it a promising tool to investigate causal relationships between these oscillations and cognitive functions (Antal and Herrmann, 2016; Fröhlich, 2015; Herrmann, Murray, Ionta, Hutt, and Lefebvre, 2016; Thut, Schyns, and Gross, 2011). Numerous studies investigated effects of tACS on perception (Kanai, Chaieb, Antal, Walsh, and Paulus, 2008; Laczó et al., 2012; Strüber et al., 2014), behavior (Antal et al., 2008; Brignani et al., 2013; Sela et al., 2012) and cognitive functions (Chander et al., 2016; Lustenberger, Boyle, Foulser, Mellin, and Fröhlich, 2015; Vosskuhl et al., 2015). A recent meta-analysis found tACS to reliably induce enhancing effects on cogni-

tive performance and perception with overall effect sizes in the small to moderate range (Schutter and Wischnewski, 2016). Furthermore, they found individually tailored, EEG guided stimulation frequencies (i.e., at participants' individual alpha frequency, IAF) and anterior-posterior montages with intensities larger or equal to 1 mA to be beneficial for the size of the stimulation effect (Schutter and Wischnewski, 2016).

Directly monitoring physiological effects of tACS during application remains challenging due to the massive artifact that is introduced to the M/EEG signals. First attempts to reconstruct brain activity during tACS have been made using a variety of methods. For example, Helfrich, Schneider, et al. (2014) applied a combination of template subtraction and principal component analysis (PCA). Neuling et al. (2015) reconstructed MEG signals using a linearly constrained minimum variance beamformer filter. Other researches applied alternative waveforms for stimulation such as sawtooths (Dowsett and Herrmann, 2016) or amplitude modulated sine waves (Witkowski et al., 2016). However, some of these methods have not been without criticism (Noury et al., 2016). While most behavioral studies rely upon online effects of tACS on behavioral measures, a large proportion of physiological studies conducted in humans measured outlasting effects of tACS in the EEG. This aftereffect is consistently reported for a variety of measures and frequency bands (Helfrich, Knepper, et al., 2014; Neuling et al., 2013; Vossen et al., 2015; Wach et al., 2013a); for an overview see Veniero et al., 2015) and has recently been demonstrated to last for up to 70 min after stimulation in the alpha band (Kasten, Dowsett, and Herrmann, 2016). Considering this long lasting effect, it is desirable to make use of the aftereffect in experimental designs offering the opportunity to measure artifact-free M/EEG signals in parallel to task performance without the need for sophisticated procedures for artifact removal. However, up to now the aftereffect has merely been observed in isolation while subjects performed simple auditory or visual vigilance tasks causing as little interference with the stimulated brain oscillation as possible (Kasten et al., 2016; Neuling et al., 2013; Vossen et al., 2015; Zaehle et al., 2010). Thus, it remains unclear whether a similar aftereffect can still be induced (or measured) if participants are engaged in a more complex task, causing stronger modulations of the stimulated frequency bands themselves. It is known, for example, that task complexity and cognitive load modulate event-related-desynchronization (ERD) patterns in the alpha band (Boiten, Sergeant, and Geuze, 1992; Dujardin, Bourriez, and Guieu, 1995; van Winsun, Sergeant, and Geuze, 1984). Furthermore, it is largely unclear whether the elicited physiological changes affect behavioral measures such as reaction times or task performance. This is especially crucial for clinical applications of tACS where long lasting stimulation effects are required to effectively recover dysfunctional oscillations, which are implicated in several neurological and psychiatric conditions (Herrmann and Demiralp, 2005; Uhlhaas

and Singer, 2006, 2012).

The current study aimed to measure both behavioral and physiological aftereffects of tACS while participants performed a mental rotation task as introduced by Shepard and Metzler (1971). Since their groundbreaking experiment, mental rotation has been excessively studied. One of the first and most robust findings was the almost linear relationship between reaction times and rotation angle which has been shown to be independent of stimulus complexity and the dimension in which the object has to be rotated (Cooper, 1975; Shepard and Metzler, 1971). Furthermore, mental rotation is one of the few domains where sex differences are consistently reported, suggesting that males tend to outperform females (Linn and Petersen, 1985; Voyer, Voyer, and Bryden, 1995). Mental rotation performance is widely used as a measure of cognitive performance and has been linked to alpha and theta oscillations in human M/EEG (Doppelmayr et al., 2002; Hanslmayr, Sauseng, Doppelmayr, Schabus, and Klimesch, 2005; Johnson and Bouchard, 2005; Klimesch et al., 2003). While theta oscillations appear to synchronize during mental rotation, alpha oscillations desynchronize as compared to a reference period prior to stimulus onset (Klimesch, Sauseng, and Hanslmayr, 2007; Michel, Kaufman, and Williamson, 1994). A phenomenon referred to as ERD/ERS (event-related desynchronization/synchronization). Stronger ERD in the alpha band has been shown to be related to higher cognitive performance especially in visual-spatial and memory tasks (Doppelmayr et al., 2002; Klimesch, 1999; Neubauer, Freudenthaler, and Pfurtscheller, 1995). Michel et al. (1994) found the duration of ERD during mental rotation to increase with the angle objects have to be mentally rotated. Additional evidence supporting the functional role of alpha desynchronization during mental rotation arises from studies using neurofeedback training (NFT) and repetitive transcranial magnetic stimulation (rTMS). In these studies, ERD in the alpha band was increased by enhancing alpha power in a reference period before stimulus onset (Hanslmayr et al., 2005; Klimesch et al., 2003; Zoefel, Huster, and Herrmann, 2011). While the NFT experiments utilized posterior electrodes to provide feedback about subjects alpha activity (Hanslmayr et al., 2005; Klimesch et al., 2003; Zoefel et al., 2011) applied rTMS over the frontal and right parietal cortex. The elicited changes on participants' alpha power/ERD were accompanied by enhanced task performance. In contrast, reaction times were not affected in these experiments. In summary, results suggest that on the one hand mental rotation performance depends on neural oscillations in the alpha band and their desynchronization during task execution. On the other hand, the desynchronization of alpha oscillations during task execution constitute regular modulations/distortions of alpha oscillations. Those can possibly distort or shorten tACS induced aftereffects. Due to these physiological properties, mental rotation is well suited to evaluate the robustness of the tACS aftereffect (the possibility to induce aftereffects in the

presence of strong interference in the stimulated frequency band). It should be noted, however, that the current study did not aim to systematically evaluate the effect of different degrees of complexity on the tACS aftereffect, but rather tested whether the effects reported during resting measurements can in principle also be induced in a more complex setting.

In order to achieve a broad characterization of the physiological and behavioral changes following tACS, the current study carried out various measures to quantify the aftereffect of tACS. Besides task performance and reaction times, we analyzed ongoing alpha power during mental rotation and resting periods as well as the mean magnitude squared coherence of ongoing alpha activity. Both measures have been used to quantify outlasting effects of tACS in the past. Several studies found increased alpha power after tACS (Kasten et al., 2016; Neuling et al., 2013; Vossen et al., 2015; Zaehle et al., 2010) during resting state measurements. We expected similar patterns in our experiment during mental rotation and during resting periods. With regard to coherence, Neuling et al. (2013) and Helfrich, Knepper, et al. (2014) reported outlasting effects of tACS on interhemispheric coherence. However, Neuling et al. (2013) found this effect only during eyes-closed measurement but not during eyes-open and suggested tACS effects to depend on brain-state. In the current analysis we tested whether interhemispheric coherence is increased for a subset of EEG electrodes during mental rotation. In addition, we evaluated event-related measures namely ERD in the alpha band and event-related potentials (ERPs). By increasing ongoing alpha power we also expected ERD in the alpha band to be increased after tACS compared to sham, as there is higher alpha power to desynchronize from when a stimulus is presented. We hypothesized this increase in ERD to be accompanied by enhanced performance in the mental rotation task in the stimulation group as compared to sham, but no changes in reaction times. However, for performance during tACS we expected a different pattern. Recent experiments (Neuling et al., 2015; Vosskuhl et al., 2016) suggested decreased ERD in the alpha band in response to visual stimulation during the application of tACS. Unfortunately, this was not explicitly tested or just indirectly inferred from reduced event-related BOLD response, respectively. Thus, these findings have to be interpreted with caution. Nevertheless, based on the available, albeit sparse evidence and the principles of entrainment, it seems reasonable to hypothesize tACS to reduce or overwrite ERD by entraining oscillations before and after stimulus presentation. Thus, we supposed performance in the mental rotation task to be reduced in the stimulation group compared to sham during the application of tACS due to this reduction in ERD. The analysis of ERPs was rather exploratory. However, latency and amplitude of P1 and N1 components of ERPs have been demonstrated to be (at least in part) generated by evoked oscillations in the alpha range (Gruber, Klimesch, Sauseng, and Doppelmayr, 2005; Klimesch, Hanslmayr, et al., 2007). Thus, the amplitude of these

components might be enhanced after tACS in the alpha band.

3.3 Materials and Methods

Twenty-three healthy subjects reporting no history of neurological or psychiatric disease received either 20 min of tACS or sham stimulation during the experiment (Figure 3.1A). Participants were medication-free at the day of measurement and gave written informed consent prior to the experiment. They were especially informed about the applied methods (EEG/tACS) and potential risks of the electrical stimulation. After signing the consent form participants filled out a questionaire assessing exclusion criteria for the experiment (especially psychiatric and neurological conditions and metal items/implants inside or outside the head). All were right-handed according to the Edinburg handedness-scale (Oldfield, 1971). Subjects were randomly assigned to either stimulation or sham group. Both groups were counterbalanced for participants' sex and time of measurement (sessions started at 10 AM or 2 PM). Data from six subjects had to be discarded. Two datasets were corrupted due to technical difficulties, three participants did not comply with the instructions or exhibited chance-level performance in the mental rotation task. A recent study suggested tACS to be only effective with low baseline power in the to-be stimulated frequency band (Neuling et al., 2013). To avoid non-responsiveness to the stimulation due to such ceiling effects, power in the IAF $\pm$ 2 Hz band during the baseline measurement was z-transformed. One subject exhibited a z-score above 1.65 (corresponding to an α-level < 0.05, one-tailed) and was excluded from further analysis. Thus, 17 participants (8 females, age: 23.41 $\pm$ 3.28 years) remained for analysis (9 in sham, 8 in stimulation group). The experiment was approved by the local ethics committee at the University of Oldenburg and conducted in accordance with the declaration of Helsinki.

3.3.1 EEG

Participants were seated in a recliner in an electrically shielded, dark room. EEG was acquired from 24 active Ag-AgCl Electrodes (ActiCap, Brain Products, Gilching, Germany), following the international 10–10 system. Electrode positions close to stimulation electrodes were left blank (Figure 3.1B). Ground electrode was placed at AFz. Position Fp1 served as reference which is the standard configuration of the ActiCap system. In addition, a vertical EOG was recorded from an electrode below the right eye. All impedances were kept below 20 kΩ. Data were digitized at a rate of 10 kHz using a 24-bit ActiChamp amplifier and stored on a computer using BrainVision PyCorder software (both Brain Products, Gilching, Germany).

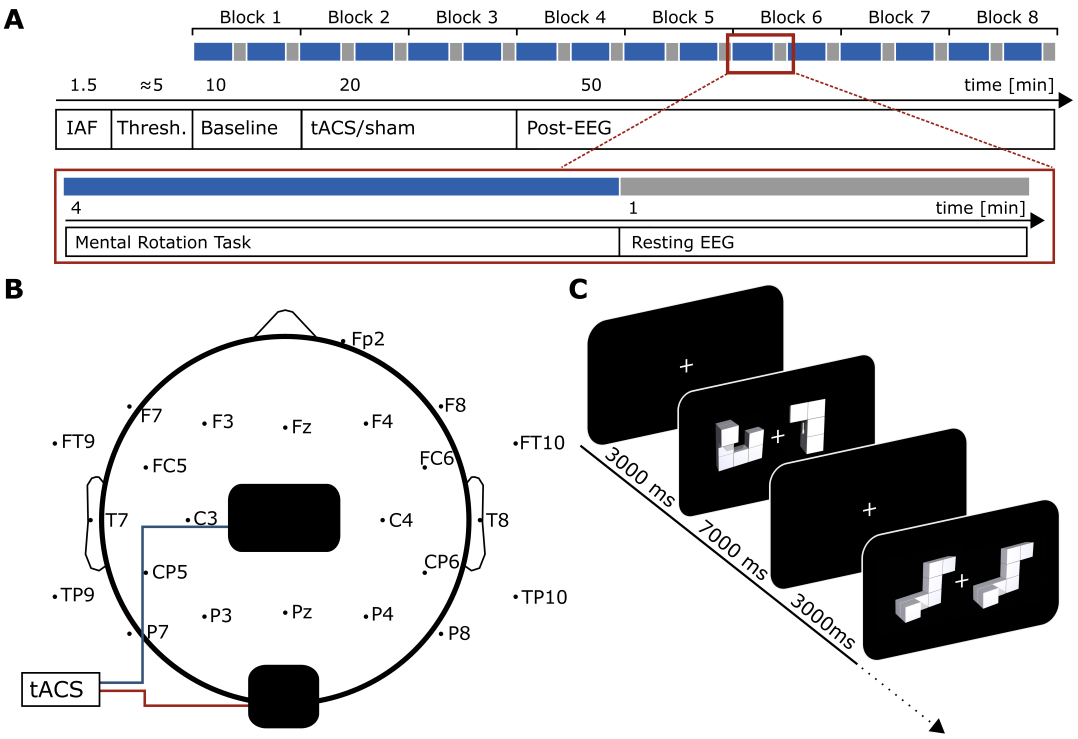

Figure 3.1: Experimental Design. (A) Time-course of the experiment. In the beginning, 90 s of eyes-closed EEG was recorded to determine participants individual alpha frequency (IAF). Afterwards, tACS intensity was adjusted to participants' sensation threshold before the actual experiment started. First, 10 min of baseline measurement were acquired. During the whole experiment participants performed a mental rotation task intermitted by 1 min resting EEG every 24 trials (4 min, red box, blue indicates mental rotation period, gray resting EEG). During resting EEG, participants performed a visual vigilance task. Each block consisted of two mental rotation and two resting periods. The baseline measurement was followed by 20 min of tACS or sham stimulation and 50 min of post-stimulation EEG. **(B)** Electrode setup. tACS electrodes (black) were positioned centered above Cz and Oz. EEG was measured from 23 positions following the international 10-10 system with electrode sites above or close to tACS electrodes left blank. **(C)** Mental rotation task. Each trial started with the presentation of a white fixation cross at the center of the screen. After 3000 ms the mental rotation stimulus display (taken from Ganis and Kievit, 2015) appeared and remained on screen for another 7000 ms. During this time, participants were asked to judge whether the two presented figures were identical (but rotated) or different. The first display contains an example for a target differing from the cue, the second for a target similar to the cue.

Prior to the main experiment, 90 s of eyes-closed resting EEG were recorded to determine participants' IAF, which was later used as stimulation frequency. EEG was split into 1 sec segments and fast Fourier transformations (FFTs) were computed on the epochs. The resulting frequency-spectra were averaged and the power peak in the 8–12 Hz range at electrode Pz was used as stimulation frequency. If no peak was evident the measurement was repeated. After stimulation intensity was adjusted to participants' sensation threshold (see "Electrical Stimulation" Section), the main-experiment started. The experiment consisted of 10 min baseline measurement, 20 min tACS or sham stimulation and another 50 min of post-stimulation EEG measurement (Figure 3.1A). Participants performed a mental rotation task similar to the classic experiment of Shepard and Metzler (1971) intermitted by 1 min resting periods throughout the experiment (Figures 3.1A,C).

3.3.2 Electrical Stimulation

tACS was delivered by a battery-operated stimulator system (DC Stimulator Plus, Neuroconn, Illmenau, Germany). Two surface conductive rubber electrodes were attached to participants' scalp using an adhesive, electrically conductive paste (ten20 conductive paste, Weaver and Co., Aurora, CO, USA). Electrodes were positioned centered above Cz (5 cm $\times$ 7 cm) and Oz (4 cm $\times$ 4 cm; Figure 3.1B). This montage has been shown to achieve highest current densities in posterior brain regions in modeling studies (Neuling, Wagner, et al., 2012) and has successfully been used in previous studies to elicit aftereffects in the alpha band (Kasten et al., 2016; Neuling et al., 2013). Furthermore, previous experiments using TMS or NFT targeted similar brain areas to enhance mental rotation performance (Hanslmayr et al., 2005; Klimesch et al., 2003; Zoefel et al., 2011). The sinusoidal current was digitally generated using Matlab 2012b (The MathWorks Inc., Natick, MA, USA), send to a digital-analog converter (Ni USB 6229, National Instruments, Austin, TX, USA) and streamed to the remote input of the stimulator. Electrode impedance was kept below 10 kΩ. Participants were stimulated at their IAF (9.82 Hz $\pm$ 1.2 Hz) with intensities adjusted to their individual sensation threshold (900 μA $\pm$ 335 μA); defined as the highest intensity at which participants' did not notice the stimulation (i.e., no phosphene or skin sensation). The thresholding was performed to rule out confounding effects of sensations such as phosphenes or tingling during stimulation. After 10 min of baseline measurement the stimulation group received 20 min of tACS with 10 s fade-in and fade-out in the beginning and the end of the stimulation. While all other parameters were kept the same, the sham group received only 30 s of tACS (including 10 s fade-in and fade-out) at the beginning of the stimulation period.

3.3.3 Mental Rotation Task

Before, during and after stimulation, participants performed a mental rotation task similar to the original experiment of Shepard and Metzler (1971). The task was presented on a computer screen (Samsung SyncMaster P247GH, 1920 $\times$ 1080 pixels, 60 Hz refresh rate) at a distance of approximately 100 cm using Psychtoolbox 3 (Kleiner et al., 2007) running on Matlab 2012b (The MathWorks Inc., Natick, MA, USA). Stimuli were taken from a recently published open-source stimulus-set (Ganis and Kievit, 2015) consisting of 48 three-dimensional objects and a total of 384 stimulus displays. Each display contains a cue object on the left and a target object on the right side which is rotated by either 0, 50, 100 or 150° on the vertical axis. The target object can be either identical to the cue (but rotated) or different; i.e., mirrored or partly mirrored in addition to the rotation, such that the two figures cannot be brought in alignment by solely rotating them (see Ganis and Kievit, 2015 for

detailed descriptions and example figures). Stimuli were presented randomly in eight blocks each comprised of 48 stimulus displays (800 $\times$ 427 pixels) with the constraint that each block contained equal numbers of rotation angles and displays containing identical and different objects. All trials started with the presentation of a fixation cross at the center of the screen. After 3000 ms a stimulus display was presented and remained on screen for 7000 ms (Figure 3.1C). Participants were asked to judge whether the target stimulus was identical or different to the cue by pressing a button with their left (identical) or right (different) index finger. They were instructed to answer as fast and accurate as possible. The time window to respond was equal to the duration of the stimulus presentation.

Every 24 trials the mental rotation task was interrupted by a 1 min resting period. To ensure participants remained attentive, a visual vigilance task similar to previous studies (Kasten et al., 2016; Zaehle et al., 2010) was implemented. A fixation cross was presented at the center of the screen and rotated by 45° for 500 ms. Stimulus onset was jittered between 30 and 40 s after beginning of the trial. Participants had to react to the rotation by pressing one of the response buttons within 2 s after stimulus onset.

The first block (48 trials) served as baseline measurement before stimulation, the two subsequent blocks (96 trials) were performed during the application of tACS or sham stimulation. The remaining five blocks (240 trials) served as post-stimulation measures of mental rotation performance. In total the experiment had a duration of approximately 80 min (Figure 3.1A).

3.3.4 Debriefing

After finishing the experiment, participants filled out a translated version of an adverse effects questionnaire evaluating commonly reported side-effects of transcranial electrical stimulation (TES; Brunoni et al., 2011). Participants had to rate the intensity of adverse effects (1—none, 2—mild, 3—moderate, 4—severe) and how much they were related to the stimulation (1—none, 2—remote, 3—probable, 4—definite). Subsequently, subjects were ask to guess whether they received actual tACS or sham stimulation to ensure they were naive towards their assigned experimental condition. All of them were informed about their experimental condition immediately afterwards.

3.3.5 Data Analysis

Data analysis was performed using Matlab 2016a (The MathWorks Inc., Natick, MA, USA) and the Fieldtrip toolbox (Oostenveld et al., 2011). For statistical analysis, R 3.2.3 (R Foundation for Statistical Computing, Vienna, Austria) was used.

3.3.5.1 Behavioral Data

Participants' performance was calculated separately for each block (48 trials, 10 min blocks). Performance during and after stimulation was normalized by performance before tACS to account for inter-individual differences. The resulting percentage values reflect performance increase during each 10 min block relative to baseline. A repeated measurements analysis of variance (rmANOVA) with the within factor block (7 levels, 2 during stimulation, 5 after stimulation) and the between factor condition (2 levels; stimulation vs. sham) was computed. Furthermore, the between factor sex (2 levels) was included to account for possible sex differences.

Reaction times (RTs) were analyzed in a similar manner. To account for the known increase in RTs with larger rotation angles, RTs were first averaged separately for each angle in each block and then normalized with their respective pre-stimulation baseline. Subsequently the normalized RTs were averaged over rotation angles such that the resulting values reflect relative change in RTs over all angles with respect to baseline for each 10 min block. Normalized RTs were finally fed into a rmANOVA with the within factor block (7 levels) and the between subject factors condition (2 levels, stimulation vs. sham) and sex (2 levels, males vs. females).

3.3.5.2 EEG

EEG data were resampled to 500 Hz and filtered between 0.3 and 100 Hz. An independent-component-analysis (ICA) was computed on tACS-free EEG signals. ICs reflecting horizontal or vertical eye movements were visually identified and rejected before backprojecting the data into sensor space. EEG data acquired during mental rotation and rest were analyzed separately. Physiological data, acquired during stimulation were not further analyzed due to the large tACS artifact.

To analyze ongoing changes in alpha power each of the pre- and post-stimulation blocks were subdivided into 5 min blocks, such that they consisted of 4 min of mental rotation task and 1 min of resting EEG. This was done to achieve higher temporal resolution of the time-course of ongoing alpha activity. Data during both conditions were analyzed separately. First EEG in each block was segmented into 1 s epochs. Subsequently, a FFT (hanning window, 2 s zero padding) was computed for each segment. Epochs containing residual artifacts were rejected and power-spectra of the first 200 artifact-free segments during mental rotation and the first 43 artifact-free segments during rest were averaged for each of the 5 min blocks. Power in the IAF band (IAF $\pm$ 2 Hz) was calculated from the averaged spectra in each block. IAF band power in the post stimulation blocks were normalized by IAF band power during the first 5 min before stimulation (normalization was applied separately

for mental rotation and resting data). In accordance with previous approaches (Kasten et al., 2016; Neuling et al., 2013; Zaehle et al., 2010) we focused on electrode Pz for subsequent analysis. In addition mean magnitude squared coherence (Equation 3.1) in the individual alpha band (IAF $\pm$ 2 Hz) between electrode pairs P3-P4 and P7-P8 was calculated for the mental rotation blocks. Coherence in the post-stimulation blocks was normalized by coherence in the pre-stimulation baseline.

$$coh_{xy} = \frac{|S_{xy}(\omega)|}{\sqrt{S_{xx}(\omega)S_{yy}(\omega)}} \tag{3.1}$$

The magnitude squared coherence for a given frequency (ω) is the function of the power spectral densities of two signals $S_{xx}(\omega)$ and $S_{yy}(\omega)$ and their cross power spectral density ($S_{xy}(\omega)$). The resulting coherence value ranges between 0 (no coherence) and 1 (perfect coherence; Bastos and Schoffelen, 2016). Relative IAF band power and relative coherence were fed into a rmANOVA with within factor block (9 levels) and between factors condition (2 levels) and sex (2 levels). In recent experiments the aftereffect appears to take some minutes until it fully builds up (Kasten et al., 2016; Neuling et al., 2013). Thus, the first block after stimulation was discarded from analysis. To ensure that the effect of tACS is frequency specific and not due to an increase in power in all frequency bands (i.e., caused by changes in impedances), two frequency bands below and above participants individual alpha band were analyzed the same way as described above. For that purpose we choose a lower band from IAF - 6 Hz to IAF - 3 Hz and an upper band from IAF + 3 to IAF + 6.

To capture event-related changes during the mental rotation task EEG was segmented into 10 s epochs starting 3 s before and ending 7 s after onset of the mental rotation stimulus. Event related alpha synchronization/desynchronization (ERS/ERD) was calculated for each trial. Pfurtscheller and Lopes Da Silva (1999) defined ERD/ERS as:

$$ERD/ERS = \frac{R - A}{R} * 100 \tag{3.2}$$

where A is the power in the frequency band of interest after stimulus presentation (test period) and R is the power during a reference period preceding stimulus presentation (Pfurtscheller and Lopes Da Silva, 1999). Positive values indicate ERD during the test period, negative values reflect ERS. Three seconds immediately before and after stimulus onset served as reference and test periods, respectively. Alpha power in both time windows was estimated by computing FFTs on a hanning-

tapered sliding window with a fixed length of 1 s moving in steps of 50 ms along each trial. Power in the IAF band (IAF $\pm$ 2 Hz) was averaged over the resulting 60 samples for reference and test period. ERD values were computed according to Equation 3.1. ERD values were averaged over trials in each block for each subject and normalized by pre-stimulation baseline. The resulting relative ERD values were fed into a rmANOVA with within factor block (5 levels) and between factors group (2 levels) and sex (2 levels). Please note that for this analysis only blocks after tACS or sham stimulation have been used. Thus, the factor time includes only five levels.

Furthermore, ERPs were calculated for the pre- and post-stimulation periods. To this end, EEG measured at electrodes P7 and P8 was segmented from -0.2 s before to 1 s after the onset of the mental rotation stimulus. Data were baseline corrected by subtracting the mean voltage of the 200 ms interval before stimulus onset from all data points. A low pass-filter at 20 Hz was applied. Artifact-free ERPs were averaged for pre- and post-stimulation periods and over electrodes. For analysis, amplitudes and latencies of three prominent ERP components were extracted from each subject, namely P100, N170 and P300. In contrast to frequency domain analysis post-stimulation data were not normalized by pre-stimulation data, instead pre- and post-stimulation ERPs were compared directly using a rmANOVAs with factors condition (2 levels), sex (2 levels) and block (2 levels).

3.4 Results

3.4.1 Debriefing

The most frequently reported side-effects (intensity rated 2 or higher) after the experiment were sleepiness (70.6%) and trouble concentrating (64.7%). Although a relatively large proportion of participants associated these adverse effects with the stimulation (47.1% rated sleepiness, 41.2% rated trouble concentrating higher than 2), Wilcoxon rank sum test revealed no differences between groups for any of the ratings (all $p > 0.1$; uncorrected). About 76% of participants indicated that they had been stimulated after finishing the experiment. Fisher's exact test for count data revealed no significant difference between groups ($OR = 5.06, p = 0.29$), suggesting that participants were not aware of their actual experimental condition.

3.4.2 Mental Rotation Task

3.4.2.1 Performance

To ensure both groups started with similar performance, a Welch two-sample t-test was performed to test for differences in baseline performance between stimulation and sham group. The test revealed no significant differences in baseline performance ($t_{(12.18)} = -1.4, p = 0.18; M_{stim} = 84.37\%, SD = 8.4, M_{sham} = 89.35\%, SD = 5.7$).

Participants in the stimulation group exhibited significantly stronger increase in mental rotation performance after stimulation than the sham group ($F_{(1,13)} = 6.04, p = 0.029, \eta^2 = 0.27$; Figure 3.2A). As expected, data revealed an effect of sex. Female participants showed a stronger performance gain than males ($F_{(1,13)} = 5.88, p = 0.031, \eta^2 = 0.27$; Figure 3.2B). However, there was no interaction of the stimulation with participants' sex ($condition \times sex : F_{(1,13)} = 2.57p = 0.13, \eta^2 = 0.13$). Furthermore, a trend for block ($F_{(6,78)} = 2.46, p = 0.07, \eta^2 = 0.04$) has been found. However, please note the relatively small effect size. None of the other interactions reached significance ($condition \times block : F_{(6,78)} = 1.55, p = 0.21, \eta^2 = 0.023; sex \times block : F_{(6,78)} = 1.68, p = 0.18, \eta^2 = 0.024; condition \times block \times sex : F_{(6,78)} = 0.93, p = 0.44, \eta^2 = 0.013$). Overall, both experimental groups enhanced performance in the mental rotation task compared to baseline during and after stimulation (stimulation: $t_7 = 3.77, p = 0.007, d = 1.33; sham : t_8 = .16, p = 0.013, d = 1.05$).

Contrary to our hypothesis a separate rmANOVA exclusively testing performance during tACS revealed a trend towards increased performance for the stimulation group already during stimulation ($F_{(1,13)} = 3.47, p = 0.085, \eta^2 = 0.19$) instead of the predicted reduction in performance. Figure 3.2C illustrates the time course of mental rotation performance for stimulation and sham group.

3.4.2.2 Reaction Times

The rmANOVA on normalized reaction times revealed neither an effect of condition ($F_{(1,13)} = 0.21, p = 0.66, \eta^2 = 0.01$), sex ($F_{(1,13)} = 0.72, p = 0.41, \eta^2 = 0.04$) or block ($F_{(6,78)} = 1.61, p = 0.20, \eta^2 = 0.03$) nor any significant interaction ($condition \times sex : F_{(1,13)} = 1.32, p = 0.027, \eta^2 = 0.07; condition \times Block : F_{(6,78)} = 1.64, p = 0.18, \eta^2 = 0.03; sex \times block : F_{(6,78)} = 0.65, p = 0.60, \eta^2 = 0.01; condition \times sex \times block : F_{(6,78)} = 0.95, p = 0.43, \eta^2 = 0.02$). Overall, both groups significantly reduced their reaction times relative to baseline during and after stimulation ($stimulation : t_7 = 6.96, p < 0.001, d = 2.46; sham : t_8 = 5.90, d = 1.97$). For an overview of reaction time results see Figures 3.2D–F.

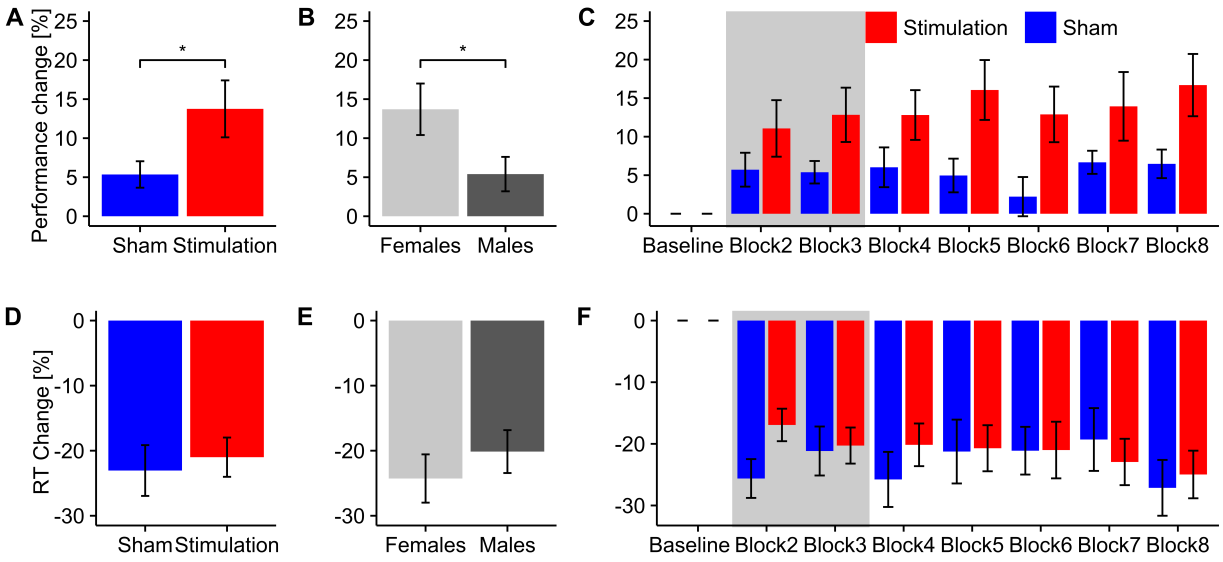

Figure 3.2: Behavioral Results. Top row: overall performance increase of the mental rotation task for **(A)** stimulation and sham group and **(B)** male and female subjects. Asterisks depicts significant differences ($* < 0.05$). Error bars depict SEM. **(C)** Time-course of the performance increase for stimulation and sham group. Gray background indicates blocks during which tACS or sham stimulation was applied. Bottom row: overall change in reaction times for **(D)** stimulation and sham group and **(E)** male and female subjects. **(F)** Time-course of reaction time changes for stimulation and sham group. Gray background indicates blocks during which tACS or sham stimulation was applied. Error bars depict SEM.

3.4.3 Electrophysiological Results

3.4.3.1 Ongoing EEG

Ongoing alpha power during mental rotation

The rmANOVA revealed a stronger increase in ongoing alpha power during mental rotation in the stimulation group compared to sham ($F_{(1,13)} = 4.68, p = 0.0496, \eta^2 = 0.21$, Figure 3.3A). Furthermore, there was a trend towards stronger power increase in the alpha band for female subjects compared to males ($F_{(1,13)} = 3.88, p = 0.07, \eta^2 = 0.18$, Figure 3.3B), as well as a significant effect of block ($F_{(8,104)} = 3.28, p = 0.002, \eta^2 = 0.06$). None of the interactions were significant ($condition \times sex$: $F_{(1,13)} = 0.07, p = 0.79, \eta^2 < 0.01; condition \times Block$: $F_{(8,104)} = 1.67, p = 0.11, \eta^2 = 0.02; sex \times block$: $F_{(8,104)} = 0.57, p = 0.80, \eta^2 = 0.01; condition \times sex \times block$: $F_{(8,104)} = 1.03, p = 0.42, \eta^2 = 0.02$). Post hoc t-tests against baseline revealed significantly increased alpha power during mental rotation in both groups ($stimulation$: $t_7 = 4.98, p < 0.001, d = 1.76; sham$: $t_8 = 3.45, p = 0.004, d = 1.15$). The time-course of ongoing alpha increase for stimulation and sham group is depicted in Figure 3.3C.

Average relative ongoing alpha power during mental rotation was significantly correlated with participants' increase in performance ($r = 0.56, t15 = 2.62, p = 0.02$; Figure 3.7A), but not with changes in reaction times ($r = 0.16, t15 = 0.63, p = 0.53$; Figure 3.7D).

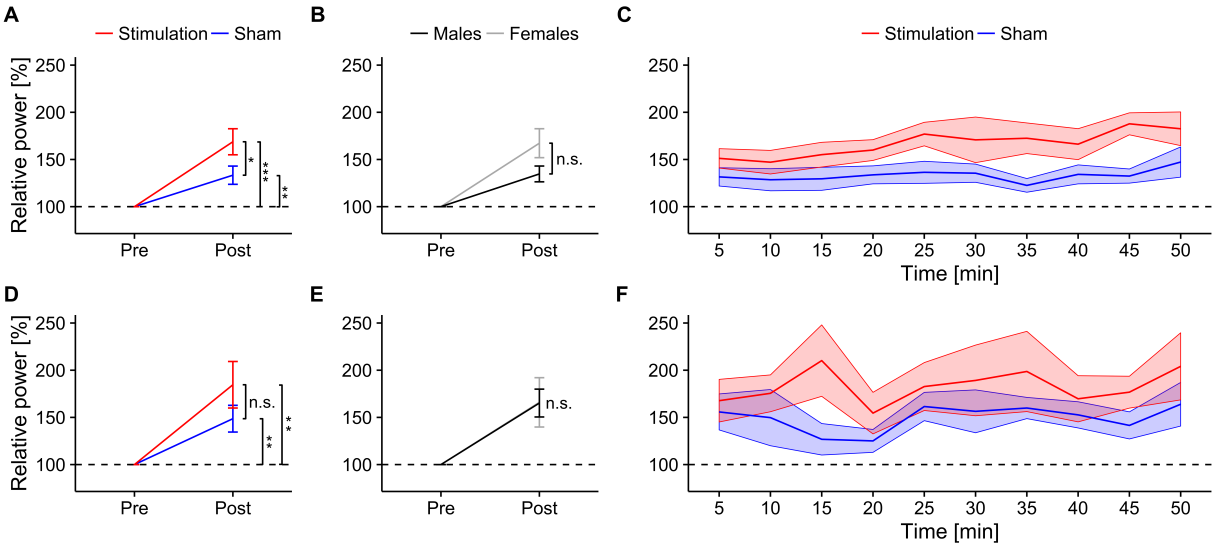

Figure 3.3: Ongoing alpha power. Top row: ongoing alpha power during mental rotation. Error bars and shaded areas depict SEM; asterisks code for significant differences ($* < 0.05, ** < 0.01, * * * < 0.001$). **(A)** Averaged relative alpha power after stimulation for stimulation and sham. **(B)** Averaged relative alpha power after stimulation for females and males. **(C)** Time-course of ongoing alpha power after stimulation for stimulation and sham group. Bottom row: ongoing alpha power during rest. **(D)** Averaged relative alpha power after stimulation for stimulation and sham. **(E)** Averaged relative alpha power after stimulation for females and males. **(F)** Time-course of ongoing alpha power after stimulation for stimulation and sham group.

To ensure frequency specific effects of the stimulation, a lower and an upper frequency band around the individual alpha band were analyzed. In the lower band, the rmANOVA only revealed a trend in the interaction between sex and block ($F_{(8,104)} = 2.99, p = 0.052, \eta^2 = 0.039$). None of the main effects or the other interactions reached significance ($condition: F_{(1,13)} = 1.24, p = 0.29, \eta^2 = 0.07, sex: F_{(1,13)} = 0.18, p = 0.68, \eta^2 = 0.01; block: F_{(8,104)} = 1.74, p = 0.18, \eta^2 = 0.023; condition \times sex: F_{(1,13)} < 0.01, p = 0.92, \eta^2 < 0.01; condition \times block: F_{(8,104)} = 0.47, p = 0.67, \eta^2 < 0.01; condition \times sex \times block: F_{(8,104)} = 1.19, p = 0.31, \eta^2 = 0.02$). The rmANOVA for the upper band revealed no significant main effects or interactions ($condition: F_{(1,13)} = 0.49, p = 0.50, \eta^2 = 0.02; sex: F_{(1,13)} = 0.01, p = 0.92, \eta^2 < 0.01; block: F_{(8,104)} = 1.25, p = 0.30, \eta^2 = 0.04; condition \times sex: F_{(1,13)} = 0.13, p = 0.73, \eta^2 < 0.01; condition \times block: F_{(8,104)} = 0.46, p = 0.62, \eta^2 = 0.01; sex \times block: F_{(8,104)} = 1.60, p = 0.22, \eta^2 = 0.05; condition \times sex \times block: F_{(8,104)} = 0.76, p = 0.47, \eta^2 = 0.02$).

Ongoing alpha power during rest

The rmANOVA revealed no significant effects of condition ($F_{(1,13)} = 1.63, p = 0.22, \eta^2 = 0.07$), sex ($F_{(1,13)} < 0.01, p = 0.97, \eta^2 < 0.01$) or block ($F_{(8,104)} = 1.25, p = 0.30, \eta^2 = 0.03$) nor any significant interactions ($condition \times sex: F_{(1,13)} = 1.43, p = 0.25, \eta^2 = 0.06; condition \times block: F_{(8,104)} = 0.66, p = 0.57, \eta^2 = 0.02; sex \times block: F_{(8,104)} = 0.60, p = 0.61, \eta^2 = 0.02; condition \times sex \times block: F_{(8,104)} =$

$0.40, p = 0.75, \eta^2 = 0.01$). However, both groups exhibited significantly increased power during resting periods relative to baseline after stimulation ($stimulation : t_7 = 3.43, p = 0.005, d = 1.2; sham : t_8 = 3.43, p = 0.004, d = 1.14$). Overview and time-course of ongoing alpha increase for stimulation and sham group during rest is depicted in Figures 14D–F. Average relative ongoing alpha power during rest was significantly correlated with participants' increase in performance ($r = 0.62, t_15 = 3.05, p = 0.008$; Figure 3.7B) but not with changes in reaction times ($r = -0.21, t_15 = 0.84, p = 0.42$; Figure 3.7E).

EEG coherence during mental rotation

Relative coherence between electrodes P3 and P4 was significantly higher in the stimulation group than in the sham group ($F_{(1,13)} = 7.04, p = 0.019, \eta^2 = 0.28$; Figure 3.4A). There were no significant sex differences ($F_{(1,13)} = 0.06, p = 0.81, \eta^2 < 0.01$; Figure 3.4B) or effects of block ($F_{(1,13)} = 0.90, p = 0.52, \eta^2 < 0.02$) but a significant three-way interaction between condition, block and sex ($F_{(8,104)} = 2.20, p = 0.033, \eta^2 = 0.04$). None of the other interactions reached significance ($condition \times sex : F_{(1,13)} = 0.27, p = 0.61, \eta^2 = 0.02; condition \times block : F_{(8,104)} = 0.54, p = 0.83, \eta^2 = 0.01; sex \times block : F_{(8,104)} = 1.17, p = 0.33, \eta^2 = 0.02$). Post hoc t-tests show a trend towards increased coherence during mental rotation compared to baseline only for stimulation ($t_7 = 1.80, p = 0.058, d = 0.64$) but not for sham ($t_8 = -2.41, p = 0.98, d = 0.80$). Refer to Figure 3.4C for an overview of the time-course of the coherence change.

The rmANOVA revealed no effects of condition ($F_{(1,13)} = 3.10, p = 0.1, \eta^2 = 0.14$; Figure 3.4D), sex ($F_{(1,13)} = 0.40, p = 0.54, \eta^2 = 0.02$; Figure 3.4E) or block ($F_{(8,104)} = 0.38, p = 0.93, \eta^2 < 0.01$) on relative coherence between electrodes P7 and P8. None of the interactions reached significance ($ondition \times sex : F_{(1,13)} = 0.09, p = 0.76, \eta^2 < 0.01; condition \times block : F_{(8,104)} = 0.87, p = 0.54, \eta^2 = 0.02; sex \times block : F_{(8,104)} = 1.13, p = 0.35, \eta^2 = 0.02; condition \times sex \times block : F_{(8,104)} = 0.81, p = 0.60, \eta^2 = 0.02$). Neither stimulation ($t_7 = 0.46, p = 0.32, d = 0.16$), nor sham group ($t_8 = -2.20, p = 0.97, d = 0.73$) exhibited increased coherence between electrodes P7 and P8 relative to baseline. Refer to Figure 3.4F for an overview of the time-course of the coherence change.

3.4.3.2 Event-related EEG

Event-related-desynchronization (ERD)

ERD increased significantly stronger in the stimulation than in the sham group ($F_{(1,13)} = 4.86, p = 0.046, \eta^2 = 0.26$; Figure 3.5A). There were no effects of sex ($F_{(1,13)} = 2.13, p = 0.17, \eta^2 = 0.13$; Figure 3.5B), block ($F_{(4,52)} = 2.05, p = 0.13, \eta^2 = 0.01$), or significant interactions ($condition \times sex : F_{(1,13)} =$

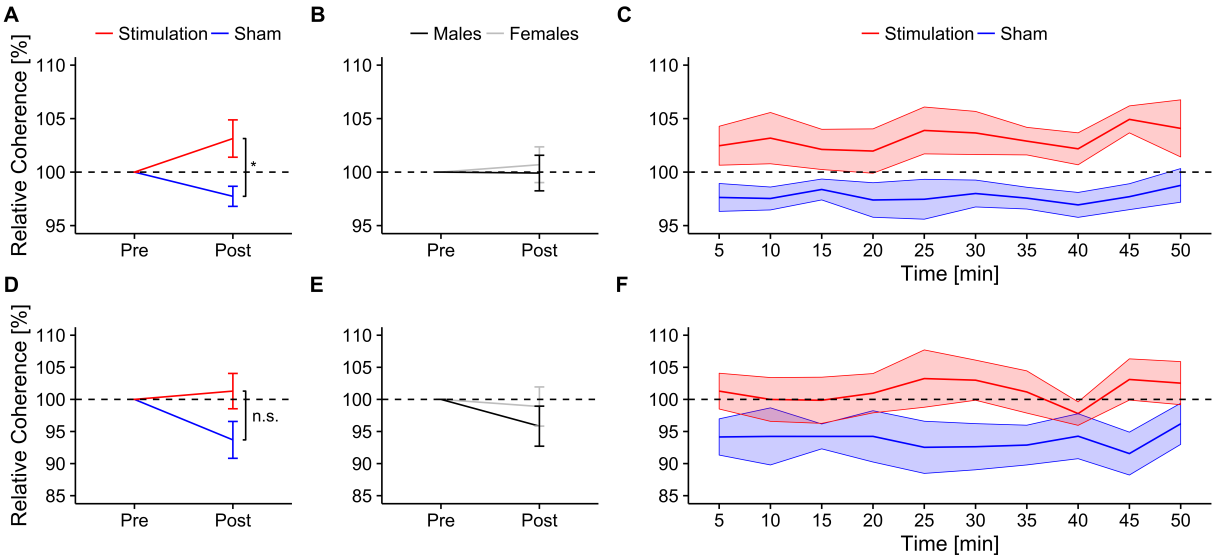

Figure 3.4: Ongoing alpha coherence..Ongoing normalized alpha coherence during mental rotation. Top row: normalized coherence between electrode P3 and P4. Error bars and shaded areas depict SEM; asterisks code for significant differences (< 0.05). **(A)** Averaged normalized coherence after stimulation for stimulation and sham. **(B)** Averaged normalized coherence after stimulation for females and males. **(C)** Time-course of normalized coherence after stimulation for stimulation and sham group. Bottom row: normalized coherence between electrode P7 and P8. **(D)** Averaged normalized coherence after stimulation for stimulation and sham. **(E)** Averaged normalized coherence after stimulation for females and males. **(F)** Time-course of normalized coherence after stimulation for stimulation and sham group.

$1.16, p = 0.30, \eta^2 = 0.08; condition \times block : F_{(4,52)} = 2.15, p = 0.12, \eta^2 = 0.012; sex \times block : F_{(4,52)} = 1.11, p = 0.35, \eta^2 < 0.01; condition \times sex \times block : F_{(4,52)} = 0.19, p = 0.86, \eta^2 < 0.01$). Only the stimulation group exhibited a trend towards increased ERD after stimulation compared to baseline ($stimulation : t_7 = 1.84, p = 0.053, d = 0.65; sham : t_8 = 0.94, d = 0.58$). The time-course of relative ERD after stimulation is depicted in Figure 3.5C, time-frequency spectra and ERD topographies are shown in Figure 3.6.

Relative ERD after stimulation was significantly correlated with participants' performance increase ($r = 0.59, t_15 = 2.83, p = 0.01$; Figure 3.7C), but not with changes in reaction times ($r = -0.12, t_15 = 0.45, p = 0.65$; Figure 3.7F).

ERD values contain information about the relation of oscillatory activity before (reference period) and after stimulus onset (test period; see Equation 3.2). Therefore, the observed effect on ERD can be driven by either an increase of alpha power in the reference period, by a decrease of alpha power in the test period or a combination thereof. To further resolve to what extent changes in oscillatory activity in reference and test periods caused the effect the raw spectra used for the calculation of ERD values were extracted and separately analyzed following the previous approach (averaging for each block and normalization with the pre stimulation baseline) and analyzed using rmANOVAs with factors condition (2 levels, stimulation vs. sham) and time (5 levels). The factor sex was not included

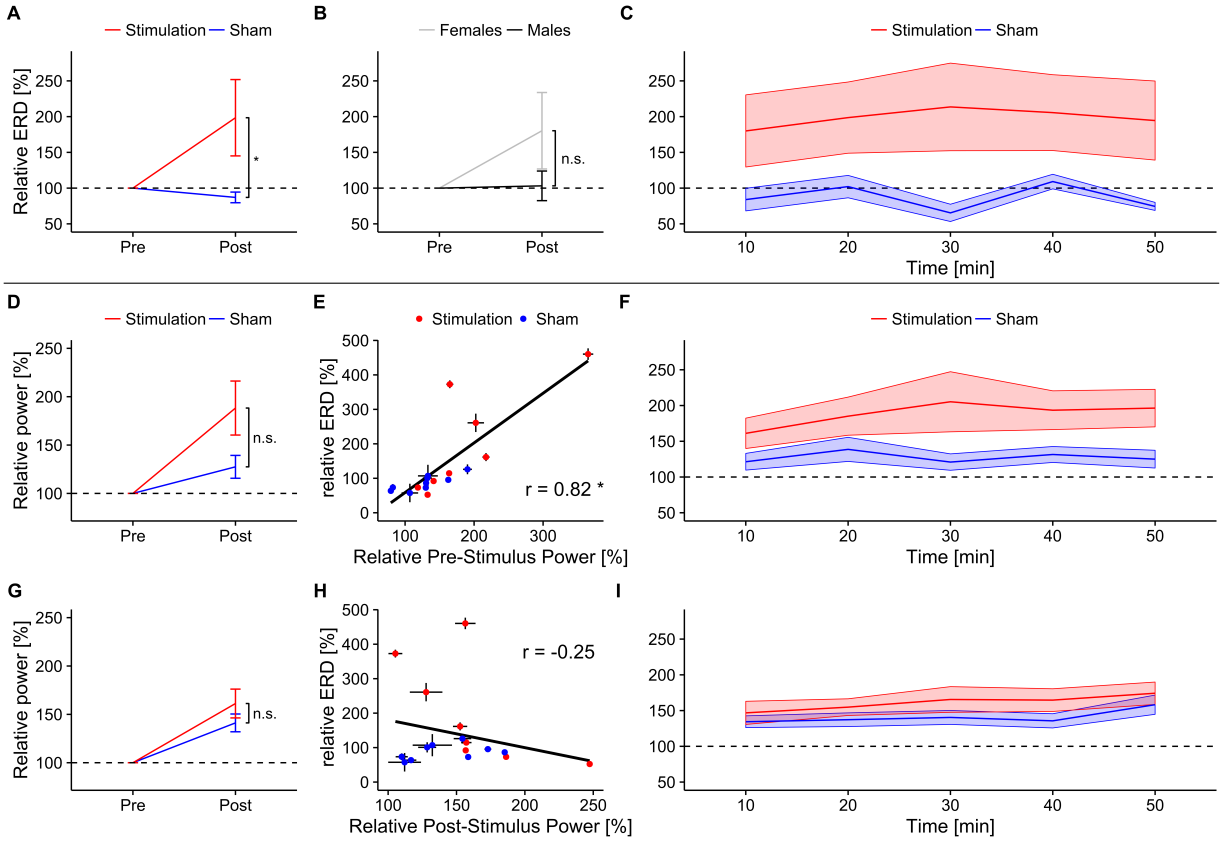

Figure 3.5: Event-related-desynchronization (ERD). Error bars and shaded areas depict SEM; asterisks code for significant differences ($* < 0.05, n.s.$ = not significant). **(A)** Overall relative ERD in the individual alpha band for stimulation and sham group. **(B)** Overall relative ERD in the individual alpha band for female and male subjects. **(C)** Time-course of relative ERD after stimulation. Bottom rows show relative alpha power 3 s before (reference period; middle row) and after stimulus onset (test period; bottom row). **(D)** Overall relative pre-stimulus alpha power (reference period) for stimulation and sham group. **(E)** Scatterplot depicting the correlation between relative pre-stimulus alpha power (test period) and relative ERD. **(F)** Time-course of relative pre-stimulus alpha power for stimulation and sham group. **(G)** Overall relative post-stimulus alpha power for stimulation and sham group. **(H)** Scatterplot depicting the correlation between relative post-stimulus alpha power and relative ERD. **(I)** Time-course of relative post-stimulus alpha power for stimulation and sham group.

as it did not yield significant results in the ERD analysis.

The rmANOVA on alpha power in the reference period revealed a trend for the factor condition ($F_{(1,15)} = 4.37, p = 0.054, \eta^2 = 0.2$) but no effect of block ($F_{(4,60)} = 2.35, p = 0.11, \eta^2 = 0.02$) and no interaction ($condition \times block$: $F_{(4,60)} = 2.38, p = 0.11, \eta^2 = 0.02$; Figures 3.5D,F). For alpha power in the test period, a significant effect of block ($F_{(4,60)} = 6.66, p < 0.001, \eta^2 = 0.06$) but no effect of condition was found ($F_{(1,15)} = 1.38, p = 0.26, \eta^2 = 0.07$). The analysis did not reveal a significant interaction ($F_{(4,60)} = 0.84, p = 0.50, \eta^2 < 0.01$; Figures 3.5G,I). Only relative reference period alpha power was significantly correlated with the change in ERD ($r = 0.82, t_15 = 5.47, p < 0.001$; Figure 3.5E) but not test period alpha power ($r = -0.25, t_15 = -0.98, p = 0.34$; Figure 3.5H).

Event-related potentials (ERP)

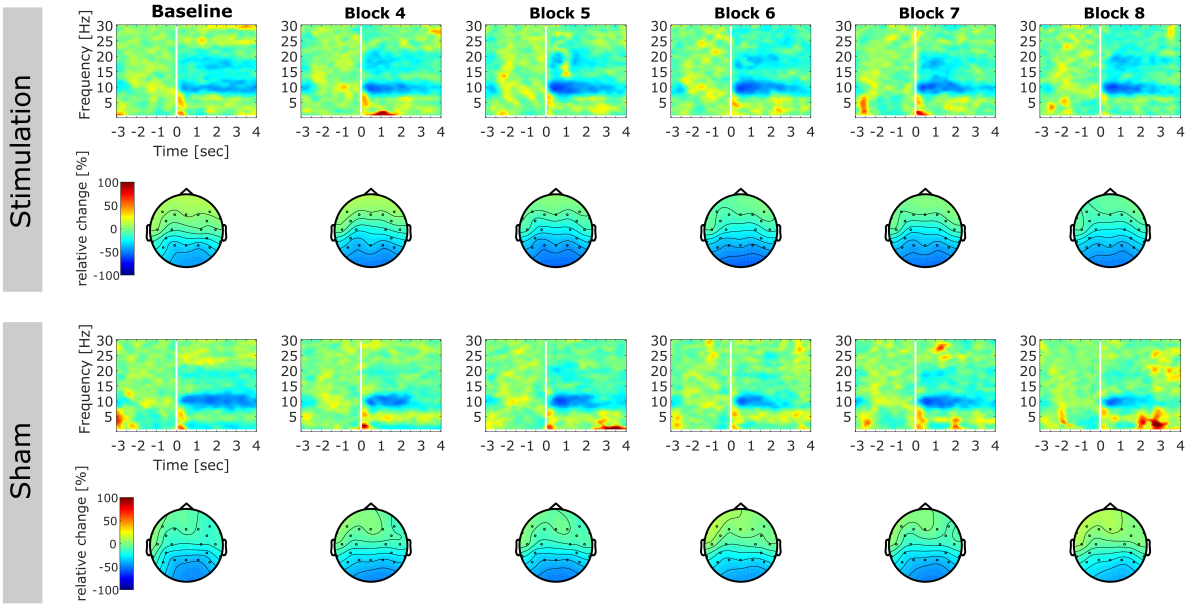

Figure 3.6: Event-related relative power change. Time-frequency representations (TFRs) and topographies reflecting relative change in spectral power after onset of the mental rotation stimulus with respect to baseline (3000 ms prior to stimulus onset until stimulus onset). TFRs are averaged over subjects for each block on electrode Pz. Topographies illustrate relative change in alpha power (8–12 Hz) in the time window 0–3000 ms after stimulus onset. First column displays pre-stimulation baseline. Later columns illustrate post stimulation blocks. Please note that blocks 2 and 3 were performed during stimulation and were discarded from analysis. Top rows: TFRs and topographies of the stimulation group. Bottom rows: TFRs and topographies of the sham group.

Statistical analysis of ERP components revealed significant main effects of block for P100 amplitude ($F_{(1,13)} = 6.18, p = 0.03, \eta^2 = 0.12$) and latency ($F_{(1,13)} = 9.83, p = 0.007, \eta^2 = 0.03$), as well as for N170 latency ($F_{(1,13)} = 5.93, p = 0.03, \eta^2 = 0.03$) and for P300 amplitude ($F_{(1,13)} = 43.72, p < 0.001, \eta^2 = 0.29$). Furthermore, analysis revealed a significant effect of sex on P100 latency ($F_{(1,13)} = 8.90, p = 0.01, \eta^2 = 0.40$). However there were no significant tACS related changes (no condition $\times$ block interactions) in any of the extracted ERP components (all $p > 0.18$). The full results of the ERP analysis are summarized in Table 3.1. Refer to Figure 3.8 for an overview of pre- and post-stimulation ERPs. Please note, that in contrast to the frequency domain analysis post-stimulation data were not normalized by pre-stimulation data. Instead, pre- and post-stimulation ERPs were compared directly using rmANOVAs with factors condition (2 levels), sex (2 levels) and block (2 levels). Thus, an effect of tACS would show up as an interaction of the factors condition and block.

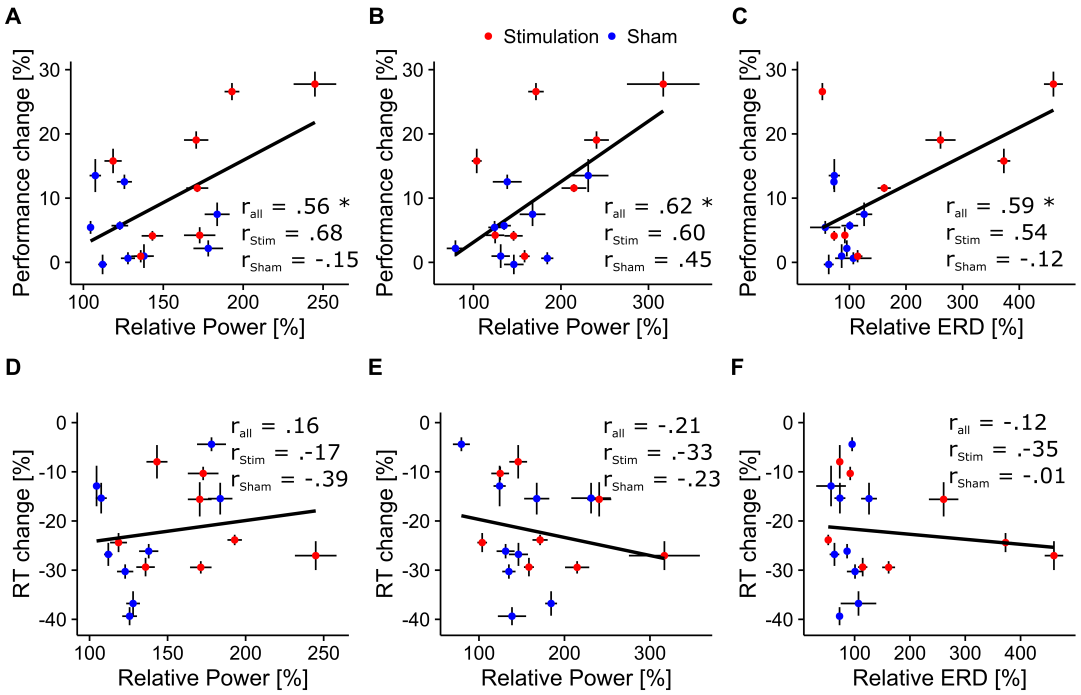

Figure 3.7: Correlations between behavioral and physiological measures. Scatterplots depicting correlations between behavioral and physiological aftereffect measures. Asterisks indicate correlations significantly differing from zero. Black bars around the dots indicate their SEM. Top row: correlation between overall performance increase and **(A)** relative ongoing alpha power during mental rotation, **(B)** relative ongoing alpha power during rest, **(C)** relative ERD. Bottom row: correlation between overall change in reaction times and **(D)** relative alpha power during mental rotation, **(E)** relative alpha power during rest, **(F)** relative ERD.

3.5 Discussion

So far, research on behavioral effects of tACS mainly focused on online effects of the stimulation. While most studies on physiological effects of tACS rely on aftereffects of the stimulation and performed resting-state measurements (Kasten et al., 2016; Neuling et al., 2013; Vossen et al., 2015; Zaehle et al., 2010). The current study combined a complex task, namely mental rotation, with measurements of the outlasting physiological effects of tACS on alpha oscillations, demonstrating both a behavioral and an electrophysiological aftereffect of tACS in parallel.

While there were no effects on participants' reaction times, performance in the mental rotation task was significantly enhanced in the stimulation group as compared to sham. This is in accordance with previous results suggesting increased performance with enhanced reference alpha power, but no facilitation of reaction times (Hanslmayr et al., 2005; Klimesch et al., 2003; Zoefel et al., 2011). The behavioral effects were accompanied by changes in ongoing and event-related alpha activity. Ongoing individual alpha power and coherence during mental rotation were significantly increased compared to sham. This extends previous findings obtained during simple auditory or visual vigilance tasks (Kasten et al., 2016; Neuling et al., 2013; Vossen et al., 2015; Zaehle et al., 2010). Furthermore,

Table 3.1: Analysis of variance (ANOVA) results of event-related-potential (ERP) analysis. Results of repeated measurements analysis of variance (rmANOVA) on amplitudes and latencies of ERP components (P100, N170 and P300). Baseline ERPs were compared to post-stimulation ERPs. No normalization was applied. Asterisks indicate significant effects. Upper case T indicates trends ($p < 0.1$).

	F	p	η^2		F	p	η^2
P100 Amplitude				**P100 Latency**			
Condition	0.99	0.34	0.05	*Condition*	0.35	0.56	0.02
Sex	2.46	0.14	0.12	*Sex*	8.90	0.01*	0.39
Block	6.17	0.03*	0.12	*Block*	9.83	0.007*	0.03
Condition × *Sex*	1.20	0.29	0.06	*Condition* × *Sex*	0.13	0.72	<0.01
Condition × *Block*	<0.01	0.94	<0.01	*Condition* × *Block*	0.22	0.65	<0.01
Sex × *Block*	1.36	0.26	0.02	*Sex* × *Block*	1.45	0.25	<0.01
Condition × *Sex* × *Block*	0.47	0.50	0.01	*Condition* × *Sex* × *Block*	0.20	0.67	<0.01
N170 Amplitude				**N170 Latency**			
Condition	2.42	0.14	0.15	*Condition*	0.06	0.80	<0.01
Sex	0.55	0.47	0.03	*Sex*	1.97	0.18	0.12
Block	0.08	0.78	<0.01	*Block*	5.93	0.03*	0.03
Condition × *Sex*	0.08	0.77	<0.01	*Condition* × *Sex*	2.41	0.14	0.15
Condition × *Block*	0.93	0.35	<0.01	*Condition* × *Block*	0.40	0.54	<0.01
Sex × *Block*	4.27	0.06^T	<0.01	*Sex* × *Block*	<0.01	0.97	<0.01
Condition × *Sex* × *Block*	0.19	0.67	<0.01	*Condition* × *Sex* × *Block*	0.01	0.92	<0.01
P300 Amplitude				**P300 Latency**			
Condition	0.65	0.43	0.04	*Condition*	0.03	0.87	<0.01
Sex	0.48	0.50	0.03	*Sex*	1.50	0.24	0.06
Block	43.72	<0.001*	0.28	*Block*	0.05	0.81	<0.01
Condition × *Sex*	0.31	0.59	0.02	*Condition* × *Sex*	0.31	0.59	0.02
Condition × *Block*	1.99	0.18	0.02	*Condition* × *Block*	0.26	0.62	<0.01
Sex × *Block*	0.38	0.55	<0.01	*Sex* × *Block*	0.94	0.35	0.03
Condition × *Sex* × *Block*	1.77	0.21	0.02	*Condition* × *Sex* × *Block*	2.32	0.15	0.07

ERD in the individual alpha band was increased in the stimulation group compared to sham. A more detailed analysis revealed some evidence that the observed effect on ERD is probably driven by an increase in pre-stimulus oscillatory power compared to sham while alpha power after stimulus onset in the stimulation group remained similar to the sham group. It is known from previous research, that the effect of tACS is context dependent (Neuling et al., 2013; Ruhnau et al., 2016). However, in these studies permanent changes in context were compared (stimulation and measurement during eyes-closed vs. eyes-open). The current pattern of results suggests that transient changes in context and stimulation effect can occur even on a single trial level which has to be taken into account as these can potentially mask stimulation effects in physiological measurements. Additionally, the finding is in agreement with the theoretical framework of previous NFT and rTMS studies, which aimed to facilitate

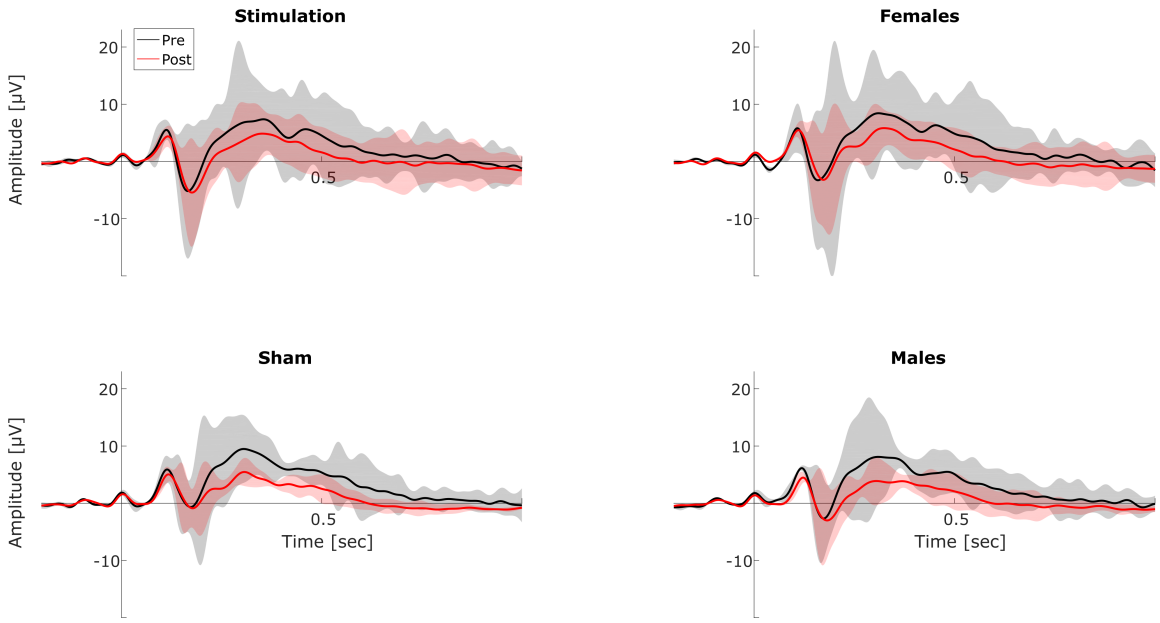

Figure 3.8: Event-related-potentials (ERPs). Grand average ERPs before (black) and after stimulation (red). Shaded areas depict SEM. **(A)** Averaged ERPs before vs. after stimulation for stimulation group. **(B)** Averaged ERPs before vs. after stimulation for female subjects. **(C)** Averaged ERPs before vs. after stimulation for sham group. **(D)** Averaged ERPs before vs. after stimulation for male subjects.

ERD and mental rotation performance by enhancing alpha power in a reference period (Hanslmayr et al., 2005; Klimesch et al., 2003; Zoefel et al., 2011).

Surprisingly, an effect of tACS was not evident in the resting periods which intermitted the mental rotation task. However, this null finding might be explained by the relatively small amount of data (43 trials per block) that was available for analysis. Furthermore, it is worth noticing that although not significant, the data still point to the same direction as previous findings (Kasten et al., 2016; Neuling et al., 2013; Vossen et al., 2015). Similar to recent results (Kasten et al., 2016; Neuling et al., 2013), the effect of tACS appears to be limited to the stimulated alpha band, as there were no significant effects on neighboring frequency bands. By applying tACS below participants' individual sensation threshold, we further ruled out, that the observed effects were due to the exposure of skin sensations or the perception of phosphenes. In contrast to the observed changes in performance and in the frequency domain, ERPs were not systematically modulated by tACS. To explain this finding, it should be considered that our stimulation protocol was designed to target ongoing oscillations in the alpha band and was applied independent of stimulus presentation. The induced oscillations contributing to the P1-N1 complex in ERPs, however, are phase locked to the stimulus presentation and might therefore be unaffected by tACS (Gruber et al., 2005; Klimesch, Hanslmayr, et al., 2007). A more elaborated design, aligning the tACS waveform with the latency of the to-be targeted ERP component

might be able to elicit changes in their amplitude. The prominent decrease in P300 amplitude over time is in line with previous research suggesting P300 habituation when a task becomes more automatic and requires less attentional resources (Courchesne, 1978; Ravden and Polich, 1998; Romero and Polich, 1996).

The widely observed sex differences in mental rotation (Linn and Petersen, 1985; Voyer et al., 1995) were also evident in the current data. Female subjects exhibited stronger improvement in the mental rotation task compared to men. Similar observations have been previously made in studies with children and adolescents suggesting that females have more benefits from training and repetition in the domain of mental rotation than males (Neubauer, Bergner, and Schatz, 2010; Tzuriel and Egozi, 2010). However, this is possibly due to lower initial performance and thus more potential for improvement. In addition, females also exhibited a trend towards stronger enhancement of ongoing alpha activity during mental rotation which vanishes during the resting periods, providing a physiological correlate of the aforementioned performance gain. The current results do not suggest that the effects of tACS were modulated by participants' sex. There is growing evidence that the effects of tACS and brain stimulation in general are highly dependent on the context of application (Feurra et al., 2013; Neuling et al., 2013; Ruhnau et al., 2016; Silvanto, Muggleton, and Walsh, 2008). For female subjects, alpha oscillations have been found to be modulated by menstrual cycle (Brötzner, Klimesch, Doppelmayr, Zauner, and Kerschbaum, 2014) offering a potential source of variance that has hardly been controlled for so far. Furthermore, sex differences and menstrual cycle are among the factors determining the induction of cortical plasticity using other non-invasive brain stimulation techniques such as rTMS or tDCS (Ridding and Ziemann, 2010). Thus, while there was no evidence for an overall interaction between participants' sex and the tACS effects in the current study, the possibility that tACS effects of females might be modulated by the menstrual cycle cannot completely be ruled out; especially as the current experiment was not tailored to explicitly study sex differences and is therefore possibly underpowered to detect moderate influences of participants' sex.

Contrary to our initial hypothesis, there was no evidence for a decrease in performance during tACS application. If at all, mental rotation performance of the stimulation group rather increased already during tACS. This is surprising given that decreased ERD was apparent in previous experiments investigating online effects of tACS (Neuling et al., 2015; Vosskuhl et al., 2016). However, it should be acknowledged that this finding was rather a visual observation and not statistically tested or indirectly inferred from a reduction of BOLD signal strength, respectively. Furthermore, both studies utilized a different type of task than the current study (visual change detection task). An important prerequisite for successful entrainment is the presence of a self-sustained oscillator (Pikovsky et al.,

2003). Comparing our mental rotation task with the visual change detection task used by Neuling et al. (2015) and Vosskuhl et al. (2016) it is likely that mental rotation involves much stronger ERD up to a complete blocking of alpha oscillations during task execution; thus offering no possibility for entrainment. It is known that ERD in the alpha band is modulated by task demands and complexity, with more demanding tasks resulting in facilitated ERD (Boiten et al., 1992; Dujardin et al., 1995; van Winsun et al., 1984). During a visual change detection task, relatively simple stimuli (the rotation of the fixation cross) are used and the amount of cognitive load for task execution is low. Thus, residual alpha activity might still be present after stimulus onset offering the possibility to be entrained. In the first case ERD would be increased during tACS due to enhanced pre-stimulus alpha power and subsequent vanishing thereof after stimulus onset. In the latter case ERD would be decreased due to entrained residual alpha activity in the pre- and post-stimulus period. Unfortunately, the current experiment was not optimized for tACS artifact removal techniques applying template subtraction combined with PCA (Helfrich, Schneider, et al., 2014). We utilized less EEG channels and the stimulation frequency was set to participants' IAF in order to achieve a maximal stimulation effect rather than being tailored to fit to the sampling frequency of the EEG. This is required for optimal artifact removal. For these reasons, it was not possible to reliably reconstruct EEG signals during stimulation and directly investigate the desynchronization patterns. Further experiments optimized for the still challenging task to remove the tACS artifact or a replication of the current findings using fMRI would be beneficial to resolve these seemingly contradicting results.

The current study extends previous results as it demonstrates tACS to elicit a robust and behaviorally relevant aftereffect in the alpha band during a classic mental rotation task (Ganis and Kievit, 2015; Shepard and Metzler, 1971). While the increase of ongoing alpha power during mental rotation was similar to previous studies on the tACS aftereffect (Kasten et al., 2016; Neuling et al., 2013), the improvement of mental rotation performance was comparable to studies using rTMS or five consecutive days of NFT, respectively (Klimesch et al., 2003; Zoefel et al., 2011). The current study employed a Cz-Oz montage to modulate subjects' oscillatory activity in the alpha band in posterior brain regions. However, we did not control for other possible montages. Klimesch et al. (2003) found similar effects of rTMS applied over frontal and parietal cortex on mental rotation performance. Thus, it might be possible that the effects reported in the current experiment might also be achieved with other (i.e., frontal-) montages.

In relation to previous tACS studies, the current experiment achieved relatively strong effect sizes with regard to participants performance even though stimulation intensity was on average slightly below the 1 mA that have been reported to be beneficial by Schutter, 2016. However, it should be

noted that this value is by no means a threshold necessary to achieve effects but rather provides a rough orientation about the relationship between stimulation intensities and effect sizes that are to be expected. Especially in combination with the benefits of individually guided stimulation at participants' IAF, results appear to fall in a reasonable range as less energy is needed to entrain an oscillation the closer the driving frequency is to the intrinsic frequency of the oscillator (Pikovsky et al., 2003; Schutter, 2016). Given the reliable effects of tACS, it might be a suitable method to complement or substitute NFT in experimental as well as in clinical settings. However, direct comparisons of the effects of tACS and NFT are yet missing as well as studies investigating how far paradigms combining NFT with tACS stimulation might lead to stronger or faster effects than each of the methods alone.

We would like to encourage further research to put a stronger emphasis on outlasting behavioral and physiological effects during the investigation of tACS. So far, the vast majority of studies carried out post stimulation measurements of only few minutes, if at all (Veniero et al., 2015). Prolonged paradigms monitoring longer periods of task performance and/or physiological changes after tACS might add additional insights to the mechanisms and long-term effects of tACS. However, when adapting this approach several crucial aspects should be taken into account. While the current study was carried out to target the amplitude of alpha oscillations and its task related modulations (ERD), tACS is potentially capable to modulate several other properties of an oscillation, such as its frequency (Vosskuhl et al., 2015), coherence (Helfrich, Schneider, et al., 2014; Strüber et al., 2014) or phase (Neuling, Rach, Wagner, Wolters, and Herrmann, 2012). However, depending on the targeted modality aftereffects are more or less likely to occur. Especially when directly modulating the frequency of an oscillation, synchronization theory would predict neural oscillators to return to their intrinsic eigenfrequency shortly after the external driving force (the stimulation) is switched off (Pikovsky et al., 2003). Thus, no sustained changes of frequency are to be expected. Indeed, this pattern has been recently observed in a study tailored to recover EEG signals during tACS by means of template subtraction and PCA (Helfrich, Schneider, et al., 2014). When targeting amplitude or coherence, aftereffects are produced quite reliably (Helfrich, Schneider, et al., 2014; Neuling et al., 2013; Strüber et al., 2014; Veniero et al., 2015; Vossen et al., 2015; Zaehle et al., 2010). Complimented by the current findings, we conclude that the tACS aftereffect can potentially be used to study causal relationships between behavior and a variety of properties of brain oscillations such as coherence or amplitude but not their frequency. The current results provide first evidence that a prolonged effect of tACS can be induced during complex tasks. However, it remains unclear to what extent the aftereffect of tACS might interact with task complexity as this factor was not varied in the current design. In a next step, it would be desirable to directly compare different tasks with varying

levels of complexity to further understand under which conditions and to which degree of complexity aftereffects can be induced with tACS.

3.6 Acknowledgments

This work was supported by a grant of the German Research Foundation (DFG, SPP 1665 HE 3353/8-1) awarded to CSH. Parts of the study were conducted as part of the Master Thesis of FHK. The underlying raw data and analysis scripts are available upon request.

Chapter 4

Study III: Facilitated Event-Related Power-Modulations during Transcranial Alternating Current Stimulation (tACS) Revealed by Concurrent tACS-MEG

Published as:

Kasten, FH., Maess, B., Herrmann, CS., (2018) Facilitated Event-Related Power-Modulations during Transcranial Alternating Current Stimulation (tACS) Revealed by Concurrent tACS-MEG. *eNeuro*., (in Press)

Author Contributions:

Designed research: FHK, BM, CSH

Perfomed Research: FHK, BM

Analyzed Data: FHK

Wrote paper: FHK, BM, CSH

4.1 Abstract

Non-invasive approaches to modulate oscillatory activity in the brain are increasingly popular in the scientific community. Transcranial alternating current stimulation (tACS) has been shown to modulate neural oscillations in a frequency-specific manner. However, due to a massive stimulation artifact at the targeted frequency, little is known about effects of tACS during stimulation. It remains unclear how the continuous application of tACS affects event-related oscillations during cognitive tasks. Depending on whether tACS influences pre- or post-stimulus oscillations, or both, the endogenous, event-related oscillatory dynamics could be pushed in various directions or not at all. A better understanding of these effects is crucial to plan, predict, and understand outcomes of solely behavioral tACS experiments. In the present study, a recently proposed procedure to suppress tACS artifacts by projecting MEG data into source-space using spatial filtering was utilized to recover event-related power modulations in the alpha-band during a mental rotation task. MEG data of 25 human subjects was continuously recorded. After 10-minute baseline measurement, participants received either 20 minutes of tACS at their individual alpha frequency or sham stimulation. Another 40 minutes of MEG data were acquired thereafter. Data were projected into source-space and carefully examined for residual artifacts. Results revealed strong facilitation of event-related power modulations in the alpha-band during tACS application. These results provide first direct evidence that tACS does not counteract top-down suppression of intrinsic oscillations, but rather enhances pre-existent power modulations within the range of the individual alpha (= stimulation) frequency.

4.2 Visual Abstract

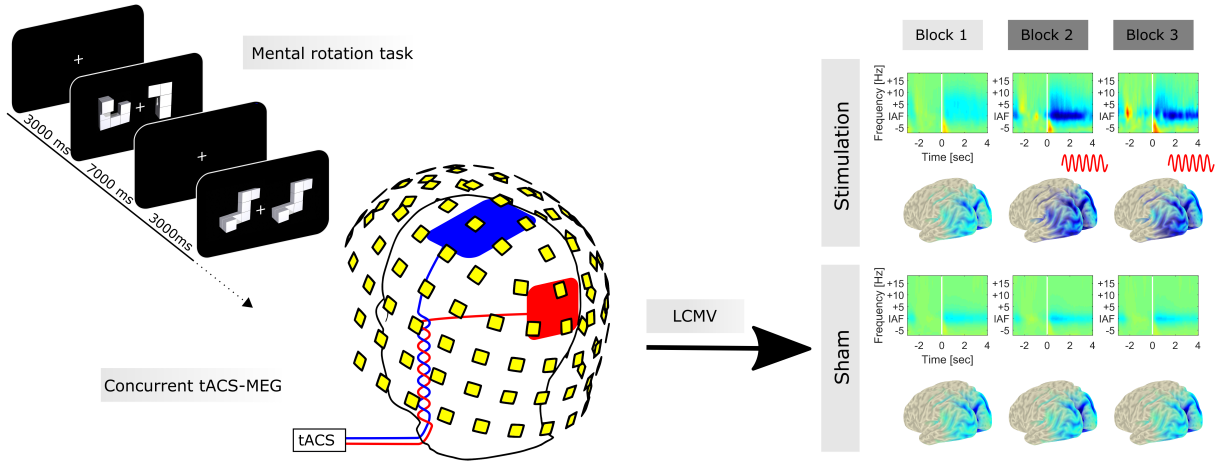

4.3 Significance Statement

Transcranial alternating current stimulation (tACS) is increasingly used in cognitive neuroscience to study the causal role of brain oscillations for cognition. However, online effects of tACS largely remain a “black box” because of an intense electromagnetic artifact encountered during stimulation. The current study is the first to employ a spatial filtering approach to recover, and systematically study, event-related oscillatory dynamics during tACS, which could potentially be altered in various directions. TACS facilitated pre-existing patterns of oscillatory dynamics during the employed mental rotation task, but did not counteract or overwrite them. In addition, control analyses and a measure to quantify tACS artifact suppression are provided that can enrich future studies investigating tACS online effects.

4.4 Introduction

Oscillatory activity of neuronal assemblies is a ubiquitous phenomenon in the brain observed within and between different brain structures and across species (Buzsáki, 2006). Over the past decades, these oscillations have been linked to a variety of brain functions, such as memory, perception, and cognitive performance (Basar et al., 2000; Buzsáki, 2006; Klimesch, 1999; Klimesch, Sauseng, and Hanslmayr, 2007). Traditionally, these relationships were fruitfully investigated using imaging techniques such as electro- or magnetoencephalography (EEG/ MEG). However, in their nature, these approaches are correlational and cannot resolve causal relationships between neural oscillations and cognitive processes. The recent (re-)discovery of non-invasive transcranial electrical stimulation (tES) now allows to directly probe these causal relationships (Herrmann, Strüber, et al., 2016).

The application of oscillatory currents through the scalp by means of transcranial alternating current stimulation (tACS) has been shown to modulate endogenous brain oscillations in a frequency-specific manner (Fröhlich and McCormick, 2010; Helfrich, Schneider, et al., 2014; Ozen et al., 2010; Zaehle et al., 2010). Effects of tACS during stimulation have been primarily investigated in animals (Fröhlich and McCormick, 2010; Kar, Duijnhouwer, and Krekelberg, 2017; Ozen et al., 2010) and with computational models (Ali et al., 2013; Fröhlich and McCormick, 2010; Negahbani et al., 2018; Reato et al., 2010). Due to a massive artifact introduced to electrophysiological signals, studies on tACS effects in humans have mostly been restricted to behavioral measures (Kar and Krekelberg, 2014; Lustenberger et al., 2015; Marshall et al., 2006), blood oxygen level–dependent (BOLD)- signal effects (Alekseichuk, Diers, Paulus, and Antal, 2016; Cabral-Calderin et al., 2016; Violante et al., 2017;

Vosskuhl et al., 2016), and aftereffects in M/EEG (Kasten et al., 2016; Neuling et al., 2015; Stecher et al., 2017; Veniero et al., 2015; Vossen et al., 2015; Wach et al., 2013a; Zaehle et al., 2010). In case of M/EEG, a frequency specific increase in oscillatory power after stimulation is consistently reported (Kasten et al., 2016; Neuling et al., 2013; Vossen et al., 2015; Zaehle et al., 2010). It is often assumed that the underlying mechanism of action of tACS is entrainment of neural activity to the external driving force, which is observed in computational and animal models (Ali et al., 2013; Fröhlich and McCormick, 2010; Negahbani et al., 2018; Ozen et al., 2010; Reato et al., 2010). Direct evidence for entrainment of brain oscillations to tACS in humans is, however, largely missing so far.

Besides sustained effects on the power of spontaneous oscillations after the stimulation, tACS has more recently been demonstrated to alter event-related oscillatory dynamics in the context of a cognitive task (Kasten and Herrmann, 2017). In that study, event-related desynchronization (ERD) was enhanced after tACS application, accompanied by improved performance in a classic mental rotation (MR) task (Kasten and Herrmann, 2017; Shepard and Metzler, 1971). The amount of ERD in the alphaband has previously been linked to MR performance (Klimesch et al., 2003; Michel et al., 1994). Although an increase in task performance has already been observed during tACS, the precise oscillatory dynamics during tACS remain unclear (Kasten and Herrmann, 2017). Given that many tACS studies rely solely on behavioral measures, an understanding of the effect of tACS on eventrelated oscillations is crucial. Depending on whether the stimulation merely affects pre- or post-stimulus oscillations or both, tACS may increase, decrease, or not modulate ERD/ERS. Each of these scenarios would result in different behavioral outcomes to be expected. The current study aims to provide a first step toward understanding the effects of tACS on event-related power modulations during stimulation. To this end, the experiment of Kasten and Herrmann (2017) was repeated in an MEG scanner. The application of linearly constrained minimum variance beamforming (LCMV; Van Veen et al., 1997) on MEG recordings has been shown to substantially suppress electromagnetic artifacts encountered during tES (Neuling et al., 2015; Soekadar et al., 2013). Although this approach will never completely remove artifacts from the signal (Mäkelä et al., 2017; Noury et al., 2016; Noury and Siegel, 2017), artifact suppression may still be sufficient to recover changes in event-related dynamics during tACS (Neuling et al., 2017; Noury and Siegel, 2018).

In the present study, LCMV was used to attempt to recover the event-related power modulations in the alpha-band encountered during MR. Based on previous behavioral results, an increase in alpha-power modulation during tACS was hypothesized (Kasten and Herrmann, 2017). The measure to capture tACS effects (absolute power difference instead of relative change) was carefully chosen to be robust against the possible influence of residual artifacts. Careful control analyses were conducted

to rule out that the observed effects can be attributed to a residual artifact.

4.5 Materials and Methods

4.5.1 Participants

Twenty-five healthy volunteers were randomly assigned to one of two experimental conditions. They received either 20 min of tACS or sham stimulation during the course of the experiment. All were right-handed according to the Edinburgh Handedness Inventory (Oldfield, 1971) and had normal or corrected-to-normal vision. Participants gave written informed consent before the experiment and reported no history of neurologic or psychiatric conditions. The experiment was approved by the Commission for Research Impact Assessment and Ethics at the University of Oldenburg and was conducted in accordance with the Declaration of Helsinki. Three subjects exhibited low tolerance to skin or phosphene sensations while determining the individual stimulation intensity (see Electrical stimulation). Due to the resulting low stimulation currents (below 0.4 mA), these subjects were excluded from the analysis. Furthermore, two participants were excluded as they did not exhibit alpha modulation in response to the cognitive task during the baseline block. Data of 20 subjects (10 in stimulation group, 10 in sham group, age: 26 $\pm$ 3 years, 8 females) remained for analysis. Although the groups were initially counterbalanced for participants' sex, the exclusion of subjects resulted in an imbalance in the sham group (7 males and 3 females vs. 5 males and 5 females in the stimulation group).

4.5.2 Magnetoencephalogram

Neuromagnetic activity was recorded at a rate of 1 kHz using a 306-channel whole-head MEG system (Elekta Neuromag Vectorview, Elekta Oy) with 102 magnetometers and 204 orthogonal, planar gradiometers, sampling from 102 distinct sensor locations. An online bandpass filter between 0.1 and 330 Hz was applied. The experiment was conducted in a dimly lit, magnetically shielded room (MSR; Vacuumschmelze) with participants seated below the MEG helmet in upright position. Before the experiment, three anatomic landmarks (nasion and left and right posterior tip of tragi) were digitized using a Fastrack (Polhemus), along with the location of five head position indicator (HPI) coils, and $>$200 head shape samples to allow continuous head-position tracking and later coregistration with anatomic MRIs.

After finishing the preparations, individual alpha frequency (IAF) was determined from a 3 min,

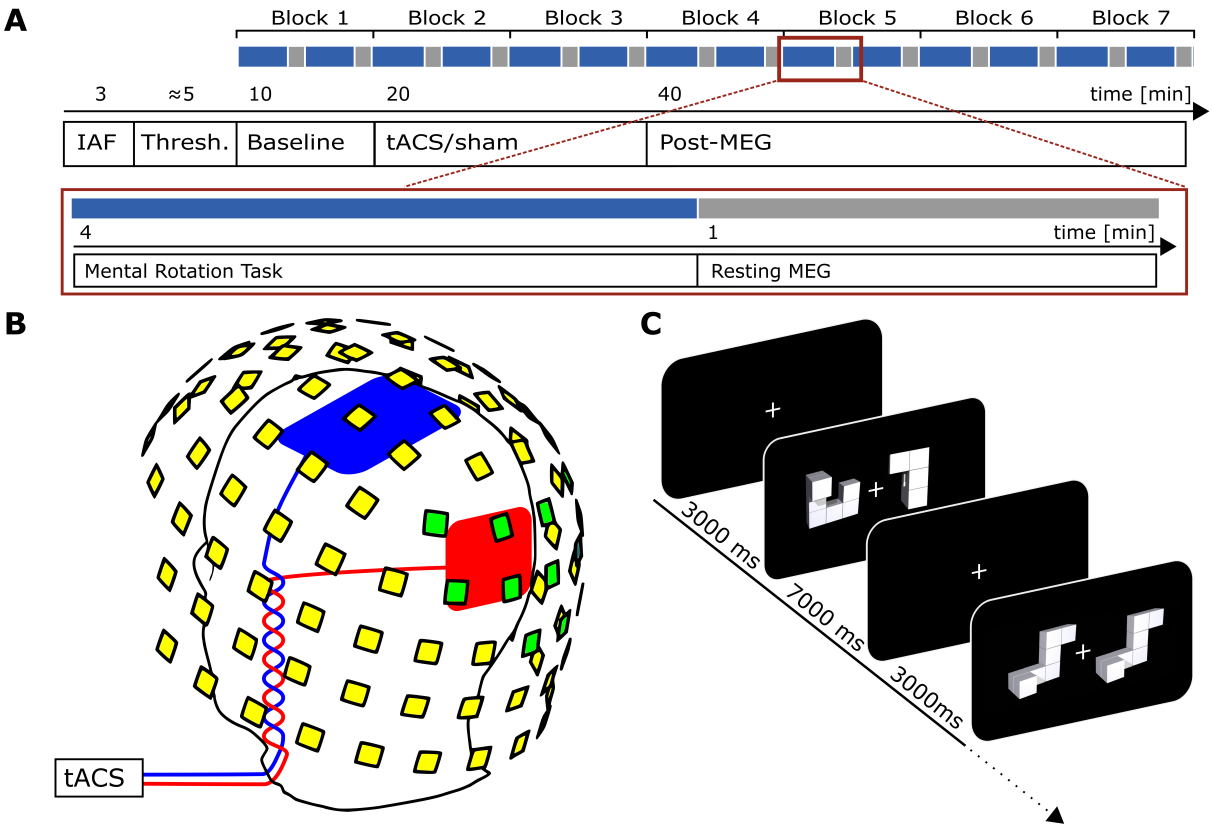

Figure 4.1: Experimental procedures. **(A)** Time course of the experiment. Blue indicates periods during which the MR task was performed; gray indicates intermittent resting periods. **(B)** Positions of stimulation electrodes (red/blue) and layout of MEG sensors (yellow/green). Stimulation electrodes were placed centered above Cz (7 × 5 cm) and Oz (4 × 4 cm) of the international 10-10 system. MEG was recorded from 102 locations. Each location contains a sensor triplet of one magnetometer and two orthogonal planar gradiometers, resulting in a total of 306 channels. Sensor locations used to determine participants' individual alpha frequency are marked green. **(C)** Mental rotation task. Each trial started with the presentation of a white fixation cross at the center of the screen. After 3000 ms, a mental rotation stimulus (two objects) was presented and remained on screen for another 7000 ms. During this time participants were required to judge whether the two objects presented were either different (example depicted in 2nd display) or identical (but rotated; 4th display). **(A)** and **(C)** are adapted from Kasten and Herrmann (2017).

eyes-open, resting-state MEG recording. Data were segmented into 1 s epochs. Fast Fourier transforms (FFTs) were computed for each of the segments using the Fieldtrip toolbox (Oostenveld et al., 2011). The power peak in the averaged spectra, in the 8–12 Hz band, was determined in a set of posterior sensors showing most pronounced alpha activity by visual inspection. The identified frequency was used as stimulation frequency for the subsequent procedures (refer to Figure 4.1A for an overview of the time course of the experiment and Figigure 4.1B for an illustration of sensor locations used to determine participants' IAF).

4.5.3 Electrical Stimulation

Participants received either 20 min of tACS (including 10 s fade-in and fade-out) or sham stimulation (30 s stimulation in the beginning of the stimulation period, including 10 s fade-in and out) at

their individual alpha frequency (IAF). The sinusoidal stimulation signal was digitally generated at a sampling rate of 10 kHz in Matlab 2012a (32-bit, The MathWorks) and transferred to a digital-analog converter (Ni USB 6221, National Instruments). From there, the signal was streamed to the remote input of a battery-driven constant current stimulator (DC Stimulator Plus, Neuroconn), which was placed inside an electrically shielded cabinet outside the MSR. The signal was then gated into the MSR via a tube in the wall using the MRI extension-kit of the stimulator (Neuroconn). Electrical stimulation was administered by two surface conductive rubber electrodes attached to participants' scalps over electrode positions Cz (5 $\times$ 7 cm) and Oz (4 $\times$ 4 cm) of the international 10-10 system (Figure 4.1B), using an adhesive, electrically conductive paste (ten20 Conductive Paste, Weaver and Co.). Impedance was kept below 20 kΩ (including two 5 Ω resistors in the cables of the MRI extension-kit of the stimulator). Accordingly, impedance between the electrodes was limited to 10 kΩ.

To minimize confounding influences from either phosphene or skin sensations, tACS was applied below participants' individual sensation threshold, using an established thresholding procedure (Kasten et al., 2016; Kasten and Herrmann, 2017; Neuling et al., 2013; Neuling et al., 2015). To this end, participants were stimulated with an initial intensity of 500 μA at their IAF. Depending on whether participants noticed the initial stimulation, intensity was either increased or decreased in steps of 100 μA until they noticed/not noticed the stimulation. The highest intensity at which participants did not notice the stimulation was subsequently used as tACS intensity in the main experiment. The thresholding was performed for both groups to keep experimental procedures similar. The obtained intensities for the sham group were applied during the 30 s stimulation train in the beginning of the stimulation block (see above). Three participants exhibited sensation thresholds below 400 μA and were excluded from analysis. On average, participants were stimulated with 715 μA $\pm$ 301 μA (peak-to-peak; stimulation group: 680 μA $\pm$ 175 μA) at a frequency of 10.5 Hz $\pm$ 0.9 Hz. TACS or sham stimulation was applied, immediately following the baseline block, for 20 min during the second and third blocks of the behavioral experiment.

4.5.4 Mental rotation task

Visual stimuli were presented using Psychtoolbox 3 (Kleiner et al., 2007) implemented in the same Matlab code that generated the electrical stimulation signal. Visual stimuli were rear-projected onto a screen inside the MSR at a distance of $\sim$100 cm from the participant.

Subjects performed the same MR paradigm that was employed in a recent tACS-EEG study (Kasten and Herrmann, 2017). Stimuli were taken from an open-source stimulus set (Ganis and

Kievit, 2015), comprising 384 MR stimuli (pairs of 3-dimensional objects) similar to the objects used in the seminal paper of Shepard and Metzler (1971). The duration of the experiment was reduced from 8 to 7 blocks of 10 min each. Participants were familiarized with the task on a laptop during electrode preparation (16 practice trials with immediate feedback). All other parameters were kept similar. Each block consisted of 48 trials, starting with the presentation of a white fixation cross at the center of the screen. After 3000 ms, an MR stimulus was presented for 7000 ms. During this time, participants were asked to judge whether the two objects on the screen were either identical (can be brought into alignment by rotating) or different (cannot be brought into alignment by rotating) by pressing a button with their left or right index finger (Figure 4.1C). To keep visual stimulation at a constant level, the MR stimuli remained on screen for the whole 7000 ms, regardless of participants' reaction times. Every 24 trials, the task was interrupted by a 1 min resting period during which a rotation of the fixation cross had to be detected. This ensured that participants remained focused and tried to avoid head movements. The first block served as a baseline measurement before stimulation. During the second and third block, tACS or sham stimulation was applied. The remaining four blocks served as post-stimulation measurements to capture aftereffects of the stimulation (Figure 4.1A). The experiment had a total duration of 70 min.

4.5.5 Debriefing

After finishing the experiment, participants filled out a translated version of a questionnaire assessing commonly reported side effects of transcranial electrical stimulation (Brunoni et al., 2011). Subsequently, they were asked to indicate whether they believe they received tACS or sham stimulation. Finally, all subjects were informed about the aims of the experiment and their actual experimental condition.

4.5.6 Data Analysis

Data analysis was performed using Matlab 2016a (The MathWorks). MEG data processing was performed using the Fieldtrip toolbox (Oostenveld et al., 2011) embedded in custom Matlab scripts.

4.5.6.1 Behavioral Data

Analysis of performance and reaction time (RT) data followed the approach of Kasten and Herrmann (2017). Performance, in percentage correct, in each block (48 trials) was calculated and normalized by pre-stimulation baseline to account for interindividual differences. The resulting values reflect per-

formance change in each block relative to baseline. RTs were averaged separately for each rotation angle and normalized by their respective baseline RT. The normalized RTs were then averaged over angles for each block. This procedure accounts for the known increase in RT with larger rotation angles (Shepard and Metzler, 1971).

4.5.6.2 MEG processing and artifact suppression

MEG data were resampled to 250 Hz and filtered between 1 and 40 Hz using a fourth-order, zero-phase Butterworth filter. Data were projected into source-space by application of a linearly constrained minimum variance (LCMV) beamformer (Van Veen et al., 1997), a procedure that has been demonstrated to suppress artifacts originating from transcranial electrical stimulation (Neuling et al., 2015; Soekadar et al., 2013). Filter coefficients were individually estimated for each block using the noise covariance matrix, an equally spaced (1.5 cm) 889-point grid warped into Montreal Neurologic Institute (MNI) space, and single-shell headmodels (Nolte, 2003), created from individual, T1-weighted MRIs. MRIs were coregistered to the median head position in each block, estimated from continuous HPI signals using the Elekta Neuromag MaxFilter software (Elekta Oy). The signal-space separation method (Taulu, Simola, and Kajola, 2005) offered by the software was not applied, as it seemed to corrupt tACS artifact suppression after beamforming. Covariance matrices were estimated by segmenting each MEG recording into 2 s epochs. The regularization parameter λ for the LCMV beamformer was set to zero to ensure optimal artifact suppression, as suggested by Neuling et al. (2017)).

Sensor-space MEG data were segmented –5 to 7 s around the onset of the MR stimuli. Epochs were then projected into source-space using the previously obtained beamformer filters, resulting in 889 virtual channels, distributed over the brain. A time–frequency analysis was computed for all trials using Morlet wavelets with a fixed width of 7 cycles. The resulting time–frequency spectra were averaged for each block.

As mentioned above, all analysis procedures in this study were rigorously checked with respect to their robustness against the influence of residual artifacts in the data (Neuling et al., 2017; Noury et al., 2016). This involved a careful choice of the measure used to capture event-related changes in oscillatory power. Traditionally, such changes have been evaluated using the concept of event-related (de-)synchronization (ERD/ERS), which has been defined by Pfurtscheller and Lopes Da Silva (1999) as:

$$ERD/ERS = \frac{R - A}{R} * 100, \tag{4.1}$$

where R is the oscillatory power within the frequency band of interest during a reference period, before stimulus onset, and A is the power during a testing period after stimulus onset. However, assuming that residual tACS artifacts (R_{Res} and A_{Res}) are equally contributing to R and A, this would change the equation in the following way:

$$ERD/ERS = \frac{(R + R_{Res}) - (A + A_{Res})}{(R + R_{Res})} * 100. \tag{4.2}$$

Given that the residuals in R and A are uncorrelated with the task and have approximately equal strength ($R_{Res} \approx A_{Res}$), their influence cancels out in the numerator but biases the denominator of the equation, resulting in systematic underestimations of the observed power modulations:

$$ERD/ERS = \frac{R - A}{(R + R_{Res})} * 100. \tag{4.3}$$

For this reason the pure difference between reference and testing period (for the sake of clarity referred to as event-related power difference; $ER\Delta_{Pow}$) was used to more accurately capture event-related power modulations in the current study:

$$ER\Delta_{Pow} = (R + R_{Res}) - (A - A_{Res}) = R - A. \tag{4.4}$$

Power in the individual alpha-band (IAF $\pm$ 2 Hz) was extracted with the reference and test periods ranging from -2.5 to -0.5 s before and 0 to 2 s after stimulus onset, respectively.

Performance of the artifact suppression was evaluated by estimating the size of the residual artifact relative to the brain oscillation of interest (see Evaluation of artifact suppression). As will be described in more detail in Results, the beamformer successfully suppressed the tACS artifact from $\sim$2,500,000 times the size of human alpha oscillations down to a factor of 3. However, some “hot spots” showing larger residual artifacts (1:10) are apparent in the proximity of stimulator cables and

the central stimulation electrode. To avoid the inclusion of virtual channels in the analysis that contain strong residual artifacts but no physiologically meaningful effects, brain areas showing strongest alpha-power modulation in response to the onset of the MR stimuli were localized based on the first (artifact-free) block before stimulation. To this end, a dependent-sample random permutation cluster t-test (two-tailed) with 5000 randomizations and Monte Carlo estimates to calculate p-values was run to compare power in the IAF-band between the reference and test periods during the baseline block. The test was performed on the whole sample (stimulation and sham group pooled). Clusters were thresholded at an α-level of 0.01. The resulting significant negative cluster was used as a region of interest (ROI) to extract the time course of $ER\Delta_{Pow}$ from each block. To account for interindividual differences, $ER\Delta_{Pow}$ in each block was normalized by $ER\Delta_{Pow}$ in the baseline block before stimulation. To test whether the effects of tACS were specific to the alphaband, the same analysis was performed on power modulations in the lower (IAF + 3 Hz to IAF + 11 Hz) and upper(IAF + 12 Hz to IAF + 20 Hz) beta-bands within the ROI.

4.5.6.3 Evaluation of artifact supression and control analyses

As discussed earlier, the application of LCMV beamforming results in a strong, yet imperfect, suppression of the tACS artifact (Mäkelä et al., 2017; Noury et al., 2016; Noury and Siegel, 2017). It is therefore crucial to characterize the achieved artifact suppression and rule out the possibility that the effects observed during stimulation result from residual artifacts in the data, rather than a true effect of tACS on the brain.

To evaluate the artifact suppression achieved by the spatial filtering procedure, participants' alpha-power (IAF $\pm$ 2 Hz) was extracted from the pre-stimulus interval of the baseline and the two stimulation blocks. The power in the baseline block provides an estimate of participants' natural, artifact-free alpha-power, which can be compared to the power encountered during stimulation blocks before (on the sensor-level) and after (on the sensor-level) beamforming. It is therefore possible to roughly estimate the size of the stimulation artifact relative to the brain signal of interest. This artifact-to-brain-signal-ratio was calculated for each magneto- and gradiometer channel as well as for each virtual channel after LCMV. While this measure is not able to disentangle brain signal/tACS effects from a residual artifact after LCMV, it can provide an upper boundary for the size of the residual artifact and allows the inspection of its spatial distribution.

A major assumption of the presented analysis framework, for event-related power modulations during tACS, is that the (residual) artifact has similar strength during the pre- and post-stimulus in-

tervals, such that its influence cancels out when contrasting (subtracting) the two intervals (Equation 4.4). Previous studies have demonstrated that physiological processes such as heartbeat and respiration can result in impedance changes of body tissue and small body movements, which change the size of the tACS artifact (Noury et al., 2016; Noury and Siegel, 2017). To rule out a similar modulation of artifact strength occurring in an event-related manner accounting for potential effects observed on the source-level, a control analysis was conducted. Sensor-level MEG time-series during the two stimulation blocks were bandpass-filtered around the stimulation frequency (IAF $\pm$ 1 Hz), and the signal envelope was extracted using a Hilbert transform. The envelope time series was subsequently segmented analogously to the $ER\Delta_{Pow}$ analysis and demeaned. The differences in envelope amplitude during pre-stimulus (-2.5 to -0.5 s) and post-stimulus (0–2 s) interval were compared by means of a random permutation cluster t-test with Monte Carlo estimates. To rule out the possibility that these differences drive the effects observed on the source-level, the envelope differences were correlated with the $ER\Delta_{Pow}$ values obtained earlier. For comparison, the same analysis was performed for the stimulation and sham group. For the sham group, envelope differences should reflect the event-related suppression of alpha-power, commonly observed during MR, and therefore highly correlate with the source-level $ER\Delta_{Pow}$. Pre- versus post-stimulus envelope differences in the stimulation group, however, should predominantly reflect changes in the tACS artifact. High correlations between sensor-space envelope differences and source-level $ER\Delta_{Pow}$ would thus indicate that systematic modulations of the tACS artifact drive changes in $ER\Delta_{Pow}$, rather than an actual physiological effect of tACS.

4.5.6.4 Experimental design and statistical analysis

Statistical analysis was realized in a 2 $\times$ 6 mixed-effects repeated-measures design with the between subject factor condition (stimulation versus sham) and the within subject factor block (6 levels). The normalized behavioral (performance, RTs) and physiological ($ER\Delta_{Pow}$) data were analyzed using repeated-measures ANOVAs (rmANOVA). Greenhouse-Geisser corrected p-values are reported where appropriate. If significant interactions between condition and block were revealed, analysis was subsequently split into two separate rmANOVAs, one covering the effects during stimulation (factors condition, stimulation vs. sham; block, block 2 vs. block 3) and the other analyzing outlasting effects (factors condition, stimulation vs. sham; block, block 4 vs. block 7). Comparisons of single blocks were performed using two-sample t-tests. Generalized R^2 and Cohen's d values are reported as measures of effect size. Pearson's correlation coefficients were calculated to relate behavioral and

physiological effects, as well as physiological effects and stimulation intensity.

Statistical analysis was performed using R 3.2.3 (The R Core Team, R Foundation for Statistical Computing). Cluster-based permutation tests on MEG data were performed in Matlab 2016a using statistical functions implemented in the Fieldtrip toolbox (Oostenveld et al., 2011).

4.5.6.5 Code accessibility

All scripts underlying the presented results are available as Extended Data and can be accessed online via the open science framework: https://osf.io/btnu7/.

4.6 Results

4.6.1 Behavioral results

A Welch's two-sample t-test yielded a trend for slightly better raw task performance in the baseline block for the sham group compared to the stimulation group ($t_{14.9} = -2.00, p = 0.06, d = 0.9; M_{Stim} = 87.3\%, SD = 3.6\%; M_{Sham} = 91.7\%, SD = 5.9\%$). The rmANOVA on relative performance change revealed a significantly larger facilitation of MR performance, relative to baseline, in the stimulation group compared to sham ($condition : F_{(1,18)} = 4.93, p = 0.04, \eta^2 = 0.14$). Average performance during and after stimulation was $M_{Stim} = 92.3\%$ ($SD = 2.5\%$) and $M_{Sham} = 90.9\%$ ($SD = 5.6\%$), respectively.

Experimental groups did not differ with respect to their baseline RTs ($t_{16} = 0.3, p = 0.77, d = 0.13, M_{Stim} = 2763ms, SD = 848ms, M_{Sham} = 2660ms, SD = 659ms$). Analysis of the normalized RTs revealed a trend for the factor block ($F_{(5,90)} = 2.47, p = 0.07, \eta^2 = 0.03$), but no effect of stimulation ($F_{(1,18)} = 1.02, p = .33, \eta^2)0.04$). Mean reaction times during and after stimulation were $M_{Stim} = 2597ms$ ($SD = 710ms$) and $M_{Sham} = 2371ms$ ($SD = 524ms$) on average. Results of the behavioral analysis are summarized in Figure 4.2.

4.6.2 Event-related alpha modulation

Comparison of pre- and post-stimulus IAF-band power, during the baseline block, revealed a significant cluster in occipito-parietal areas ($p_{cluster} < 0.001$; Figure 4.3A) for the whole sample. The identified cluster was used as an ROI to extract the time course of $ER\Delta_{Pow}$ from the different blocks and to limit the subsequent analysis to physiologically meaningful brain regions. The subsequent rmANOVA revealed a significant main effect of block ($F_{(5,90)} = 7.22, p = 0.009, \eta^2 = 0.15$) as well

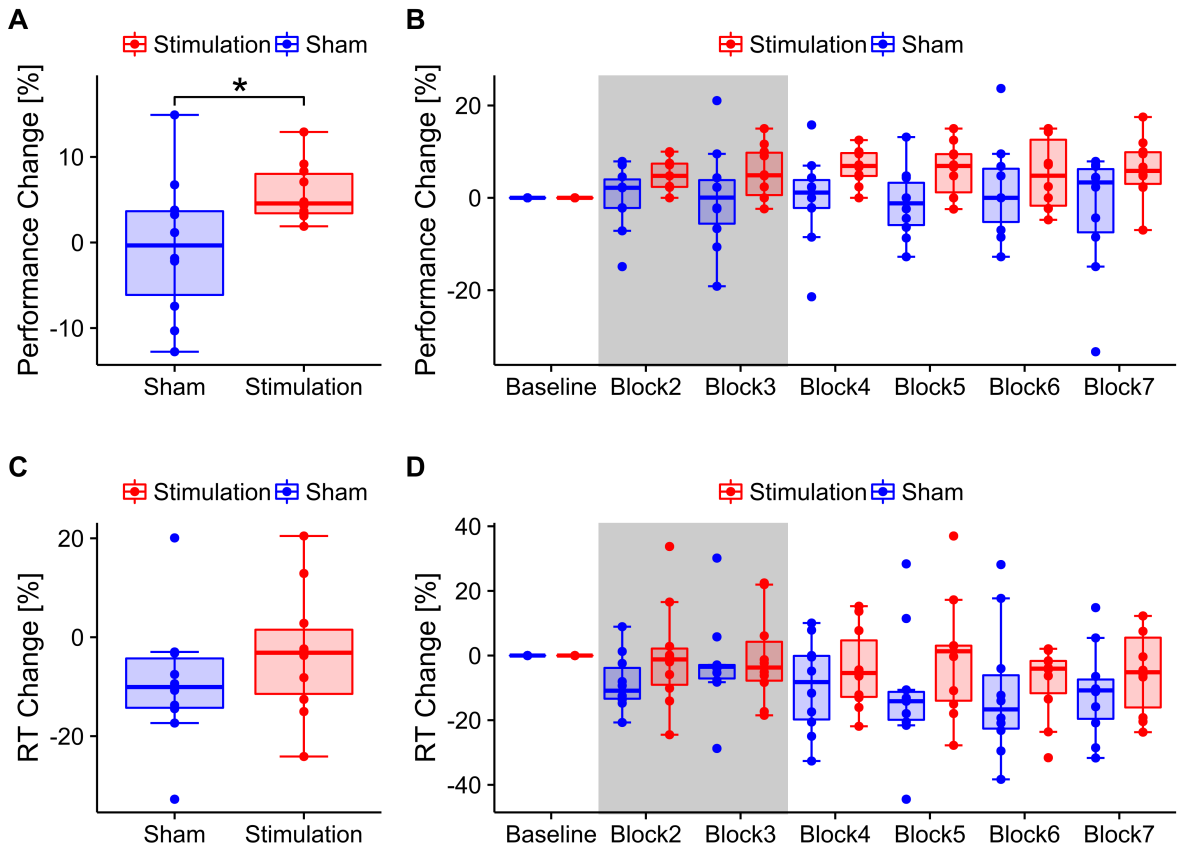

Figure 4.2: Behavioral results. **(A)** Change in task performance for stimulation and sham group, relative to baseline, pooled over all experimental blocks. Boxes indicate the 25th and 75th percentile of the sample distribution (interquartile length); lines inside the boxes mark the median. Whiskers extend to the most extreme values within 1.5 times the interquartile length. Asterisks code for significance ($*, p < 0.05$). **(B)** Change in task performance relative to baseline for stimulation and sham group depicted over experimental blocks. The gray area indicates blocks that were performed during tACS or sham stimulation. **(C)** Change in RT for stimulation and sham group relative to baseline pooled over experimental blocks. **(D)** Change in RT for stimulation and sham group relative to baseline depicted over experimental blocks. Gray area indicates blocks that were performed during tACS or sham stimulation.

as a significant condition $\times$ block interaction ($F_{(5,90)} = 6.81, p = 0.011, \eta^2 = 0.15$), and a trend for the main effect of condition ($F_{(1,18)} = 3.62, p = 0.07, \eta^2 = 0.10$). Please refer to Figure 4.3B for an overview of the time course of relative $ER\Delta_{Pow}$. To further resolve the significant interaction, separate rmANOVAs were performed on the data acquired during and after tACS. These analyses exhibited a significant main effect of condition ($F_{(1,18)} = 9.34, p = 0.007, \eta^2 = .27$) during stimulation, but not thereafter ($condition: F_{(1,18)} = 0.14, p = 0.71, \eta^2 = 0.01$; Figure 4.3C). Furthermore, a significant effect of block ($F_{(3,54)} = 3.55, p = 0.02, \eta^2 = 0.02$), as well as a significant condition $\times$ block interaction ($F_{(3,54)} = 3.10, p = 0.034, \eta^2 = 0.02$) were found in the post-stimulation data. None of the other main effects or interactions reached significance. It was not possible to further resolve the significant condition $\times$ block interaction during the poststimulation blocks. Separately testing relative $ER\Delta_{Pow}$ values of the two experimental groups against each other did not reveal significant differ-

ences for any of the blocks (all $p > 0.12$, Welch's two-sample t-test, one-tailed, uncorrected). Based on pure visual inspection, the interaction appears to be driven by a group difference during the first block after stimulation (block 4, see Figure $ER\Delta_{Pow}$B), which might be indicative of a weak tACS aftereffect during this block. Refer to Figure 4.4 for group-averaged time-frequency representations of participants' normalized alpha-power change and the corresponding source-level topographies within the analyzed ROI.

No significant correlation between the increase in $ER\Delta_{Pow}$ during stimulation and stimulation intensity was observed in the stimulation group ($r = 0.40, t_8 = 1.25, p = 0.24$). A weak, negative, non-significant correlation was observed in the sham group ($r = –0.26, t_8 = –0.78, p = 0.45$; Figure 4.3D).

To test whether the effects of tACS were specific to the alpha-band, the analysis was repeated on event-related power modulations in the lower (IAF + 3 Hz to IAF + 11 Hz) and upper (IAF + 12 Hz to IAF + 20 Hz) beta-bands within the ROI. The rmANOVA for the lower beta-band revealed a significant effect of block ($F_{(5,90)} = 15.10, p = 0.001, \eta^2 = 0.17$) as well as a significant condition $\times$ block interaction ($F_{(5,90)} = 9.37, p = 0.001, \eta^2 = 0.11$). Two separate rmANOVAs, testing the effects during and after stimulation, revealed a trend for the factor condition during stimulation ($F_{(1,18)} = 4.17, p = 0.056, \eta^2 = 0.18$) as well as a significant effect of block ($F_{(1,18)} = 4.72, p = 0.043, \eta^2 = 0.02$). After stimulation, only a trend for the factor block was found ($F_{(3,54)} = 2.28, p = 0.09, \eta^2 = 0.03$). No significant effects were found in the analysis of the upper beta-band. Figure 4.3E, F summarizes results for the lower and upper beta-band analysis (all $p > 0.1$).

There were no significant correlations between relative $ER\Delta_{Pow}$ and change in task performance during ($r_{online} = 0.3, t_{18} = 1.37, p = 0.18$) or after ($r_{offline} = 0.11, t_{18} = 0.49, p = 0.62$) stimulation. Descriptively, the correlation was higher for the sham group both during and after stimulation ($r_{Sham/online} = 0.51, t_8 = 1.67, p = 0.13$; $r_{Sham/offline} = 0.54, t_8 = 1.83, p = 0.1$) compared to the stimulation group ($r_{Stim/online} = 0.09, t_8 = 0.27, p = 0.8$; $r_{Stim/offline} = –0.16, t_8 = –0.45, p = 0.67$; Figure 4.3G, H).

4.6.3 Control analyses

To rule out the possibility that the strikingly strong facilitation of power modulation in the alpha-band was driven by residual artifacts, several control analyses were performed. In a first step, the performance of the artifact suppression achieved by LCMV was evaluated. To this end, the ratio of pre-stimulus alpha-power during the (tACS-free) baseline block and the two tACS blocks was com-

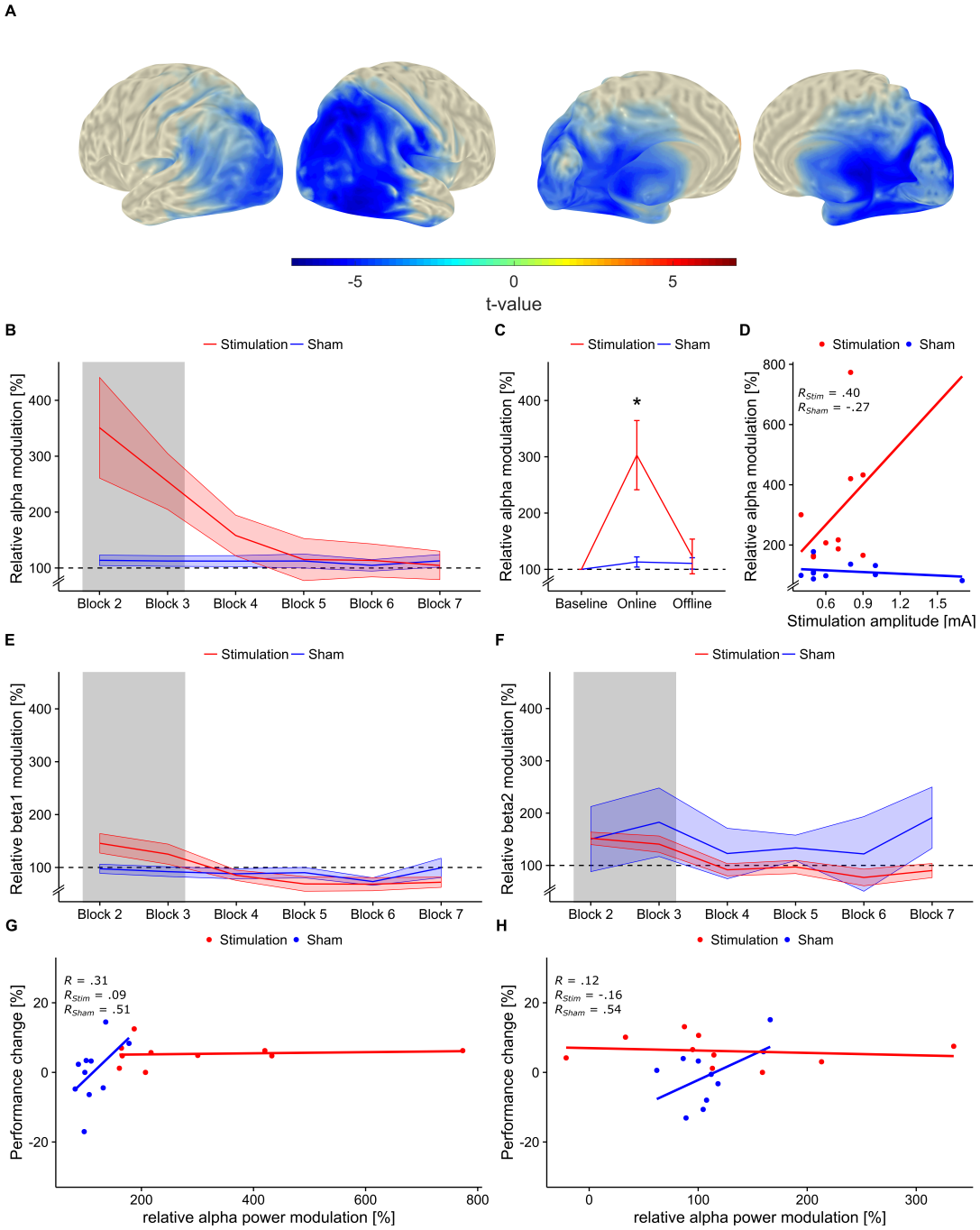

Figure 4.3: Event-related alpha-power modulation. (A) Region of interest (ROI). Significant cluster (pre- vs. post-stimulus power) in the IAF-band during the first block before tACS or sham stimulation, computed over the whole sample ($p_{cluster} < 0.001$). Topographies depict t-values mapped on an MNI standard surface. Statistical maps are thresholded at $\alpha < 0.01$. The depicted cluster (blue) was used as ROI to extract the time course of alpha-power modulation, relative to baseline, over blocks from the virtual channels. **(B)** Relative alpha-power modulation within ROI depicted for each block. The gray area indicates blocks during tACS or sham stimulation. Shaded areas represent standard error of the mean (SEM). Dashed line depicts baseline level. **(C)** Relative alpha-power modulation during tACS or sham (online) and after stimulation (offline). Error bars represent SEM; asterisks code for significant differences ($*, p < 0.05$). **(D)** Relative alpha-power modulation during stimulation correlated with stimulation intensity. Each point represents a single subject's stimulation amplitude and relative alpha-power modulation, averaged over the two stimulation blocks (blocks 2 and 3). Please note that a stimulation intensity was determined for all participants (including sham); however, only participants in the stimulation group had this intensity continuously applied during blocks 2 and 3. **(E)** Relative power modulation in the lower beta-band (IAF + 3 Hz to IAF + 11 Hz) within the ROI for each block. **(F)** Relative power modulation in the higher beta-band (IAF + 12 Hz to IAF + 20 Hz) within the ROI for each block. **(G, H)** Correlation between change in task performance and relative alpha-power modulation during **(G)** and after **(H)** tACS. High, albeit nonsignificant, correlations were evident for the sham group, but not the stimulation group.

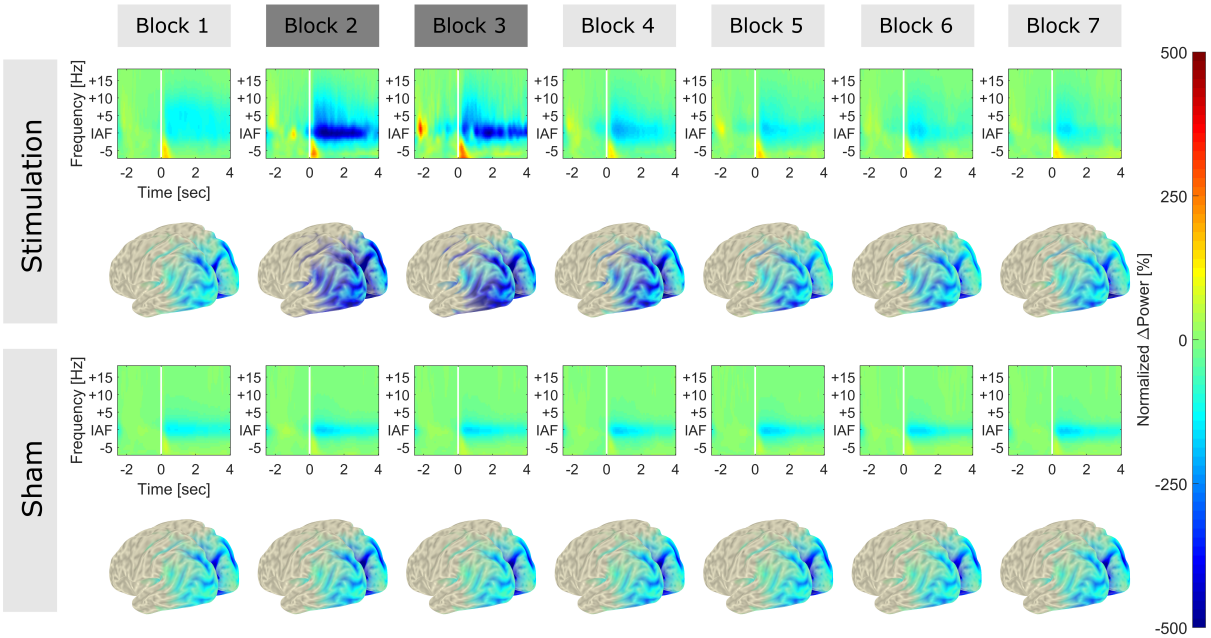

Figure 4.4: Normalized, baseline-subtracted TFRs and source topographies. TFRs and source topographies for stimulation **(top rows)** and sham group **(bottom rows)**. TFRs were aligned at IAF and averaged over subjects in each group. The range from –2.5 to –0.5 s before stimulus onset (white bar) served as reference period for baseline subtraction. Spectra were subsequently normalized by the power difference in the alpha-band (IAF $\pm$ 2 Hz) during the baseline block (block 1) before stimulation. Normalization was performed such that the data presented resemble data in the statistical analysis. Blocks 2 and 3 (dark gray) represent data acquired during tACS or sham stimulation. All other blocks (light gray) were measured in absence of stimulation. Functional maps were averaged over subjects and projected onto an MNI standard surface. Only activity within the analyzed ROI is depicted. A strong facilitation of event-related power modulation around the IAF can be observed during tACS application (block 2 and 3).

pared in sensor- and source-space. On average, this artifact-to-brain-signal ratio was 2,534,000:1 in block 2 and 2,569,000:1 in block 3 (average over all sensors and subjects) in the sensor-space data. After LCMV beamforming, the ratio was reduced to 2.72:1 in block 2 and 3.13:1 in block 3 (average over virtual sensors and subjects). The largest ratio observed in a single virtual channel of one subject after beamforming was 93.42:1. Figure 4.5 illustrates the spatial distribution of the artifact-to-brainsignal ratio on the source-level. The ratio was highest in central areas, covered by stimulation electrodes and cables. Outside of these areas, the ratio was substantially smaller and falls within a physiologically plausible range for alpha-band oscillations ($<$4:1). Overall artifact suppression appeared to be slightly worse during block 3 compared to block 2.

The event-related envelope of the sham group was consistent with the pattern of alpha-power decrease typically observed after stimulus onset in the MR task in both sensor types. This was confirmed by the permutation cluster analysis, which revealed significant positive clusters in the magnetometer and the gradiometer data ($p_{cluster} = 0.001$, Figure 4.6A, C; significant sensors are marked by black dots), and further supported by the high correlation between source-level power modulation and envelope difference of magnetometer ($r = 0.96, t_8 = 10.17, p = 0.001$; Figure 4.6B) and

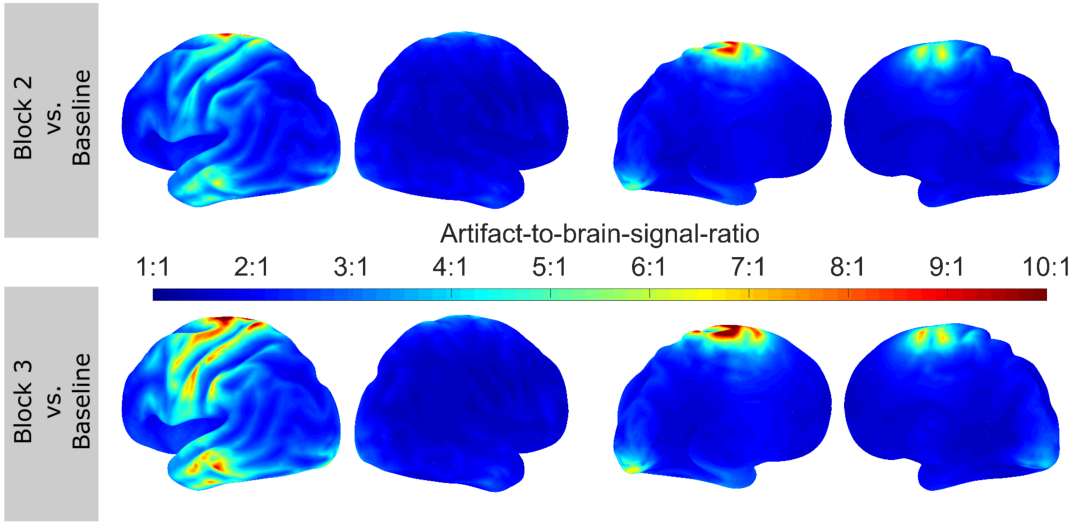

Figure 4.5: Artifact-to-brain-signal topographies. Topographies depict the average ratio between participants' pre-stimulus alphapower, estimated during the baseline block, and residual artifact in the pre-stimulus interval during block 2 **(top row)** and 3 **(bottom row)**. Results are depicted only for the stimulation group. The ratio is strongest in central areas covered by the stimulation electrodes and cables. Frontal and posterior areas within the ROI seem less affected, with the ratio falling in a physiologically plausible range (<1:4), such that residual artifact and facilitatory effects of the stimulation or spontaneous increase of alpha power cannot be disentangled. Results have to be interpreted in terms of an upper boundary for the size of the residual artifact, as each virtual channel contains a mixture of brain signal of interest and artifact.

gradiometer ($r = 0.88, t_8 = 5.23, p = 0.001$; Figure 4.6D) channels. In the stimulation group, time course and topography of the envelope overall exhibited the opposite pattern, with lower amplitudes before stimulus onset and increased amplitude thereafter. In addition, the envelope time course of gradiometers shows a prominent rhythmic activity in the range of 1–2 Hz. This could potentially reflect heartbeat-related modulations of the tACS waveform (Noury et al., 2016). However, given that this rhythmic activity was observed in only one sensor type and in a relatively systematic manner, it more likely reflects a technical artifact. Importantly, no such rhythmic modulation was evident in the time–frequency representations after LCMV (Figure 4.4). Results of the cluster analysis revealed positive clusters in the gradiometer data in only a few frontal sensors ($p_{cluster} = 0.05$; Figure 4.6, top left) as well as positive and negative clusters for some magnetometer channels ($p_{cluster} = 0.05$). No significant correlation was evident between the observed source-level power modulations and the sensor-level envelope differences in magnetometer ($r = 0.13, t_8 = 0.37, p = 0.72$) or gradiometer sensors ($r = 0.26, t_8 = 0.75, p = 0.47$). Overall, results do not support the idea that the effects observed on the source-level can be explained by systematic, task-related changes in artifact strength. Very few channels were found to exhibit significant, taskrelated power modulations. Those that did rather seemed so show a reversed pattern of artifact modulation compared to the source-level data.

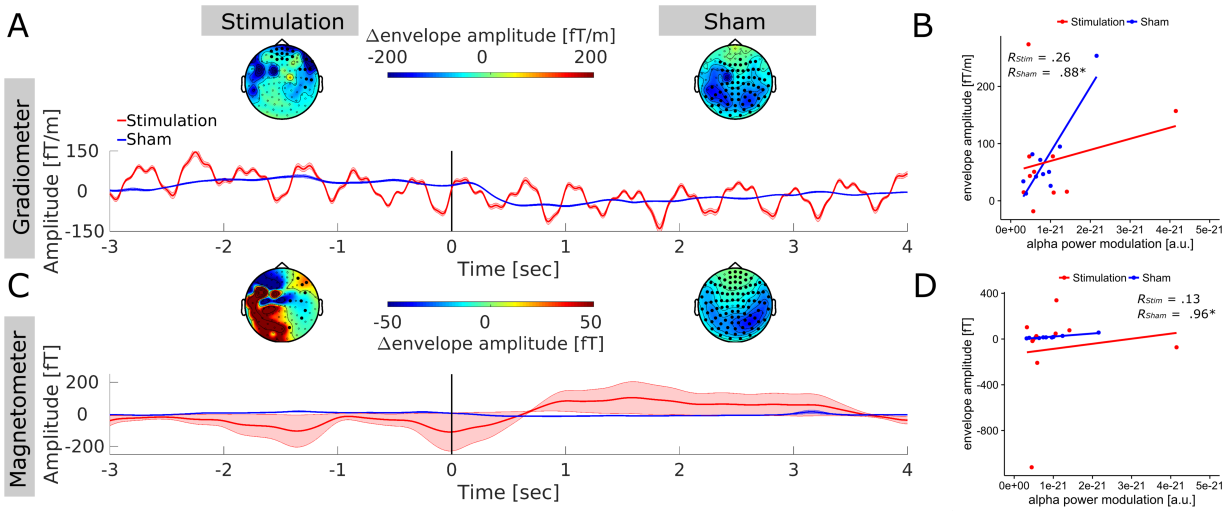

Figure 4.6: Event-related artifact envelope. (A) Topography and time course of the artifact envelope around stimulus onset in gradiometer sensors. Topographies represent the amplitude difference of the envelope, around the stimulation frequency between the reference (–2.5 to –0.5 s) and the testing periods (0–2 s). Darkened sensors mark locations in which this difference was significant. Data of the sham group is depicted for comparison and reflects the task-related modulation of endogenous alpha oscillations (visible shortly after stimulus onset, vertical black bar at 0 s) as no stimulation artifact was introduced to the data. Envelope epochs of all subjects were demeaned before averaging to enhance comparability of the envelope modulation. Shaded areas depict standard error of the mean (SEM). Gradiometer time courses were strongly dominated by rhythmic modulation around 1–2 Hz that potentially reflects a technical artifact in this sensor type. **(B)** Correlation between event-related modulation of the artifact envelope in gradiometer sensors and event-related alpha-power modulation within the ROI after beamforming. The absence of a significant (or even moderately high) correlation in the stimulation group provides supporting evidence that the effects observed in source-space are not driven by systematic event-related modulations of tACS artifact strength. **(C)** Topography and time course of the artifact envelope around stimulus onset in magnetometer sensors. **(D)** Correlation between event-related modulation of the artifact envelope in magnetometers and alpha-power modulation within ROI after beamforming. Similar to the gradiometer data, no correlation between source-level effects and artifact tACS artifact modulation was observed.

4.7 Discussion

To date, few studies have investigated the effects of tACS on oscillatory activity in the human brain during stimulation (Helfrich, Schneider, et al., 2014; Ruhnau et al., 2016; Voss et al., 2014), due to the massive electromagnetic artifact encountered during the measurement. The current study adds to this line of research by characterizing how eventrelated oscillatory activity during a cognitive task reacts to externally applied perturbations in the same frequency band. Theoretically, tACS could counteract, overwrite, or enhance the oscillations underlying performance of the task.

Results show that, rather than counteracting or overwriting the event-related down-regulation of oscillatory power during the mental rotation (MR) task, continuous application of tACS facilitated the pre-existing difference between pre- and post-stimulus power in the alpha-band. This finding indicates that tACS exerts its effects differently during pre- and post-stimulus intervals. Given that tACS is usually observed to facilitate power of the targeted brain oscillation after stimulation, the current finding seems most likely to be caused by stronger enhancement of alpha-power before stimulus on-

set (Kasten and Herrmann, 2017; Neuling et al., 2013; Veniero et al., 2015), rather than inhibition of post-stimulus alpha-power. Unfortunately, this cannot be resolved using the current data, as the contrast between pre- and post-stimulus intervals was necessary to account for residual tACS artifacts. To directly observe differential effects of tACS on event-related brain oscillations, future work might make use of amplitude-modulated tACS (AM-tACS), which has been proposed as a strategy to overcome the strong electrophysiological artifact in the range of the targeted brain oscillation (Witkowski et al., 2016). This new stimulation waveform has very recently been shown in a computational model to exhibit entrainment mechanisms similar to those of conventional sine-wave tACS (Negahbani et al., 2018). However, it should be noted that two recent studies cast doubts on whether AM-tACS is entirely free of stimulation artifacts in the range of the targeted brain oscillation (Kasten, Negahbani, Fröhlich, and Herrmann, 2018; Minami and Amano, 2017). Thus, careful assessment of brain signals recorded during stimulation would still be required.

A differential effect of tACS on pre- and post-stimulus intervals can be interpreted in terms of a short-scale state dependence of tACS effects. Several studies have demonstrated that tACS effects are state-dependent on larger time scales. On the one hand, tACS in the alpha-band seems to only be effective when the targeted brain oscillation is comparatively low in amplitude, e.g. during eyes open, but not during eyes closed (Alagapan et al., 2016; Neuling et al., 2013; Ruhnau et al., 2016). On the other hand, involvement of the targeted brain oscillation in a given state (or task) also seems necessary to successfully induce tACS effects (Feurra et al., 2013). In the simplest case, pre- and post-stimulus intervals in the current study reflect two distinct brain states (a resting or preparatory state and an MR state) that differ in terms of alphaoscillation involvement and susceptibility to tACS. This pattern is in line with predictions derived from synchronization theory, which require the presence of a selfsustained oscillator for entrainment to occur (Pikovsky et al., 2003). Consequently, tACS might exhibit its effect during the pre- but not during the post-stimulus interval where alpha oscillations are suppressed due to the task.

Although the current findings converge with observations of facilitated event-related desynchronization (ERD) after tACS (Kasten and Herrmann, 2017), it is important to emphasize that online effects of tACS (during stimulation) cannot directly be inferred from effects measured after stimulation. While computational models and animal experiments suggest entrainment as the core mechanism of online tACS effects (Fröhlich and McCormick, 2010; Ozen et al., 2010; Reato et al., 2010), there is increasing evidence that the aftereffects of tACS might be better explained by mechanisms of neural plasticity (Vossen et al., 2015; Zaehle et al., 2010). Different mechanisms of action, during and after stimulation, could in principle lead to different effects of tACS on event-related oscillations. Thus, di-

rect observations of tACS online effects are inevitable to predict and understand behavioral outcomes of tACS experiments.

The observed enhancement of event-related alphapower modulation can explain previous results of better performance in the MR task during tACS (Kasten and Herrmann, 2017). Mental rotation tasks typically feature alpha oscillations before stimulus onset, followed by taskinduced suppression of the oscillation. The suppression typically lasts until participants finish task execution (Michel et al., 1994). Studies using repetitive transcranial magnetic stimulation (rTMS) and neurofeedback training (NFT) have demonstrated facilitated MR performance when targeting spontaneous alpha oscillations during the pre-stimulus interval (Hanslmayr et al., 2005; Klimesch et al., 2003; Zoefel et al., 2011). More broadly, alpha oscillations have been suggested to enhance performance, in a variety of tasks, by suppressing activity in task-irrelevant areas of the brain or in preparation for an upcoming event, which has been referred to as “gating by inhibition” (Jensen and Mazaheri, 2010). By selectively enhancing prestimulus alpha-power, tACS could facilitate the preparatory gating and thus benefit subsequent task performance.

While the results are in agreement with previous findings (Kasten and Herrmann, 2017), they contradict observations of Neuling et al. (2015). That study reported a tendency for reduced alpha desynchronization elicited by a passive visual task during tACS. However, the authors calculated relative change (computed similarly to ERD/ERS) to capture event-related alpha desynchronization, which is vulnerable to residual artifacts in the data. As shown in Equations 4.2 and 4.3, such a residual artifact would lead to a biased (larger) denominator, resulting in systematic underestimations of ERD within the stimulated frequency band. Using the absolute power difference (here termed $ER\Delta_{Pow}$) between two time intervals within the same stimulation condition (i.e., pre-/post-stimulus alpha-power) appears to be a more robust measure to capture online effects of tACS. Using such a procedure, the residual artifact cancels out during the subtraction process. Importantly, this cancelation assumes that the strength of the residual artifact is relatively stable between conditions and uncorrelated with the task. Such systematic modulations could in principle occur if the task elicits systematic changes in physiological processes like heartbeat, respiration, or skin conductance (Noury et al., 2016). While there was no evidence for such a systematic change in artifact strength that could explain the observed pattern in the current data, the possibility has to be taken into account when using stimuli that can elicit stronger physiological responses (e.g., emotional pictures or demanding motor tasks). However, the impact of these modulations on the artifact suppression, compared to the size of the physiological effect on the brain, has not been thoroughly characterized yet.

In addition to the observed effect of tACS on power modulations in the alpha-band, the data

revealed a trend toward increased event-related power modulations in the lower beta-band during tACS. This observation could be indicative of a rather unspecific effect of tACS (Kleinert, Szymanski, and Müller, 2017). Alternatively, the effect in the lower betaband could be explained by entrainment or as a resonance phenomenon at the first harmonic of subjects' stimulation frequency (Herrmann, 2001; Herrmann, Murray, et al., 2016). Further, cross-frequency interactions between alpha and beta oscillations (Palva, 2005) could underlie the effects, resulting in co-modulation of beta oscillations stemming from tACS effects in the alpha-band.

Contradicting the previous finding of a prolonged, tACS-induced ERD increase in the alpha-band (Kasten and Herrmann, 2017) and despite the substantial online effects, only a short-lasting aftereffect during the first block after stimulation was observed, if at all. Several studies have successfully shown persistent effects of tACS on alpha-power during rest (Kasten et al., 2016; Neuling et al., 2013; Veniero et al., 2015; Vossen et al., 2015). A possible explanation for the lack of a sustained tACS effect in the current study was the relatively low stimulation intensity compared to the aforementioned experiments.

Similar to previous work (Kasten and Herrmann, 2017), a significantly stronger increase in MR performance was observed in the stimulation group compared to the sham group. Unfortunately, it cannot be ruled out that this effect might have been partly driven by differences in baseline performance between the two groups. This could also explain the absence of previously observed correlations between performance increase and facilitated alphapower modulation (Kasten and Herrmann, 2017), which would have further supported the physiological findings. Alternatively, the strong effect of tACS on participants' alpha-power modulation during stimulation might have caused ceiling effects such that, beyond a certain level, MR performance could not be facilitated any further. However, due to the differences in baseline performance, interpretability of the current behavioral results is limited. Nonetheless, this does not contradict the physiologic effects, which were the main focus of the current study. MR tasks induce comparably long-lasting event-related power modulations (Michel et al., 1994), a beneficial property when studying tACS effects on event-related oscillations. In the current experiment, this came at the cost of overall high task performance in both groups. Future studies might therefore benefit from more difficult MR paradigms (e.g., only including large rotation angles).

In addition to investigating the concurrent effects of tACS on event-related oscillations, the current study made an attempt to quantify the artifact suppression capabilities of LCMV beamforming. To this end, the oscillatory power around the stimulated frequency during tACS was compared to an artifact-free estimate of participants' natural brain signal (alpha-power). This allowed to estimate the magnitude of the stimulation artifact relative to the brain signal of interest before and after artifact

suppression. In the current study, this artifact-to-brain-signalratio was reduced from ∼2,500,000:1, before LCMV, to ∼3:1 thereafter, with stronger artifacts around stimulation electrodes and cables (∼10:1). Since the power values obtained during stimulation will always contain a mixture of residual tACS artifact and brain signal, this ratio can provide only an upper boundary for the size of the residual artifact. Alpha-power increase, by a factor of 3 or 4, falls into a physiologically plausible range for spontaneous of stimulation-induced alpha-power changes, consistent with previous work on tACS aftereffects (Kasten and Herrmann, 2017; Neuling et al., 2013; Stecher et al., 2017). The artifact-to-brain-signal ratio might nevertheless be a useful tool for future studies to assess whether a residual artifact falls within the same order of magnitude as the brain signal of interest. It might also be used to evaluate and optimize the performance of artifact suppression techniques, i.e., by tuning relevant parameters. Thus far, artifact suppression approaches have mostly been evaluated subjectively, i.e., by inspecting raw time series (time-) frequency spectra or ERPs (Helfrich, Schneider, et al., 2014; Neuling et al., 2015; Witkowski et al., 2016). The artifactto-brain-signal ratio provides a more objective evaluation of the artifact size, relative to the brain signal of interest, and is scale-free, allowing for easy comparison of different artifact suppression approaches even between different measurement modalities (EEG/MEG, LCMV, template subtraction, etc.). In addition, the mapping of residual artifact strength allows the assessment of overlap between hot spots of residual artifacts and regions of interest.

The findings presented in the current study provide the first direct insights concerning the online effects of tACS on event-related oscillations in humans. The effects were investigated using a rather simplistic approach, using only two conditions (stimulation vs. sham) and one stimulation frequency, targeting posterior alpha oscillations with a Cz-Oz montage. This path was chosen to establish an analysis framework, including controls, for the investigation of concurrent effects of tACS. Success at this stage would greatly facilitate approaches with more complex designs requiring larger sample sizes and higher computational efforts. TACS experiments generally allow for a multitude of control and contrast conditions, including alternative electrode montages and frequencies. The current study can therefore neither resolve frequency nor montage specificity of tACS effects. However, with the present results and the proposed analysis pipeline, the current study paves the way for further investigations of montage and frequency specificity of tACS effects, specifically on event-related oscillatory dynamics during various cognitive tasks.

4.8 Acknowledgements

This research was supported by a grant of the German Research Foundation (Deutsche Forschungsgemeinschaft, DFG) awarded to Christoph S. Herrman (DFG, SPP, 1665 HE 3353/8-2).

We thank Yvonne Wolf-Rosier for her invaluable efforts and assistance during data collection and Dr. Joshua Grant for proofreading this manuscript.

Chapter 5

Study IV: Non-linear transfer characteristics of stimulation and recording hardware account for spurious low-frequency artifacts during amplitude modulated transcranial alternating current stimulation (AM-tACS)

Published as:

Kasten, FH., Negahbani, E., Frohlich, F., Herrmann, CS., (2018) Non-linear transfer characteristics of stimulation and recording hardware account for spurious low-frequency artifacts during amplitude modulated transcranial alternating current stimulation (AM-tACS). *NeuroImage.*, 179, 134-143

Author Contributions:

Designed research: FHK, EN, FF, CSH

Perfomed Research: FHK

Analyzed Data: FHK

Wrote paper: FHK, EN, FF, CSH

5.1 Abstract

Amplitude modulated transcranial alternating current stimulation (AM-tACS) has been recently proposed as a possible solution to overcome the pronounced stimulation artifact encountered when recording brain activity during tACS. In theory, AM-tACS does not entail power at its modulating frequency, thus avoiding the problem of spectral overlap between brain signal of interest and stimulation artifact. However, the current study demonstrates how weak non-linear transfer characteristics inherent to stimulation and recording hardware can reintroduce spurious artifacts at the modulation frequency. The input-output transfer functions (TFs) of different stimulation setups were measured. Setups included recordings of signal-generator and stimulator outputs and M/EEG phantom measurements. 6^{th}-degree polynomial regression models were fitted to model the input-output TFs of each setup. The resulting TF models were applied to digitally generated AM-tACS signals to predict the frequency of spurious artifacts in the spectrum. All four setups measured for the study exhibited low-frequency artifacts at the modulation frequency and its harmonics when recording AM-tACS. Fitted TF models showed non-linear contributions significantly different from zero (all $p < .05$) and successfully predicted the frequency of artifacts observed in AM-signal recordings. Results suggest that even weak non-linearities of stimulation and recording hardware can lead to spurious artifacts at the modulation frequency and its harmonics. These artifacts were substantially larger than alpha-oscillations of a human subject in the MEG. Findings emphasize the need for more linear stimulation devices for AM-tACS and careful analysis procedures, taking into account low-frequency artifacts to avoid confusion with effects of AM-tACS on the brain.

5.2 Introduction

Transcranial alternating current stimulation (tACS) is receiving growing popularity as a tool to interfere with endogenous brain oscillations in a frequency specific manner (Fröhlich and McCormick, 2010; Helfrich, Schneider, et al., 2014; Herrmann et al., 2013; Ozen et al., 2010; Zaehle et al., 2010), allowing to study causal relationships between these oscillations and cognitive functions (Fröhlich, 2015; Herrmann, Murray, et al., 2016). Further, its use might offer promising new pathways for therapeutic applications to treat neurological or psychiatric disorders associated with dysfunctional neuronal oscillations (Brittain et al., 2013; Herrmann and Demiralp, 2005; Mellin et al., 2018; Uhlhaas and Singer, 2006, 2012).

While mechanisms of tACS have been studied in animals (Fröhlich and McCormick, 2010; Kar

et al., 2017; Ozen et al., 2010; Reato et al., 2010) and using computational modelling (Ali et al., 2013; Reato et al., 2010; Zaehle et al., 2010), the investigation of tACS effects in human subjects has so far mostly been studied behaviorally (Kar and Krekelberg, 2014; Lustenberger et al., 2015; Neuling, Rach, Wagner, et al., 2012), by measuring BOLD response (Cabral-Calderin et al., 2016; Violante et al., 2017; Vosskuhl et al., 2016), or by tracking outlasting effects in M/EEG signals (Kasten et al., 2016; Kasten and Herrmann, 2017; Neuling et al., 2013; Veniero et al., 2015; Vossen et al., 2015; Zaehle et al., 2010). Due to a strong electro-magnetic artifact, which spectrally overlaps with the brain oscillation under investigation, online measurements of tACS effects in M/EEG remain challenging. However, uncovering these online effects is crucial as the aforementioned approaches can only provide limited, indirect insights to the mechanisms of action during tACS in humans. In addition, online monitoring of physiological signals during stimulation may enable closed-loop applications that can provide potentially more powerful, individually tailored, adaptive stimulation protocols (Bergmann et al., 2016). Some authors applied artifact suppression techniques such as template subtraction (Dowsett and Herrmann, 2016; Helfrich, Schneider, et al., 2014; Voss et al., 2014) or spatial filtering (Neuling et al., 2015; Ruhnau et al., 2016) to recover brain signals obtained during concurrent tACS-M/EEG. However, these approaches are computationally costly, and therefore i.e. difficult to implement in closed-loop protocols. Further, their application is limited as they fail to completely suppress the artifact and analysis approaches must be limited to robust procedures to avoid false conclusions about stimulation effects (Neuling et al., 2017; Noury et al., 2016; Noury and Siegel, 2017, 2018).

As a solution to these issues, amplitude modulated tACS (AM-tACS), using a high frequency carrier signal which is modulated in amplitude by a lower frequency modulation signal, chosen to match the targeted brain oscillation has been proposed (Witkowski et al., 2016). A recent simulation study demonstrated that, similar to conventional tACS, this type of waveform is capable of entraining neuronal activity in a cortical model to the frequency of the envelope modulation, albeit to a smaller extent (Negahbani et al., 2018). Amplitude modulated waveforms contain spectral power at the frequency of the carrier signal (f_c) and two sidebands at $f_c\pm$ modulation frequency (f_m), but no power at f_m itself (see Figure 5.1 for an illustration). Consequently, the tACS artifact would be shifted into higher frequencies, elegantly avoiding spectral overlap with the targeted brain oscillation. In addition, physiologically driven modulations of artifact strength that result in side-bands around the stimulation artifact (Noury et al., 2016) would be shifted into higher frequencies in a similar manner. However, more recently low-frequency artifacts at f_m have been reported in sensor-level MEG recordings during AM-tACS (Minami and Amano, 2017). These artifacts required the application of

advanced artifact suppression algorithms (Minami and Amano, 2017). Although the authors of that study explained these artifacts by non-linear characteristics of the digital-analog conversion, a detailed investigation into these low-frequency artifacts and how they emerge during AM-tACS has not yet been provided. In fact, the process of stimulation on the one side and signal recording on the other side involves at least one step of digital-analog (generating a stimulation signal) and one step of analog-digital conversion (sampling brain signal plus stimulation artifact). The linearity of these conversions is naturally limited by properties of the hardware in use (Vargha, Schoukens, and Rolain, 2001). To further complicate the situation, the amplification involved in the recording process using M/EEG can be another potential source of nonlinearity. The amplitudes usually applied in tACS can potentially cause signals/artifacts, beyond the dynamic range where the measurement devices exhibit linear transfer characteristics (Cooper, Osselton, and Shaw, 1974). In general, all electronic components, including those that are usually idealized as being linear (e.g. resistors), exhibit some degree of non-linearity in reality, especially when operating under extreme conditions (Maas, 2003).

To shed light on the effects of non-linearity of stimulation and recording hardware on AM-tACS signals, input-output transfer functions (TFs) of different AM-tACS setups were estimated and evaluated with respect to their performance in predicting low-frequency artifacts of AM-tACS (In contrast to the frequency-domain definition of TFs commonly used in linear-system analysis, here TF refers to the input-output amplitude relation of a probe signal).

5.3 Materials and Methods

In order to characterize non-linearities inherent to different tACS setups, the transfer functions (TFs) relating input-output amplitudes of four different setups, with increasing complexity, were recorded and modeled by polynomial regression models. Additionally, AM-tACS signals were recorded to demonstrate the presence of low-frequency artifacts. TF models were applied to digital AM-signals to predict output spectra of the physical recordings.

To relate the strength of low-frequency artifacts during AM-tACS to the size of neuronal signals in the human brain, an additional MEG dataset was acquired from a human pilot subject (27 years, male, right-handed). The participant gave written informed-consent prior to the measurement. The experimental protocol was approved by the "*Commission for Research Impact Assessment and Ethics*" at the University of Oldenburg.

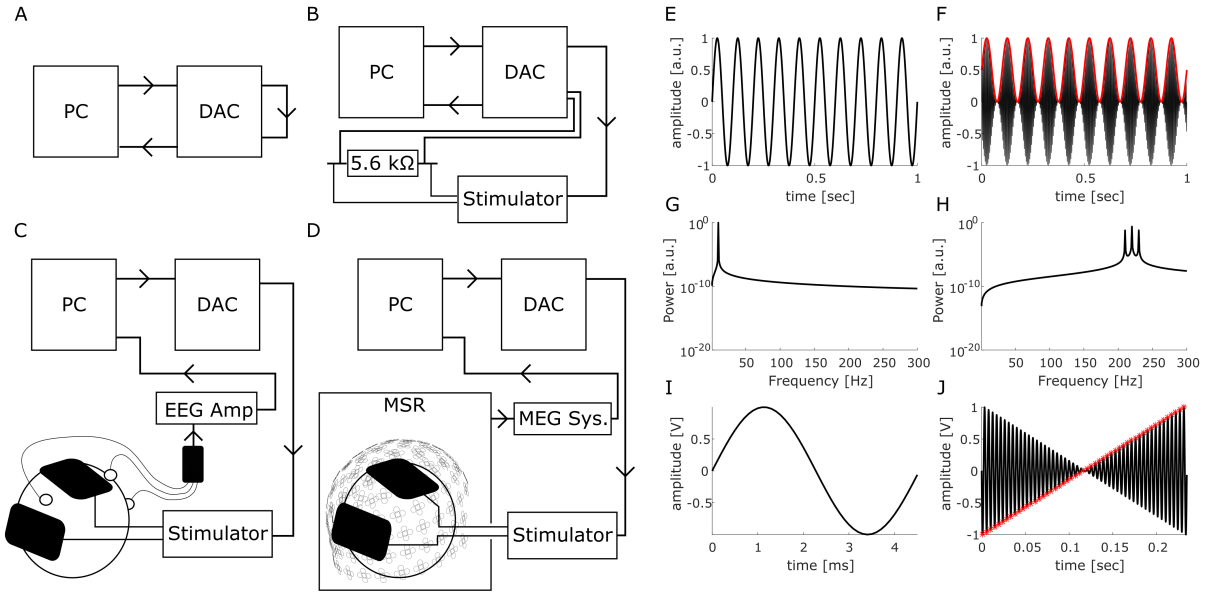

Figure 5.1: Experimental setups and signals. (A-D) Schematic representations of the evaluated setups. For details refer to the "**Test setups**" section in the manuscript. DAC: Digital-Analog converter. MSR: Magnetically shielded-room. Arrows indicate the direction of signal flow **(E,F)** Time-domain representations of a low-frequency sine-wave conventionally used for tACS **(E)** and an amplitude modulated sine-wave with a carrier frequency of 220 Hz modulated at 10 Hz **(F)**. Red curve depicts the 10 Hz envelope of the signal. **(G,H)** Frequency-domain representations of the tACS signals. While the 10 Hz sine wave exhibits its power at 10 Hz **(G)**, the amplitude modulated signal only exhibits power at the carrier frequency and two side-bands, but no power at the modulation frequency **(F)**. **(I)** Probe stimulus for measuring the setups transfer curves was a 220 Hz single-cycle sine wave. Probe stimuli of different amplitude were concatenated to a sweep **(J)**. Red asterisks mark points that were extracted as V_{out} measure. To enhance visibility of the general concept, a sweep consisting of 51 probes is displayed here. For the actual measurements of the TFs 10 sweeps with 10001 probes were used.

5.3.1 Test setups

5.3.1.1 Basic DAC recording

For the first, basic setup, a digital/analog-analog/digital converter (DAC; NiUSB-6251, National Instruments, Austin, TX, USA) recorded its own output signal. The signal was digitally generated using Matlab 2016a (The MathWorks Inc., Natick, MA, USA) and streamed to the DAC via the Data Acquisition Toolbox. The signal was generated and recorded at a rate of 10 kHz (Figure 5.1A).

5.3.1.2 DAC & tACS stimulator

In the second setup the DAC was connected to the remote-input of a battery-driven constant current stimulator (DC Stimulator Plus, Neuroconn, Illmenau, Germany). Stimulation was administered to a 5.6 kΩ resistor. The signal was recorded from both ends of the resistor using the DAC (Figigure 5.1B).

5.3.1.3 DAC & tACS recorded from phantom using EEG

In the third setup the DC Stimulator was connected to two surface conductive rubber electrodes placed on a melon serving as a phantom head. Electrodes were attached using an electrically conductive, adhesive paste (ten20, Weaver & Co., Aurora, CO, USA). The signal was recorded from an active Ag/AgCl EEG electrode (ActiCap, Brain Products, Gilching, Germany), placed between the tACS electrodes. Two additional electrodes were attached to the phantom to serve as reference and ground electrodes for the recording (positions were chosen to mimic a nose-reference and a ground placed on the forehead). The signal was generated by the DAC at a rate of 10 kHz and recorded at 10 kHz using a 24-bit ActiChamp amplifier (Brain Products, Gilching, Germany). EEG and stimulation electrode impedances were kept below 10 kΩ (Figure 5.1C).

5.3.1.4 DAC & tACS recorded from phantom using MEG

Finally, the phantom was recorded using a 306-channel whole-head MEG system (Elekta Neuromag Triux, Elekta Oy, Helsinki, Finland), located inside a magnetically shielded room (MSR; Vacuumschmelze, Hanau, Germany). Signals were recorded without internal active shielding at a rate of 1 kHz and online filtered between 0.3 and 330 Hz. The stimulation signal was gated into the MSR via the MRI-extension kit of the DC Stimulator (Neuroconn, Illmenau, Germany; Figure 5.1D).

5.3.2 Transfer function and AM-tACS measurements

A probe stimulus consisting of a one-cycle sine wave at 220 Hz was used to obtain measurements of each setups transfer function (TF). 10001 probes of linearly spaced amplitudes (V_{in}), ranging from -10 V to 10 V for the first setup, from -0.75 V to 0.75 V for the second and third setup, and from -0.5 V to 0.5 V for the MEG setup, were concatenated to a sweep stimulus with a total duration of approximately 45 s (see Figure 5.1I–J for a schematic visualization). Amplitudes had to be adjusted for setups involving the DC Stimulator to account for higher output voltages due to the 2 mA per V voltage-to-current conversion of the remote-input. The chosen input voltages correspond to a maximum output of 3 mA peak-to-peak amplitude of the DC Stimulator (a maximum current of 2 mA was chosen for the MEG setup to avoid saturation and flux trapping of MEG sensors). Ten consecutive sweeps were applied and recorded for each setup. In order to evaluate how well the obtained TF can predict artifacts in the spectrum of AM-tACS, AM-waveforms with f_c = 220 Hz and f_m = 10 Hz, 11 Hz, and 23 Hz at different amplitudes (100%, 66.7%, 33.4% and 16.16% of the maximum range applied during the TF recording) were generated. Amplitudes were chosen to produce output currents of 3 mA, 2

mA, 1 mA, and 0.5 mA when using the DC Stimulator (2 mA, 1.3 mA, 0.66 mA, 0.33 mA for the MEG setup). AM-signals were computed based on the following equation:

$$AM_{Signal}(t) = a_{Sim}\left(\left(\frac{sin(2\pi * f_m * t}{2} + \frac{1}{2}\right) * sin(2\pi * f_c * t)\right), \tag{5.1}$$

where a_{Stim} is the stimulation amplitude, f_m is the modulation frequency and f_c is the carrier frequency. The resulting signal corresponds to an AM-waveform with 50% modulation depth. Each signal was generated and recorded with 60 repetitions to increase signal-to-noise ratios.

5.3.3 Human MEG recording

In order to relate the strength of the low-frequency artifacts encountered during AM-tACS to human brain activity, an additional pilot recording involving a human subject was carried out. Three resting state recordings of 10 min each were acquired in the MEG. During two of the blocks the participant was stimulated with 1 mA of AM-tACS with f_m = 10 Hz and 23 Hz, and f_c = 220 Hz, respectively. Electrodes were positioned centered above locations Cz and Oz of the international 10-10 system. The remaining block was acquired in absence of stimulation (participant was physically disconnected from the stimulator by removing the cables from the electrodes). Recording settings were similar to the MEG phantom measurement described above. The participant was instructed to keep the eyes closed throughout the recordings.

5.3.4 Data analysis

Data analysis was performed using Matlab 2016a (The MathWorks Inc., Natick, MA, USA). The Fieldtrip toolbox (Oostenveld et al., 2011) was used to import and segment M/EEG recordings and to analyze the human MEG recordings. All scripts and underling datasets are available online (https://osf.io/czb3d/).

5.3.4.1 Data processing and transfer function estimation

The recorded sweeps were epoched into segments containing single cycles of the sine-waves used as probes. All segments were baseline corrected and the peak-amplitude (V_{out}) of each epoch was extracted by identifying the minimum (for $V_{in} < 0$) or maximum values (for $V_{in} \geq 0$) within each segment. A 6th-degree polynomial regression model was fitted to each repetition of the sweep to

predict V_{out} (recorded peak amplitudes) as a function of V_{in} (generated peak amplitudes) using a least-square approach:

$$\hat{V_{out}} = f(V_{in}), \tag{5.2}$$

with:

$$f(V_{in}) = \beta_6 * V_{in}^6 + \beta_5 * V_{in}^5 + \beta_4 * V_{in}^4 + \beta_3 * V_{in}^3 + \beta_2 * V_{in}^2 + \beta_1 * V_{in} + \beta_0 \tag{5.3}$$

The fitting procedure was performed separately for each sweep to obtain measures of variance for each of the coefficients. Coefficients were averaged subsequently and the resulting function was used to model each systems TF. R^2-values were calculated as measures for goodness of fit.

In order to evaluate the performance of the TF models in predicting low-frequency AM-tACS artifacts of the setups, the digitally generated AM-tACS signals were fed through the TF models. Subsequently, the predicted output signals were compared to the AM-tACS recordings acquired for each setup. To this end, power spectra of the original digital, the predicted and the recorded AM-signals were computed using Fast Fourier Transform (FFT) implemented in Matlab. The resulting power spectra of the AM-waveforms were averaged over the 60 repetitions. For the MEG recording, results are presented for an exemplary parieto-occipital gradiometer sensor (MEG2113).

5.3.4.2 Identification of low-frequency artifacts

To identify systematic artifacts in the spectrum of the AM-signal in the noisy recordings, the averaged power spectra were scanned for artifacts within a range from 2 Hz to 301 Hz. Artifacts were defined as the power at a given frequency being altered by at least 5% as compared to the mean power of the two neighboring frequencies. The identified artifacts were statistically compared to the power in the two neighboring frequency bins using student's t-tests. Bonferroni-correction was applied to strictly account for multiple comparisons. To allow additional comparisons of the relative strength of the low-frequency artifacts between the different setups, the ratio of the low-frequency artifacts at f_m and the artifact originating from the carrier waveform (f_c) was computed for each of the 60 spectra in each AM-tACS recording condition. The obtained ratios were then averaged.

5.3.4.3 Simulation

To evaluate the effect of each non-linear term in the TF models on the output signal, a simulation was carried out. To this end, an amplitude modulated signal with f_c = 220 Hz and f_m = 10 Hz was evaluated by simplified TFs with all coefficients set to zero, except for the linear and one additional non-linear term. These coefficients were set to one in each run. This procedure leads to exaggerated output spectra that do not realistically resemble the recorded AM-signals. However, they are well suited to illustrate how the input waveform is affected by each of the non-linear terms in the TF.

In addition to the AM-signal, a temporal interference (TI) signal was simulated. TI stimulation has recently been proposed as a tool to non-invasively stimulate deep structures of the brain (Grossman et al., 2017). TI stimulation consists of two externally applied, high frequency sine waves with slightly differing frequencies that result in an amplitude modulation in areas where their electric fields overlap. Since the generation of this AM-waveform is mathematically different as compared to the other AM-tACS approach, this signal was separately modeled based on the following equation:

$$TI_{Signal}(t) = a_{Stim} * \frac{(sin(2\pi * f_1 * t) + sin(2\pi * f_2 * t))}{2} \tag{5.4}$$

with f_1 = 200 Hz and f_2 = 210 Hz. The overlap of these two frequencies results in an amplitude modulation at 10 Hz.

5.3.4.4 Human MEG data

Due to high noise levels in the magnetometer sensors, analysis of the human MEG recording was restricted to gradiometers. Signals obtained from the human pilot subject were high-pass filtered at 1 Hz using a 4^{th}-order forward-backward Butterworth filter and subsequently epoched into 300 non-overlapping segments of 2 s. FFTs (Hanning window, 4 s zero-padding) were computed on each of the segments. The resulting power spectra were subsequently averaged for each of the 10 min blocks. The planar gradient magnitude over pairs of orthogonal gradiometers at each sensor location was calculated as the summed power of the two in each frequency bin. Participant's peak-power in the alpha band (8 Hz–12 Hz) over all sensors during the stimulation-free recording was extracted from the spectrum and used as reference to quantify artifact strength at f_m and f_c. In order to test its effectiveness in suppressing AM-tACS artifacts, the same analysis pipeline was performed after MEG data underwent spatiotemporal Signal Space Separation (tSSS; Taulu and Simola, 2006; Taulu

et al., 2005) applied via the MaxFilter™ Software (Elekta Oy, Helsinki, Finnland).

5.4 Results

5.4.1 Systematic artifacts at modulation frequency of AM-tACS and harmonics

Analysis of the AM-tACS recordings identified systematic artifacts at f_m and its harmonics that statistically differed from power at neighboring frequencies in all setups (all $p < .05$; Figure 5.2, 5.3). The relative strength of these artifacts was comparatively small for the most simple setup ($\sim$0.00000002% of the strength of the artifact at f_c) and increased with complexity of the setups under investigation (DAC + Stimulator: $\sim$0.00006%, DAC + Stimulator + EEG: $\sim$0.012%, DAC + Stimulator + MEG: $\sim$0.001%). Figure 5.4 provides an overview of the f_m/f_c-ratios in the different measurement conditions (modulation frequencies, intensities, setups). In addition, stronger distortions at harmonic frequencies of f_m were observed for the more complex setups and with increasing intensities (Figure 5.2, 5.3). Apart from low-frequency artifacts at the modulation frequency, some of the recordings showed additional side-bands around the carrier frequency, which was most pronounced in the EEG setup (Supplementary Figure S1 and S2).

5.4.2 Setups exhibit non-linear transfer characteristics

To obtain a model of the TF of each setup, 6^{th}-degree polynomial regression models were fitted to the input-output amplitudes of the probe stimuli. All setups tested in this study exhibited coefficients of the non-linear terms of the fitted TFs significantly differing from zero.

In setups 1, 2, and 4 all model coefficients significantly differed from zero (all $p < .004$; bonferroni corrected). For the EEG setup, coefficients β_2 ($p < .02$), β_5($p < .004$) and β_6 ($p < .007$) significantly differed from zero. Results are summarized in Table 5.1. High goodness of fit values were achieved for all setups under investigation ($R^2 > .99$), indicating that the polynomial functions provide powerful models to describe the input-output characteristics of the setups. Importantly, the non-linearities found during this analysis are subtle compared to the contribution of the linear terms in each TF. This leads to the impression of linearity when visually inspecting each setups' TF (Figure 5.2,5.3 top panel). However, as it will be shown in the following, these small deviations from linearity are sufficient to cause the low frequency artifacts observed during the AM-tACS recordings.

Table 5.1: Transfer function coefficients tested for deviation from zero. Coefficients of the 10 polynomial functions fitted for each setups TF recordings were tested against zero using student's t-test (two-sided, bonferroni corrected). Mean and standard deviation are shown for each coefficient.

	$Mean$	$Std.$	df	T	p
DAC					
β_0	-1.05e-05	4.80e-06	9	-6.92	$<$.001*
β_1	0.9988	1.86e-05	9	$>$100	$<$.001*
β_2	-3.28e-06	7.02e-07	9	-14.79	$<$.001*
β_3	-3.75e-07	7.16e-08	9	-16.56	$<$.001*
β_4	9.99e-08	2.31e-08	9	13.69	$<$.001*
β_5	3.73e-09	5.77e-10	9	20.41	$<$.001*
β_6	-6.32e-10	1.72e-10	9	-11.63	$<$.001*
DAC + Stimulator					
β_0	0.0042	0.0009	9	15.37	$<$.001*
β_1	10.8640	0.0123	9	$>$100	$<$.001*
β_2	-0.0686	0.0153	9	-14.14	$<$.001*
β_3	-0.0904	0.0324	9	-8.83	$<$.001*
β_4	0.1838	0.0606	9	9.54	$<$.001*
β_5	0.0809	0.0484	9	5.28	$<$.001*
β_6	-0.1702	0.0712	9	-7.56	$<$.001*
EEG					
β_0	-0.0001	0.0001	9	-5.27	$<$.001*
β_1	0.1736	0.0007	9	$>$100	$<$.001*
β_2	0.0024	0.0017	9	4.44	.002*
β_3	-0.0006	0.0024	9	-0.81	.44
β_4	0.0035	0.0069	9	1.64	.14
β_5	-0.0058	0.0035	9	-5.30	$<$.001*
β_6	-0.0118	0.0078	9	-4.80	.001*
MEG					
β_0	-0.0009	0.0002	9	-16.35	$<$.001*
β_1	11.3235	0.0576	9	$>$100	$<$.001*
β_2	0.0267	0.0121	9	6.97	$<$.001*
β_3	0.3033	0.0393	9	24.41	$<$.001*
β_4	-0.5931	0.1532	9	-12.24	$<$.001*
β_5	-1.1228	0.2065	9	-17.19	$<$.001*
β_6	2.1034	0.5192	9	12.81	$<$.001*

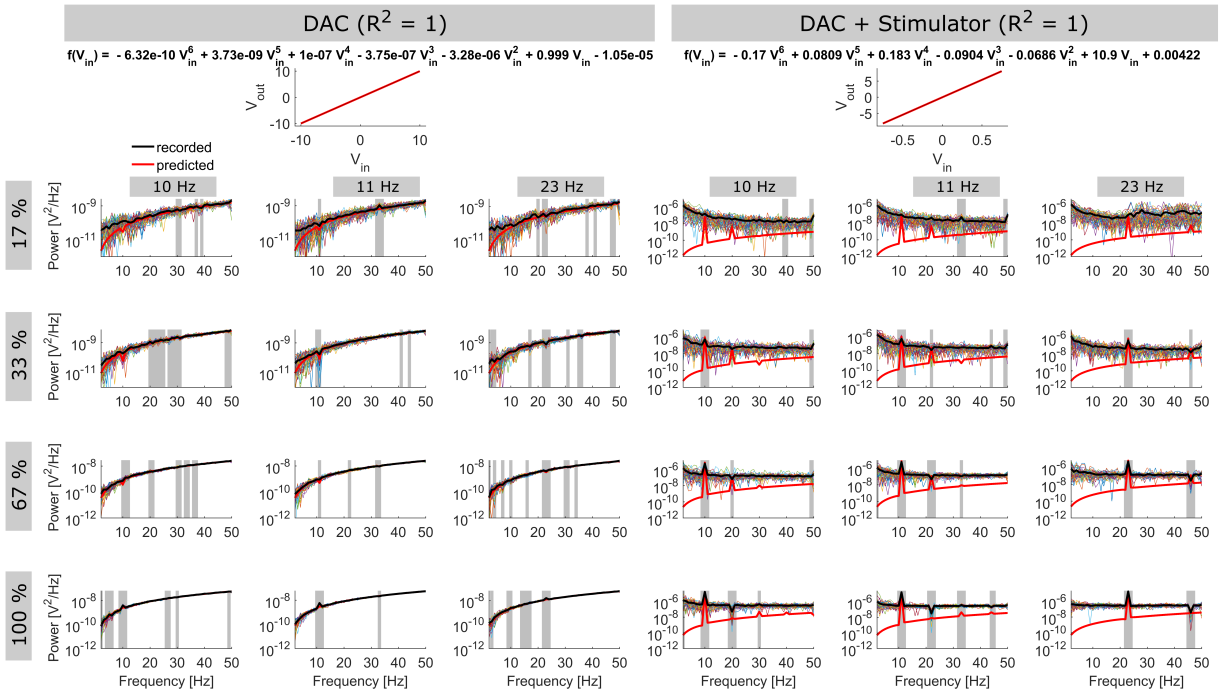

Figure 5.2: Transfer functions (top row) and spectra (lower rows) of setups of the DAC and Stimulator setup. TFs **(top)** show recorded probe stimulus amplitudes in relation to their input amplitudes (V_{out}/V_{in}; black dots), as well as the course of the TF model (red line). The corresponding function is displayed in the title. Spectra show average power at each frequency in the different AM-recordings (black line). Thin colored lines show power spectra for each of the 60 repetitions. Red line shows the spectrum predicted by evaluating the digital AM-signal by the estimated TF of the setup. Grey areas indicate frequencies significantly differing in power compared to the two neighboring frequencies ($p < .05$, bonferroni corrected). Please note the different scaling of the power spectra. To enhance visibility, spectra are limited to the frequency range between 1 Hz and 50 Hz. Please refer to the Supplementary Materials for an alternative version of the figure, covering the full frequency range between 1 and 300 Hz.

5.4.3 Transfer functions predict frequency of spurious artifacts

When applying the TF models to the digital AM-waveforms, the resulting spectra provide accurate predictions of the systematic low-frequency artifacts at f_m of the AM-signal and its first harmonics in the recordings. For the first two setups, where the TF models' goodness of fit is equal to 1, the predicted spectra also capture the amplitudes of low-frequency artifacts with relatively high accuracy (Figure 5.2). For the two later setups, however, the predicted spectrum apparently underestimates amplitudes of the recorded spectrum (Figure 5.3). In summary, results suggest that the polynomial functions fitted to the data successfully captured the non-linear process leading to the low-frequency artifacts at f_m, although for the later setups, that exhibited more noise during the measurements, accuracy of the fits seems not sufficient to accurately predict the artifacts amplitudes. This seems not surprising as the TF models can only provide an approximation of the true non-linearity of the system. In addition, the application of a TF to a pure digital AM-signal can never completely capture the effects of the recording process that involves measurement of noise and external interferences (i.e. line-

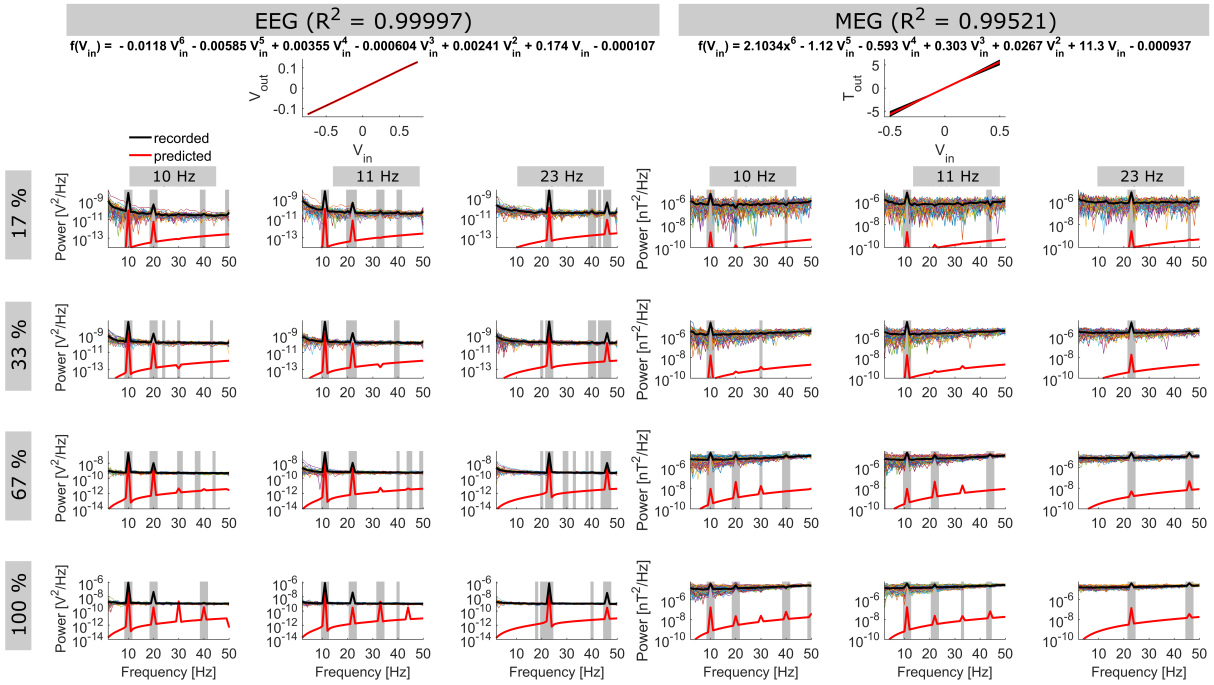

Figure 5.3: Transfer functions (top row) and spectra (lower rows) of the EEG and MEG setup. TFs (top) show recorded probe stimulus amplitudes in relation to their input amplitudes (V_{out}/V_{in}; black dots), as well as the course of the TF model (red line). The corresponding function is displayed in the title. Output values (V_{out}) for the MEG setup are expressed in nT. Spectra show average power at each frequency in the different AM-recordings (black line). Thin, colored lines show power spectra for each of the 60 repetitions. Red line shows the spectrum predicted by evaluating the digital AM-signal by the estimated TF of the setup. Grey areas indicate frequencies significantly differing in power compared to the two neighboring frequencies ($p < .05$, bonferroni-corrected). Please note the different scaling and units of the power spectra. To enhance visibility, spectra are limited to the frequency range between 1 Hz and 50 Hz. Please refer to the Supplementary Materials for an alternative version of the figure, covering the full frequency range between 1 and 300 Hz.

noise). In an attempt to incorporate each system's noise, the AM-tACS measurements were repeated with an additional prototypical noise signal computed from 10 one-second recordings of a 300 Hz sine wave. This noise signal was added to the signal predicted by the TF model (we thank an anonymous reviewer for suggesting this approach; please refer to the Supplementary Materials for details of the method). Unfortunately, the estimated noise-levels were not always comparable to those during the AM-tACS measurements. Especially for the more complex setups, noise levels appeared to depend on properties of the signal fed through the setup. In those cases were good noise-levels were obtained, the predicted spectra resembled the recorded signals pretty well. Nevertheless, the artifact peaks at the modulation frequency and its harmonics were still underestimated in most cases, likely due to the remaining deviation between the modeled and the true underlying transfer characteristics of the system (Supplementary Figures S3 and S4).

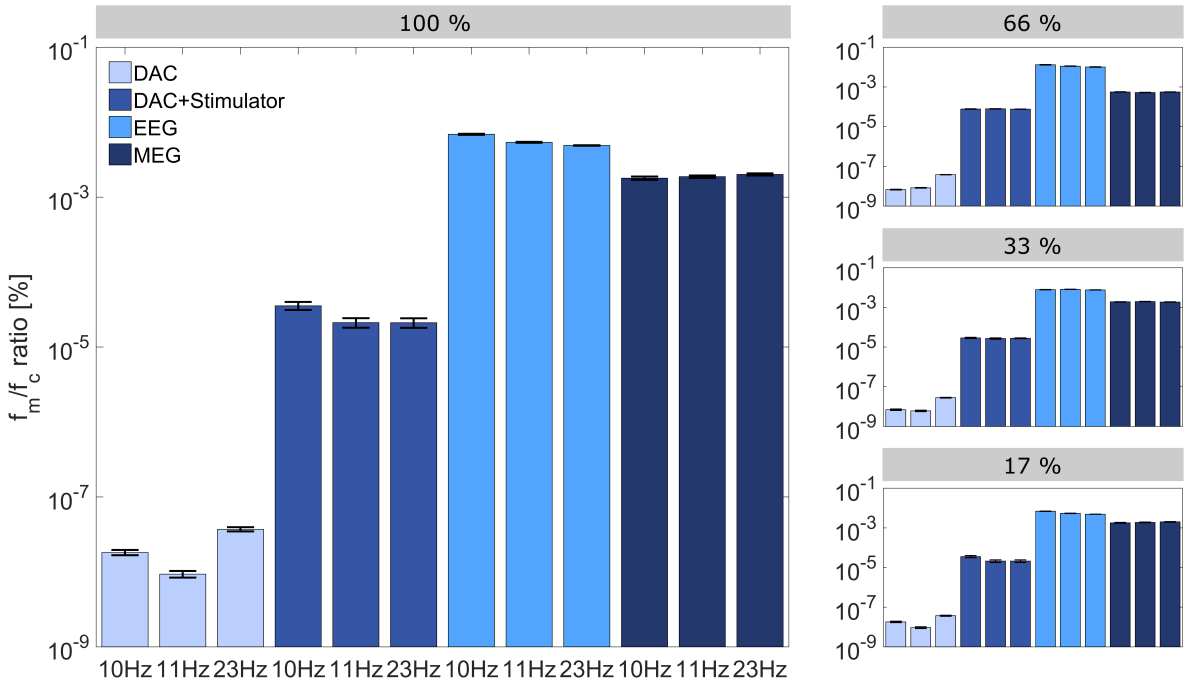

Figure 5.4: Ratio between artifact at f_m and f_c. Bar plots depict the average ratio between the low-frequency artifact extracted at f_m and the artifact at f_c computed over the 60 repetitions in each measurement condition. The different setups tested are color coded, error bars depict standard error of the mean. **(Left)** Ratios for each f_m for the 100% intensity condition. **(Right)** Ratios for the remaining intensities. Overall the relative strength of the low-frequency artifact at f_m increases with the complexity of the setup under investigation. Please not the logarithmic scaling of the vertical axis.

5.4.4 Simulating the isolated effect of non-linear TF-terms

Based on the results presented so far, it was possible to characterize the non-linearity of each setup and to demonstrate that the estimated TF can be used to predict artifacts in the recorded AM-signals. However, since the obtained TFs are rather complex, a simulation was carried out to model how each of the non-linear terms of the TFs contributes to the generation of low-frequency artifacts during AM-tACS. Spectra and output signals obtained from this simulation are depicted in Figure 5.5. While a solely linear TF did not change the spectral content of the AM-waveform (Figure 5.5 top left), polynomial terms with odd exponents $>$1 resulted in additional side bands around f_c of the AM-signal (Figure 5.5 middle, bottom left). In contrast, terms with even exponents induced artifacts at f_m and its harmonics (Figure 5.5 right column) by asymmetrically modulating the input waveform around zero. The higher the exponent of the polynomial terms, the more sidebands and higher harmonics are introduced to the spectrum, respectively. A separate simulation for an AM-signal resulting from temporal interference (Grossman et al., 2017) yielded a similar result (Supplementary Figure S5).

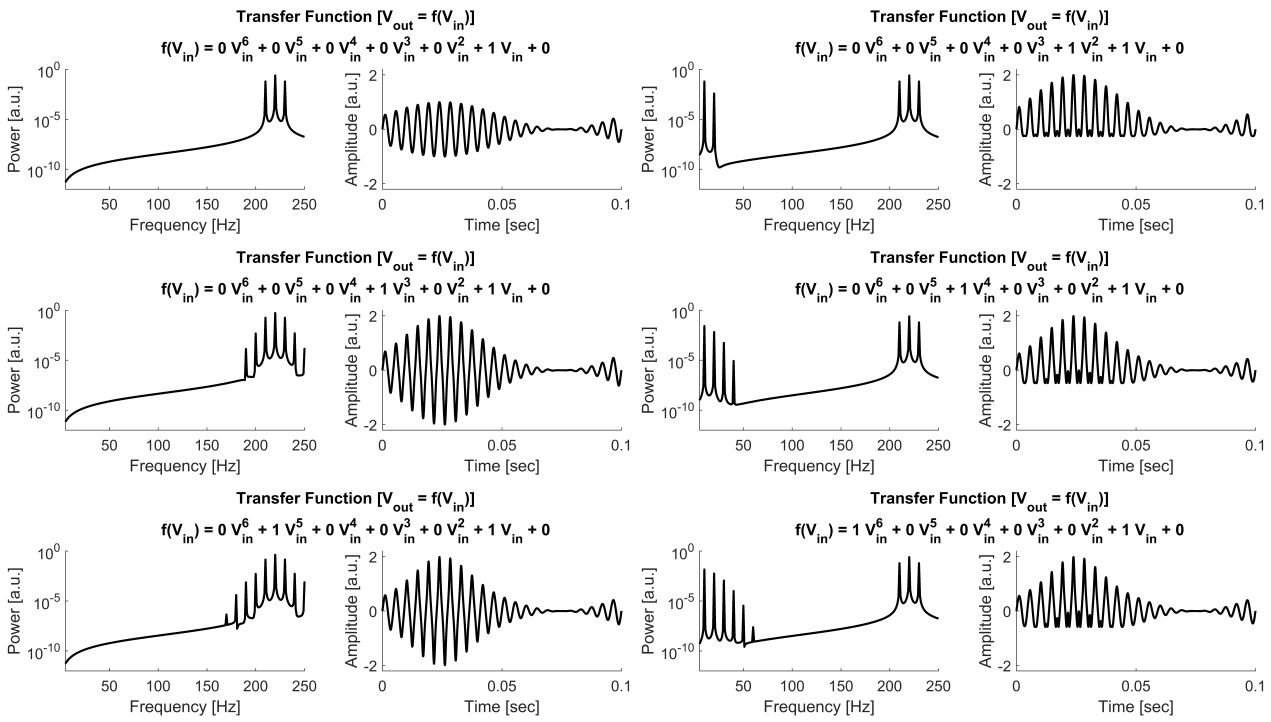

Figure 5.5: Simulation results. Frequency- (**1**st **and 3**rd **column**) and time-domain (**2**nd**and 4**th **column**) representations of the output signals resulting from evaluating the digital AM-waveform using a simplified TF. To enhance visibility only the first 100 ms (1 cycle) of the output signals are depicted in the time-domain plots. A solely linear TF **(top left)** perfectly resembles the input spectrum. Setting the coefficient of an additional polynomial term with an odd-valued exponent to 1 resulted in additional side bands around f_c (**middle** and **bottom left**). In contrast, setting the coefficient of an additional polynomial term with an even-valued exponent to 1 resulted in artifacts at f_m and its harmonics (**3**rd **and 4**th **column**). The higher the exponent of the polynomial terms, the more side-bands/harmonic artifacts they introduced. Time-courses of the output waveforms illustrate the asymmetric modulation around zero caused by the even-valued exponents of the TF (**4**th **column**). The polynomial function applied to generate each output signal is depicted on top of each plot.

5.4.5 AM-tACS artifacts in human MEG data

Participant's maximum power within the alpha-band over all sensors during the stimulation-free recording was identified at 11.25 Hz. Power in this frequency bin was used to reference the strength of AM-tACS artifacts at f_m = 10 Hz and 23 Hz. In addition, participant's peak alpha-power was compared against power at f_c = 220 Hz, which is comparable to artifact strength encountered during conventional tACS. Power spectra obtained from the two AM-tACS recording blocks exhibit artifacts at the modulation frequencies and their harmonics (Figure 5.6 top panel). Without the application of tSSS, the low-frequency artifact during AM-tACS was 522 (f_m = 10 Hz) and 861 (f_m = 23 Hz) times larger as compared to the pilot subject's natural alpha-peak power. The stimulation artifact at f_c was $\sim$90,000,000 times stronger than participant's natural alpha power. The application of tSSS resulted in strong suppression of artifact peaks during the AM-tACS recordings at f_m and its harmonics, as well as around f_c (Figure 5.6, bottom panel). The ratio between spectral power at $f_m$during AM-tACS and natural alpha-peak power was reduced to 1.8 (f_m = 10 Hz) and 1.1 (f_m = 23 Hz). While such

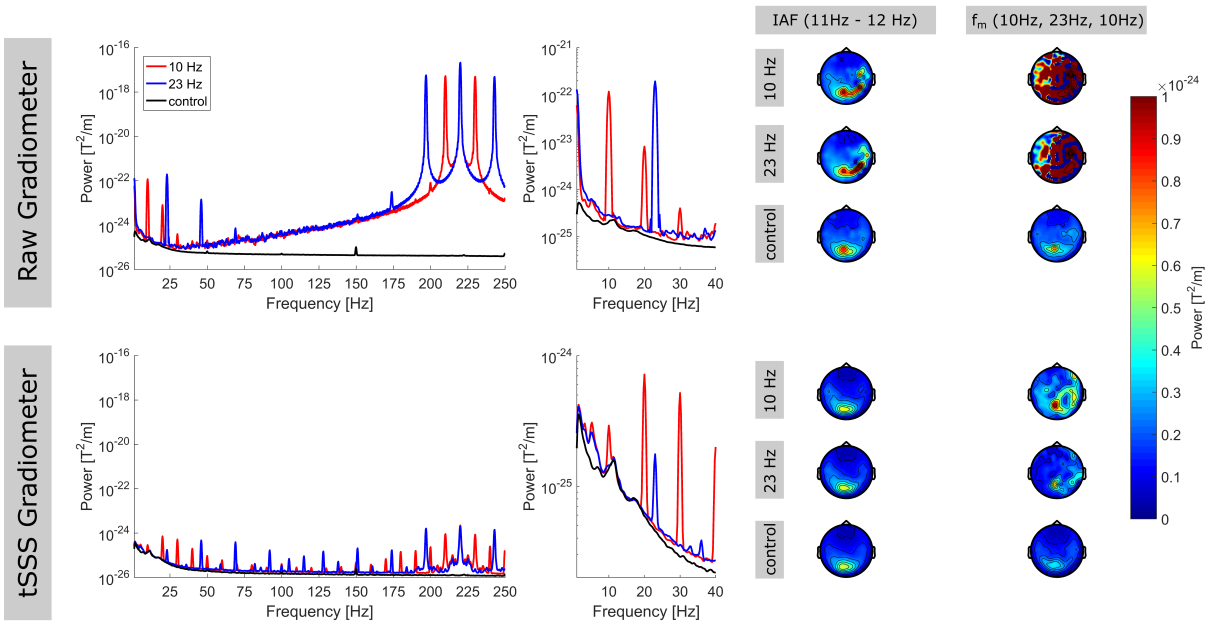

Figure 5.6: Low-frequency artifacts in human MEG data. (Top left) Power spectra obtained during the three pilot measurement blocks (10 Hz and 23 Hz amplitude modulation and control) without application of artifact cleaning approaches. **(Top right)** Topographies depict participant's power within in the individual alpha band (11 Hz–12 Hz) and power at f_m (10 Hz and 23 Hz; for the control condition power at 10 Hz is depicted). Both spectra and topographies are evident of low-frequency artifacts during AM-tACS occurring at f_m and its harmonics. These artifacts are substantially stronger as compared to participants' natural alpha band activity. **(Bottom)** Spectra and topographies depict the same data as above after the application of tSSS. Although tSSS resulted in a substantial suppression of all AM-tACS artifact peaks (at f_m and its harmonics as well as the main artifact peak around $f_c \pm f_m$), the spectra are still dominated by distortions originating from AM-tACS.

ratios fall into a physiologically plausible range for a natural or AM-tACS induced power change (and frequency shift), the spatial distribution of power at f_m still exhibits distortions in the proximity of the electrode cables, indicating the presence of residual artifacts in the data (Figure 5.6, bottom right). This is further supported by the presence of additional artifact peaks at harmonic frequencies of f_m. In addition to the reduction of low-frequency artifacts, a suppression of power at f_c was observed (reduced to 14 times the size of participant's alpha peak power). In summary, results confirm the presence of low-frequency artifacts in concurrent AM-tACS MEG recordings, which are substantially larger than signals originating from the brain. Even after the application of artifact cleaning by means of tSSS, residual artifacts at f_m and its harmonics remained present in the recordings.

5.5 Discussion

Amplitude modulated transcranial alternating current stimulation (AM-tACS) offers a promising new approach to investigate online effects of tACS using physiological recordings. While in theory AM-tACS should not exhibit artifacts within the frequency range of brain signals, the current study demon-

strates that non-linear transfer characteristics of stimulation and recording hardware reintroduce such artifacts at the modulation frequency and its harmonics. These artifacts are likely too small to modulate brain activity themselves, as they are several orders of magnitude smaller as compared to conventional tACS waveforms. However, as shown during an MEG pilot recording, artifacts at the modulation frequency can still be substantially larger than human alpha oscillations. Consequently, physiological recordings during AM-tACS must not be considered artifact-free in the range of the modulation frequency. Rather, the extent of low-frequency artifacts has to be evaluated carefully and taken into account to ensure valid conclusions from the data.

The setups evaluated for the current study have been build based on a limited set of hardware components. Thus, the extent of non-linearity might differ for hardware combinations using other stimulator or recording systems. However, since all electronic components exhibit some degree of non-linearity (Maas, 2003), the general process underlying the generation of low-frequency AM-tACS artifacts is potentially applicable to all setups. Only the size of these artifacts may differ depending on the (non-)linearity of the setup (Figure 5.4). The current study provides a framework to measure and estimate a setup's transfer characteristics and evaluate the strength of these low-frequency artifacts arising from its non-linearities. Interestingly, the DAC itself exhibited comparatively weak artifacts, while the more complex setups showed stronger artifacts at the modulation frequency and several harmonics. In fact, the addition of the tACS stimulator to the setup increased artifact strength at the modulation frequency by approximately three orders of magnitude. Changing the recording system to MEG/EEG added another three to four orders of magnitude to the artifact strength relative to the expected artifact at the carrier frequency. This indicates that artifact strengths of the systems might be primarily driven by non-linearities of the stimulator and the recording systems, rather than the DAC. The latter has been suggested as the source of non-linearities by previous authors (Minami and Amano, 2017). In contrast to the DAC, these devices perform different steps of signal conversion and amplification, which could indicate that these processes may have actually stronger contribution to artifact generation than the digital-analog conversion.

The results from concurrent recording of MEG during AM-tACS from a human subject suggest that the size of low-frequency artifacts can be substantially stronger than neural signals of interest. For the current recording, low-frequency artifacts were about 500–800 times larger than the subject's natural alpha oscillations during eyes-closed. Such a single recording can of course only provide a very rough estimate of the artifact strength. Nevertheless, these results emphasize the practical relevance of these artifacts. As seen during the comparison of the different test setups, the strength of low-frequency artifacts during AM-tACS can strongly vary between different setups. Consequently,

there might be hardware combinations where low-frequency artifacts might even fall into the range of human brain activity and thus be potentially confused with stimulation effects on the brain (i.e. observed in the current study after tSSS application to the pilot recording). Especially, in cases where spatial information is missing (i.e. recording from only few EEG sensors), such artifacts in the spectrum might be hard, if not impossible, to be disentangled from stimulation effects.

To obtain a model of each setup's transfer characteristics, polynomial regression models were fitted to the probe-signal recordings. The degree of the models was chosen as a tradeoff between sufficient complexity to capture each setup's non-linearity and simplicity to retain a straightforward, interpretable model. Unfortunately, traditional approaches for model selection, i.e. based on adjusted R^2 or Akaike Information Criterion, that start from a simple intercept or a saturated model, are not applicable to the data at hand, as the non-linearities observed in the setups are very subtle. A simple linear model would already account for a huge proportion of the input-output recordings' variance. Adding additional higher degree terms to the model does not sufficiently increase the explained variance to counteract the penalty implemented in most model evaluation metrics. However, as seen in the simulated data, only these terms account for the low-frequency artifacts observed in the AM-tACS recordings by asymmetrically modulating the input signals around zero. While a single additional non-linear term would already be sufficient to explain the generation of a low-frequency artifact at f_m and its first harmonic frequency (Figure 5.5), simulation results indicated that higher order non-linear terms are necessary to also model potential higher harmonics of the low-frequency artifact and additional side-bands around f_c (Supplementary Figs. S1 and S2). By implementing a 6^{th}-degree polynomial model, TFs were in principle able to capture low-frequency artifacts up to the 5th harmonic of the modulation frequency and four additional side-bands around f_c.

Given that the low-frequency AM-tACS artifacts are several orders of magnitude smaller than the artifact arising during conventional tACS (or at the carrier frequency), they are potentially easier to correct/suppress by application of beamforming (Chander et al., 2016; Witkowski et al., 2016) or spatiotemporal signal space separation in the MEG (Minami and Amano, 2017; Taulu and Simola, 2006; Taulu et al., 2005) and independent or principal component analysis (ICA/PCA) in the EEG (Helfrich, Schneider, et al., 2014). In the current study, the application of tSSS with standard settings (suggested by the manufacturer) to a concurrent AM-tACS-MEG recording apparently resulted in non-optimal suppression of the low-frequency artifacts. Even worse, after tSSS application the artifact at the modulation frequency was suppressed to a size that falls into a plausible range for actual tACS effects on the brain. Only by inspecting topographies and power at harmonic frequencies of f_c, the spectral peak at f_m itself could be identified as a potential residual artifact. This observation

emphasizes the need for further studies, carefully and systematically evaluating the efficiency of artifact suppression algorithms in the context of AM-tACS to avoid erroneous conclusions. Such studies should also consider the possibility that the low-frequency artifacts, originating from non-linearities of the hardware in use, might potentially be subject to physiologically driven non-linear modulations (Noury et al., 2016; Noury and Siegel, 2017), thus resulting in additional side-band peaks around the low-frequency artifacts.

The optimal solution to overcome the reported low-frequency artifacts would be the optimization of stimulation and recording hardware with respect to their linearity. Neither have devices for transcranial electric stimulation currently available been purposefully designed to apply AM-tACS, nor are recording systems for brain activity intended to record AM-waveforms at intensities as observed during AM-tACS. Devices exhibiting more linear transfer characteristics (i.e. observed for the DAC in setup 1) would decrease the size of the artifacts compared to the signal of interest such that their influence eventually becomes negligible. Until such devices are available, careful analysis procedures have to be carried out to ensure trustworthy results from concurrent AM-tACS-M/EEG experiments. The current study proposes an analysis framework that enables researchers to check their AM-tACS setups for non-linearities and spurious low-frequency artifacts. This may help to disentangle actual effects of the stimulation on the brain from artifacts introduced by the stimulation in future work, and aid the development process of new, specialized AM-tACS hardware.

5.6 Acknowledgements

This research was supported by the Neuroimaging Unit of the Carl von Ossietzky University Oldenburg funded by grants from the German Research Foundation (3T MRI INST 184/152-1 FUGG and MEG INST 184/148-1 FUGG). Christoph S. Herrmann was supported by a grant of the German Research Foundation (DFG, SPP, 1665 3353/8-2). This work was supported in part by the National Institute of Mental Health of the National Institutes of Health under award numbers R01MH111889 and R01MH101547 (PI: Flavio Frohlich). The content is solely the responsibility of the authors and does not necessarily represent the official views of the National Institutes of Health.

The authors would like to thank Katharina Duecker for her assistance during acquisition of human MEG data.

Chapter 6

General Discussion

6.1 Effects of tACS on Spontaneous and Event-related Oscillations

Transcranial alternating current stimulation receives increasing popularity as a tool to investigate causal relationships between brain oscillations and cognitive functions. However, the precise mechanisms of the method are poorly understood so far. The first three studies in the current thesis aimed to further characterize effects of tACS on spontaneous and event-related oscillations.

The first study demonstrated a sustained effect of a single session of 20 min tACS on spontanous oscillations in the alpha range that lasted for up to 70 min. After this time, the power increase was not significantly different from sham stimulation, due to a natural alpha increase in the control group. Very recently, Wischnewski et al. (2018) replicated this duration when applying tACS in the beta range over the primary motor cortex. In their study, authors successfully abolished tACS aftereffects when participants received the NMDA receptor antagonist dextromethorphan, but observed aftereffects of similar duration when a placebo was provided.

Sustained effects of tACS on spontaneous oscillations in different frequency bands have been observed in a variety of studies (Neuling et al., 2013; Veniero et al., 2015; Vossen et al., 2015; Wischnewski et al., 2018; Zaehle et al., 2010). However, many associations between brain oscillations and cognitive functioning or psychiatric disorders are based on event-related oscillatory activity. Whether tACS can modulate such event-related oscillations and into which direction poses a complex, yet important problem. It has been demonstrated that tACS effects depend on brain-states, with some states being more susceptible to stimulation than others (Feurra et al., 2013; Neuling et al., 2013; Ruhnau et al., 2016). Event-related oscillations can be seen as a transition between two (or even more) such brain-states (for simplicity a pre- and a post-stimulus state will be assumed in the following). Depending on the susceptibility of these states to the stimulation, the pattern of event-related oscillatory activity may be altered into different directions or left unaffected, with different effects to-be expected on the behavioral level. In a clinical context, this determines whether the stimulation results in symptom improvement or decline. Thus, a general theory predicting how event-related oscillations are modulated by tACS is desirable to be able to derive hypotheses for solely behavioral experiments and to design effective stimulation protocols for treatment purposes.

Study 2 and 3 aimed to investigate tACS effects in the context of a cognitive task. Results indicate that tACS does not only affect spontaneous oscillations, but can also alter patterns of event-related oscillatory activity during and after stimulation. In study 2, the increased event-related desynchronization (ERD) after tACS appeared to be driven by a stronger alpha enhancement during the pre-stimulus interval. Performance in the mental rotation task used in both experiments has been linked

to ERD in the alpha band (Klimesch et al., 2003; Michel et al., 1994). In this task, alpha oscillations are typically observed during the pre-stimulus interval, but are suppressed while executing the mental rotation (Michel et al., 1994). Based on the findings in only one task it is difficult to propose a general model about how tACS exerts its effects on event-related oscillations. However, some hypotheses can be derived from the selective enhancement of pre-stimulus oscillations, which can be tested by applying tACS during a variety of different tasks, that induce event-related synchronization (ERS) and event-related desynchronization (ERD).

Following the principles of synchronization theory, entrainment to an external driving force can only occur in the presence of a self sustained oscillator (Pikovsky et al., 2003). Based on this view, tACS may only affect pre- or post-stimulation intervals during which the targeted oscillation is present, but not those during which it is suppressed. Similarly, strengthening neural circuits underlying an oscillation by induction of spike-timing dependent plasticity through tACS (Vossen et al., 2015; Wischnewski et al., 2018; Zaehle et al., 2010) may increase their capability to oscillate at higher amplitudes, or in higher synchrony. However, the actual increased oscillatory activity can still only be observed when these circuits are activated, but not when their activity is suppressed. Consequently, tACS would affect pre-stimulus oscillations during ERD and post-stimulus oscillations during ERS, thus facilitating pre-existent patterns of both ERD and ERS.

The above hypothesis cannot be verified with experimental data currently available, as event-related oscillations have rarely been targeted with tACS so far. More research in this area targeting ERD and ERS in different frequency bands is needed to derive general and valid predictions about tACS effects on ERD/ERS, opening a wide field for future research. The above considerations may only hold for induced, but not evoked oscillatory activity. Here, continuous application of tACS may disrupt the phase reset of the targeted evoked oscillation if the stimulation is not temporally aligned with the onset of the event (or vice versa). Indeed, Wischnewski and Schutter (2017) recently observed diminished evoked delta in response to feedback signals in a decision making task after stimulating participants with tACS in the delta range. Conversely, aligning the stimulation with the event-related phase reset, might be able to facilitate the evoked oscillation.

While effects of tACS on the task induced modulation of alpha power were observed in study 2 and 3, study 3 failed to replicate the sustained effect on alpha power modulation after the stimulation was switched off. Although outlasting effects of tACS are well documented in the literature (Neuling et al., 2013; Veniero et al., 2015; Vossen et al., 2015; Wach et al., 2013a; Wach et al., 2013b; Wischnewski et al., 2018; Zaehle et al., 2010), several studies in the past did not observe such effects (Clayton, Yeung, and Kadosh, 2018; Fekete, Nikolaev, Knijf, Zharikova, and van Leeuwen, 2018;

Stecher and Herrmann, 2018). Strikingly, in study 3 the induction of an aftereffect failed despite strong effects observed during stimulation. This raises the question which factors determine successful induction of stimulation aftereffects and how on- and offline effects relate to each other. An obvious discrepancy between the two experiments is the reduced stimulation intensity in study 3 (680 μA vs. 1200 μA and 900 μA in studies 1 and 2). Although the intensity was strong enough to elicit a strong online effect, higher intensities might be necessary to induce processes of synaptic placticity, that seem most likely to explain tACS aftereffects (Vossen et al., 2015; Wischnewski et al., 2018; Zaehle et al., 2010). Apart from stimulation intensity, a variety of factors are suspected to modulate brain stimulation effects in the field of tDCS and TMS that may also apply to tACS. Those factors modulating the induction of plasticity include participants' sex, age, medication and genetics as well as time of day (Krause and Cohen Kadosh, 2014; Ridding and Ziemann, 2010). Further, individual anatomy such as skull thickness and folding of the cortex may alter the amount of current ariving at the targeted brain regions (Laakso, Tanaka, Koyama, De Santis, and Hirata, 2015). A factor with high prevalence in the population is the intake of nicotine, which has been shown to reduce or abolish tDCS and TMS induced aftereffects (Grundey et al., 2012; Thirugnanasambandam et al., 2011). In the context of tACS, the influence of these factors may be even more complex and severe, as they might not only modulate the susceptibility to the induction of aftereffects, but could also affect the targeted oscillations themselves. Cigarette smoking and withdrawal for example are known to affect the amplitude of alpha and theta oscillations as well as the dominant alpha frequency in the EEG (Domino et al., 2009; Herning, Jones, and Bachman, 1983) and could potentially confound or mask stimulation effects. Identifying these factors, understanding their influence and ideally finding ways to counteract them, will be an important challenge for future research. An important aid in this context might be to investigate the relation between on- and offline effects.

6.2 Implications for concurrent tACS-M/EEG

Recent years have seen the development of a variety of approaches to recover online effects of tACS in M/EEG (Dowsett and Herrmann, 2016; Helfrich, Schneider, et al., 2014; Kohli and Casson, 2015; Neuling et al., 2015; Witkowski et al., 2016). At the same time, it also became clear, that these approaches suffer from imperfections that compromise their artifact suppression capabilities (Mäkelä et al., 2017; Noury et al., 2016; Noury and Siegel, 2018) and limit their application due to residual artifacts that remain in the data. The presence of such artifacts can severely bias results and may lead to invalid conclusions about tACS effects, if not appropriately taken into account. Based on

the work in the field on concurrent tACS-M/EEG, including the two studies presented in chapters 4 and 5, some general requirements and suggestions for measurements of tACS online effects can be derived to ensure validity of results.

First and foremost, it seems useful to assume that concurrent tACS-M/EEG recordings will never be completely free of tACS-artifacts, even after the application of suppression methods such as template subtraction or LCMV beamforming. A general problem for concurrent tACS-M/EEG is how to prove the successful artifact removal of a given method. Due to the spectral overlap of the brain signal of interest and the stimulation artifact, disentangling tACS effects on brain oscillations from tACS artifacts is challenging, if not impossible under realistic experimental conditions. Consequently, even if a method capable of perfect artifact suppression would be available, proving such complete artifact removal seems hardly feasible. Findings presented in study 4 (chapter 5) indicate that even during amplitude modulated tACS (AM-tACS), a method that should in theory not exhibit any spectral overlap between brain signal and tACS artifact, hardware non-linearities can unexpectedly reintroduce artifacts with such spectral overlap. However, once the fact that concurrent tACS-M/EEG data are always contaminated with some degree of tACS induced artifacts is accepted, one can tailor experiments, analysis pipelines and control analyses to be robust against their influence.

In study 3 (presented in chapter 4), this was realized by contrasting two intervals (before and after stimulus presentation) during the same tACS condition. The respective power values in the frequency band of interest during stimulation were subtracted before comparing this difference to tACS-free conditions. As shown in equation 4.4 this procedure implements an additional cancellation of residual tACS artifacts, while preserving the event-related dynamics. Given that the residual artifact in the contrasted data segments is approximately the same, the measure is robust against its influence. The use of relative measures such as ERD/ERS (Pfurtscheller and Lopes Da Silva, 1999) in this context would have lead to erroneous ERD results biased towards smaller values (equations 4.1 - 4.3) and ultimately invalid conclusions about the tACS effect. As a consequence, it is recommendable to carefully evaluate whether analysis methods and output measures are robust or prone to be biased by imperfect artifact removal.

The consequences of residual artifacts on absolute (power difference) and relative measures (ERD/ERS) can be illustrated by a simple simulation. To this end, 100 pairs of data points (A and R), were generated for the pre- (R) and post-stimulus intervals (A). Values for R were sampled from a uniform distribution with values ranging between 1 and 100 (arbitrary units). Values for A were computed by multiplying the respective R values by a random weight between 0 and 1, which ensured that values for A were always smaller or equal to R. Power difference and ERD in absence

of an artifact were computed for each pair of data points (according to equations 4.1 and 4.4). The results serve as the ”ground truth” for the simulation. Next, a residual artifact was added to R and A. The artifact was multiplied by random weights to allow for random fluctuations of artifact strength between A and R of up to 10%. Artifact contaminated power differences and ERDs were computed based on the following equations:

$$PowerDiff. = (R + T * wR) - (A + T * wA) \tag{6.1}$$

$$ERD = \frac{(R + T * wR) - (A + T * wA)}{(R + T * wR)} * 100, \tag{6.2}$$

where T is the strength of the residual artifact and wA and wR are weights to introduce random fluctuation in artifact strength between the conditions. The simulation was run for different artifacts strengths ranging from 1 to 4000 (arbitrary units). As the average size of R is 50, this corresponds to brain signal to artifact ratios of 0.02 to 80. Results of the simulation are summarized in Figure 6.1.

Figure 6.1 A and B illustrate the effect of an artifact that is on average three times the size of R on ERD and power difference. This artifact to brain signal ratio is similar to the one estimated for the residual artifact in study 3. While the artifact imposes a highly significant difference between the ”true” ERD values and the artifact contaminated, the calculation of a power difference still provides a robust estimate of the average difference in the sample although with increased variance. When different amplitudes were tested, even residual artifacts as little as 10% of the size of R resulted in significantly biased ERD values (Figure 6.1 C). In contrast, power difference values, were not vulnerable to such systematic bias. However, with increasing artifact strength the estimated average power difference becomes more noisy (Figure 6.1 C) and correlation between artifact contaminated power differences and original data decays (Figure 6.1 D).

The subtraction approach described above relies on some important assumptions. In order to cancel out successfully, the strength of the residual tACS artifact must be uncorrelated with the task and of approximately equal size within the contrasted conditions. Recent work has shown, that physiological processes such as heart beat and respiration can systematically modulate the tACS induced artifact in MEG and EEG recordings (Noury et al., 2016; Noury and Siegel, 2018). In the MEG, these modulations have been suggested to originate from small body or head movements, which

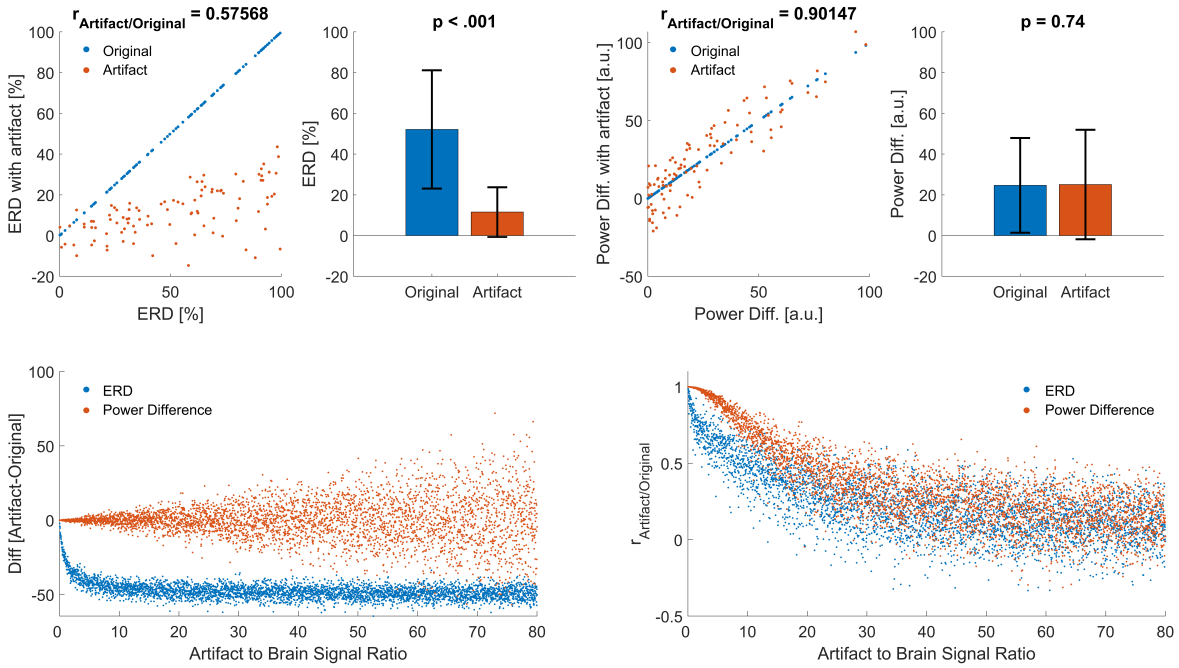

Figure 6.1: Simulation ERD vs. Power Difference. **(A)** Simulated ERD values with (orange) and without (blue) addition of a residual artifact to pre- and post-stimulus interval. Bar plots depict the resulting average ERD values for 100 simulated data points. Error bars depict standard deviation. The presence of a residual artifact resulted in a significantly reduced ERD. **(B)** Results of the same simulated data with power difference computed instead of ERD. While the addition of a residual artifact adds additional variance to the average power difference, no systematic bias is introduced. **(A)** and **(B)** depict results for a residual artifact approximately 3 times larger than R. **(C)** Difference between the original and artifact contaminated data for ERD (blue) and Power difference (orange) measure for different artifact strengths. Small artifact strength already results in substantial difference between the original and the artifact contaminated data, while the computed power difference becomes more noisy with increasing artifact strengths. Each dot represents the difference of the two averages of a simulation run. **(D)** Correlation between original and artifact contaminated ERD and power difference values for different artifact strengths. Compared to the power difference, ERD values exhibit a steeper decay of correlation with increasing artifact strength.

change the distance between the sensor array and the stimulation electrode. In EEG, changes in body impedance seem most likely to explain the findings (Noury et al., 2016). If these underlying processes hold true, a multitude of other processes may exert modulations of tACS artifact strength in a similar manner (e.g. systematic head movements in MEG during button presses). If some of these processes are systematically affected by experimental conditions (e.g. increasing heart-rate with stimulus onset), the assumption of uncorrelated artifact fluctuations may not hold. In order to rule out such systematic modulations by the task, a control analysis was implemented in study 3. In a first step, the envelope of the artifact was extracted on the sensor level and tested for significant task induced modulations. Afterwards, the obtained modulation indexes were correlated with the physiological effects observed after artifact suppression to test whether the modulation of tACS artifact strength was driving these effects. While the results of this control analysis did neither suggest substantial task induced tACS artifact modulation, nor correlated with the physiological effects ob-

served after artifact suppression, it is important to emphasize that this finding cannot be generalized to all tasks and should be tested for every new experiment. Paradigms that elicit stronger physiological responses, such as emotional/fearful stimuli or tasks involving strong motor responses, may be capable of systematically modulating tACS artifact strength by changing heart-rates, respiration frequencies, skin conductance or by triggering subtle body/head movements (Palomba, Angrilli, and Mini, 1997; Pollatos, Herbert, Matthias, and Schandry, 2007). Importantly, even in the absence of systematic modulations by a task, the aforementioned physiological processes can impose random fluctuations in artifact strength. As seen in the above simulation, such fluctuation add variance (or noise) to the estimated power difference. The subtraction approach thus requires efficient artifact reduction before it can be applied, as increased noise in the obtained difference values may shadow stimulation effects. In order to judge whether the subtraction approach can realistically account for residual artifacts in the data, it seems useful to report its size along with the results. In study 3, the brain-signal-to-artifact-ratio was introduced as a measure to accomplish this task more objectively than pure visual inspection. The measure can be used to compute an upper boundary for the size of a residual artifact relative to an estimate of the brain signal of interest (e.g. alpha power) during a stimulation-free interval.

The subtraction of two experimental conditions is obviously not innovative. In the context of source-localization, such contrasts are in fact a common strategy to overcome the center of head bias of the LCMV beamformer (Van Veen et al., 1997). It is, however, important to emphasize that when new approaches for tACS artifact removal/suppression such as LCMV or AM-tACS are introduced, the computation of contrasts imposes a second, implicit layer of artifact removal to the analysis pipeline. Consequently, one may overlook residual artifacts in the data after application of the original method. Such application of implicit or undisclosed artifact removal was performed in two recent studies proposing LCMV beamforming (Neuling et al., 2015) and AM-tACS (Witkowski et al., 2016) as solutions to overcome tACS artifacts in MEG. The first study presented contrasts to demonstrate the artifact suppression capabilities of LCMV (Neuling et al., 2015), the second applied SAM beamforming, a time domain beamformer exhibiting similar artifact suppression capabilities as LCMV (Soekadar et al., 2013), on MEG data acquired during AM-tACS. The application of these methods is not problematic per-se, as long as it is ensured that results are not systematically biased by a residual artifact. However, in both cases these additional procedures may have masked the presence of residual artifacts that were later identified (Minami and Amano, 2017; Noury et al., 2016) and which limit the application of both approaches. In order to allow for transparent evaluation of an approach and its limitations, the artifact suppression capabilities of the whole analysis pipeline need

to be considered and those of single processing steps should be explicitly disclosed.

Dealing with tACS artifacts to recover online effects of the stimulation constitutes a complex problem with many pitfalls that can, in the worst case, lead to erroneous conclusions about tACS effects. However, if carefully performed and accompanied by appropriate controls, artifact reduction approaches can also provide important insights to the fundamental mechanisms of the method and foster our understanding of brain oscillations in general.

6.3 Limitations

As with all research, some limitations apply to the presented work. To begin with, all stimulation protocols used for the first three studies were limited to the alpha band and compared effects against sham stimulation. In addition, only one montage (Cz-Oz) was applied throughout all experiments. Accordingly, the current work cannot provide evidence that tACS can exhibit similar effects in other frequency bands, or by stimulating different brain regions. With regard to the duration of tACS aftereffects on spontaneous oscillations, a similar effect of tACS has recently been reported after stimulation in the beta frequency band over the primary motor cortex (Wischnewski et al., 2018). In case of event-related oscillations, more research is needed in order to generalize the current findings.

In a similar manner, the potentially limited generalizability of the tACS artifact suppression pipeline should be emphasized. The combination of LCMV and contrasting of conditions has been performed while stimulating in the alpha band. Alpha oscillations are the most dominant oscillatory activity in the awake brain and exhibit the highest amplitudes. This feature makes alpha oscillations a convenient target for brain stimulation and might also aid the recovery of event-related oscillations during tACS. As seen in the simulation (Figure 6.1), a smaller residual artifact relative to the brain oscillation of interest, or in other words, a large brain oscillation of interest relative to the residual artifact, benefits the cancellation of the residual artifact. As the amplitude of brain oscillations decays towards higher frequencies, the recovery of event-related activity might turn out to be more difficult in other frequency bands. Another factor that has not been systematically evaluated so far, is the role that the montage of stimulation electrodes might play for the effectiveness of artifact suppression using LCMV. Especially montages with electrodes positioned very close to each other, or that apply different stimulation waveforms at the same time could compromise the artifact suppression capabilities of the LCMV if the artifacts are less spatially correlated over sensors (Mäkelä et al., 2017; Van Veen et al., 1997).

6.4 Conclusions

Investigating brain oscillations by means of transcranial alternating current stimulation is still a comparatively young field that showed rapid developments in the past years. The current work contributes to these advances by showing that tACS can not only elicit long lasting changes on spontaneous oscillations, but is also capable of altering event-related oscillatory activity. Especially the latter, broadens the range of potential treatment options for neurological and psychiatric disease that are linked to abnormal event-related oscillations. In addition, more precise knowledge about tACS effects on event-related oscillatory activity would allow to improve predictions about behavioral effects of the stimulation and their interpretation. Nevertheless, important questions, such as which factors determine successful stimulation, remain unresolved.

Understanding the processes and mechanisms happening during stimulation is one of the most important challenges in the field. While the current findings can provide some first insights into these effects, the proposed analysis framework and recommendations may aid future research to obtain robust effects during stimulation and to validate those with appropriate control analyses.

References

Alagapan, S., Schmidt, S. L., Lefebvre, J., Hadar, E., Shin, H. W., & Fröhlich, F. (2016). Modulation of Cortical Oscillations by Low-Frequency Direct Cortical Stimulation Is State-Dependent. *PLOS Biology*, *14*(3), e1002424. doi:10.1371/journal.pbio.1002424

Alekseichuk, I., Diers, K., Paulus, W., & Antal, A. (2016). Transcranial electrical stimulation of the occipital cortex during visual perception modifies the magnitude of BOLD activity: A combined tES–fMRI approach. *NeuroImage*, *140*, 110–117. doi:10.1016/j.neuroimage.2015.11.034

Ali, M. M., Sellers, K. K., & Frohlich, F. (2013). Transcranial Alternating Current Stimulation Modulates Large-Scale Cortical Network Activity by Network Resonance. *Journal of Neuroscience*, *33*(27), 11262–11275. doi:10.1523/JNEUROSCI.5867-12.2013

Amzica, F., & Steriade, M. (1998). Electrophysiological correlates of sleep delta waves. doi:10.1016/S0013-4694(98)00051-0

Antal, A., Alekseichuk, I., Bikson, M., Brockmöller, J., Brunoni, A., Chen, R., ... Paulus, W. (2017). Low intensity transcranial electric stimulation: Safety, ethical, legal regulatory and application guidelines. *Clinical Neurophysiology*, (In Press, Accepted Manuscript). doi:10.1016/j.clinph.2017.06.001

Antal, A., Bikson, M., Datta, A., Lafon, B., Dechent, P., Parra, L. C., & Paulus, W. (2014). Imaging artifacts induced by electrical stimulation during conventional fMRI of the brain. *NeuroImage*, *85*, 1040–1047. doi:10.1016/j.neuroimage.2012.10.026. arXiv: NIHMS150003

Antal, A., Boros, K., Poreisz, C., Chaieb, L., Terney, D., & Paulus, W. (2008). Comparatively weak after-effects of transcranial alternating current stimulation (tACS) on cortical excitability in humans. *Brain Stimulation*, *1*(2), 97–105. doi:10.1016/j.brs.2007.10.001

Antal, A., & Herrmann, C. S. (2016). Transcranial Alternating Current and Random Noise Stimulation: Possible Mechanisms. *Neural Plasticity*, *2016*, 1–12. doi:10.1155/2016/3616807

Arroyo, S., Lesser, R. P., Gordon, B., Uematsu, S., Jackson, D., & Webber, R. (1993). Functional significance of the mu rhythm of human cortex: an electrophysiologic study with subdural elec-

trodes. *Electroencephalography and Clinical Neurophysiology*, *87*(3), 76–87. doi:10.1016/0013-4694(93)90114-B

Barker, A. T., Jalinous, R., & Freeston, I. L. (1985). Non-invasive magnetic stimulation of human motor cortex. *Lancet (London, England)*, *1*(8437), 1106–7. Retrieved from http://www.ncbi.nlm.nih.gov/pubmed/2860322

Basar, E., Basar-Eroglu, C., Karakas, S., & Schürmann, M. (2000). Brain oscillations in perception and memory. *International journal of psychophysiology : official journal of the International Organization of Psychophysiology*, *35*(2-3), 95–124. doi:10.1016/S0167-8760(99)00047-1

Bastos, A. M., & Schoffelen, J.-m. (2016). A Tutorial Review of Functional Connectivity Analysis Methods and Their Interpretational Pitfalls. *Frontiers in Systems Neuroscience*, *9*(January), 175. doi:10.3389/fnsys.2015.00175

Bennett, M. (2000). The concept of long term potentiation of transmission at synapses. *Progress in Neurobiology*, *60*(2), 109–137. doi:10.1016/S0301-0082(99)00006-4

Berger, H. (1929). Uber das Elektroenkephalogramm des Menschen. *Archiv fur Psychatrie*, *87*, 527–570.

Bergmann, T. O., Karabanov, A., Hartwigsen, G., Thielscher, A., & Siebner, H. R. (2016). Combining non-invasive transcranial brain stimulation with neuroimaging and electrophysiology: Current approaches and future perspectives. *NeuroImage*, *140*, 4–19. doi:10.1016/j.neuroimage.2016.02.012

Bikson, M., Inoue, M., Akiyama, H., Deans, J. K., Fox, J. E., Miyakawa, H., & Jefferys, J. G. R. (2004). Effects of uniform extracellular DC electric fields on excitability in rat hippocampal slices in vitro. *The Journal of Physiology*, *557*(1), 175–190. doi:10.1113/jphysiol.2003.055772

Bindman, L. J., Lippold, O. C. J., & Redfearn, J. W. T. (1964). The action of brief polarizing currents on the cerebral cortex of the rat (1) during current flow and (2) in the production of long-lasting after-effects. *The Journal of Physiology*, *172*(3), 369–382. doi:10.1113/jphysiol.1964.sp007425

Boiten, F., Sergeant, J., & Geuze, R. (1992). Event-related desynchronization: the effects of energetic and computational demands. *Electroencephalography and Clinical Neurophysiology*, *82*(4), 302–309. doi:10.1016/0013-4694(92)90110-4

Boksem, M. A., Meijman, T. F., & Lorist, M. M. (2005). Effects of mental fatigue on attention: An ERP study. *Cognitive Brain Research*, *25*(1), 107–116. doi:10.1016/j.cogbrainres.2005.04.011

Boyle, M. R., & Frohlich, F. (2013). EEG feedback-controlled transcranial alternating current stimulation. In *2013 6th international ieee/embs conference on neural engineering (ner)* (pp. 140–143). doi:10.1109/NER.2013.6695891

Brignani, D., Ruzzoli, M., Mauri, P., & Miniussi, C. (2013). Is transcranial alternating current stimulation effective in modulating brain oscillations? *PloS one*, *8*(2), e56589. doi:10.1371/journal.pone.0056589

Brittain, J.-S., Probert-Smith, P., Aziz, T. Z., & Brown, P. (2013). Tremor Suppression by Rhythmic Transcranial Current Stimulation. *Current Biology*, *23*(5), 436–440. doi:10.1016/j.cub.2013.01.068

Brötzner, C. P., Klimesch, W., Doppelmayr, M., Zauner, A., & Kerschbaum, H. H. (2014). Resting state alpha frequency is associated with menstrual cycle phase, estradiol and use of oral contraceptives. *Brain Research*, *1577*(1), 36–44. doi:10.1016/j.brainres.2014.06.034

Brunoni, A. R., Amadera, J., Berbel, B., Volz, M. S., Rizzerio, B. G., & Fregni, F. (2011). A systematic review on reporting and assessment of adverse effects associated with transcranial direct current stimulation. *The International Journal of Neuropsychopharmacology*, *14*(08), 1133–1145. doi:10.1017/S1461145710001690

Busch, N. A., Dubois, J., & VanRullen, R. (2009). The Phase of Ongoing EEG Oscillations Predicts Visual Perception. *Journal of Neuroscience*, *29*(24), 7869–7876. doi:10.1523/JNEUROSCI.0113-09.2009. arXiv: 1507.02142

Butz, M., Gross, J., Timmermann, L., Moll, M., Freund, H. J., Witte, O. W., & Schnitzler, A. (2004). Perilesional pathological oscillatory activity in the magnetoencephalogram of patients with cortical brain lesions. *Neuroscience Letters*, *355*(1-2), 93–96. doi:10.1016/j.neulet.2003.10.065

Buzsáki, G. (2006). *Rhythms of the Brain*. doi:10.1093/acprof:oso/9780195301069.001.0001

Buzsáki, G., & Lopes Da Silva, F. (2012). High frequency oscillations in the intact brain. doi:10.1016/j.pneurobio.2012.02.004. arXiv: 15334406

Cabral-Calderin, Y., Williams, K. A., Opitz, A., Dechent, P., & Wilke, M. (2016). Transcranial alternating current stimulation modulates spontaneous low frequency fluctuations as measured with fMRI. *NeuroImage*, *141*, 88–107. doi:10.1016/j.neuroimage.2016.07.005

Cajochen, C., Brunner, D. P., Krauchi, K., Graw, P., & Wirz-Justice, A. (1995). Power Density in Theta/Alpha Frequencies of the Waking EEG Progressively Increases During Sustained Wakefulness. *Sleep*, *18*(10), 890–894. doi:10.1093/sleep/18.10.890

Chaieb, L., Antal, A., Pisoni, A., Saiote, C., Opitz, A., Ambrus, G. G., ... Paulus, W. (2014). Safety of 5 kHz tACS. *Brain Stimulation*, *7*(1), 92–96. doi:10.1016/j.brs.2013.08.004

Chander, B. S., Witkowski, M., Braun, C., Robinson, S. E., Born, J., Cohen, L. G., ... Soekadar, S. R. (2016). tACS Phase Locking of Frontal Midline Theta Oscillations Disrupts Working Memory Performance. *Frontiers in Cellular Neuroscience*, *10*(May), 1–10. doi:10.3389/fncel.2016.00120

Clarke, A. R., Barry, R. J., McCarthy, R., & Selikowitz, M. (2001). Age and sex effects in the EEG: Differences in two subtypes of attention-deficit/hyperactivity disorder. *Clinical Neurophysiology*, *112*(5), 815–826. doi:10.1016/S1388-2457(01)00487-4

Clayton, M. S., Yeung, N., & Kadosh, R. C. (2018). The effects of 10 Hz transcranial alternating current stimulation on audiovisual task switching. *Frontiers in Neuroscience*, *12*(FEB), 1–12. doi:10.3389/fnins.2018.00067

Cohen, J. (1992). A power primer. *Psychological Bulletin*, *112*(1), 155–159. doi:10.1037/0033-2909.112.1.155

Cole, S. R., & Voytek, B. (2017). Brain Oscillations and the Importance of Waveform Shape. doi:10.1016/j.tics.2016.12.008

Cooper, L. A. (1975). Mental rotation of random two-dimensional shapes. *Cognitive Psychology*, *7*(1), 20–43. doi:10.1016/0010-0285(75)90003-1

Cooper, R., Osselton, J. W., & Shaw, J. C. (1974). Recording Systems. In *Eeg technology* (2nd, Chap. 4, pp. 47–79). doi:10.1016/B978-0-407-16001-9.50001-8

Courchesne, E. (1978). Changes in P3 waves with event repetition: long-term effects on scalp distribution and amplitude. *Electroencephalography and clinical neurophysiology*, *45*(6), 754–66. doi:10.1016/0013-4694(78)90143-8

Creutzfeldt, O. D., Fromm, G. H., & Kapp, H. (1962). Influence of transcortical d-c currents on cortical neuronal activity. *Experimental Neurology*, *5*(6), 436–452. doi:10.1016/0014-4886(62)90056-0

Daniel, R. S. (1967). Alpha and theta EEG in vigilance. *Perceptual and motor skills*, *25*(3), 697–703. doi:10.2466/pms.1967.25.3.697

Domino, E. F., Ni, L., Thompson, M., Zhang, H., Shikata, H., Fukai, H., ... Ohya, I. (2009). Tobacco smoking produces widespread dominant brain wave alpha frequency increases. *International Journal of Psychophysiology*, *74*(3), 192–198. doi:10.1016/j.ijpsycho.2009.08.011

Doppelmayr, M., Klimesch, W., Stadler, W., Pöllhuber, D., & Heine, C. (2002). EEG alpha power and intelligence. *Intelligence*, *30*, 289–302. doi:10.1016/S0160-2896(01)00101-5

Dowsett, J., & Herrmann, C. S. (2016). Transcranial Alternating Current Stimulation with Sawtooth Waves: Simultaneous Stimulation and EEG Recording. *Frontiers in Human Neuroscience*, *10*(March), 1–10. doi:10.3389/fnhum.2016.00135

Dujardin, K., Bourriez, J. L., & Guieu, J. D. (1995). Event-related desynchronization (ERD) patterns during memory processes: effects of aging and task difficulty. *Electroencephalography and Clinical Neurophysiology/ Evoked Potentials*, *96*(2), 169–182. doi:10.1016/0168-5597(94)00284-L

Fekete, T., Nikolaev, A. R., Knijf, F. D., Zharikova, A., & van Leeuwen, C. (2018). Multi-electrode alpha tACS during varying background tasks fails to modulate subsequent alpha power. *Frontiers in Neuroscience*, *12*(JUN). doi:10.3389/fnins.2018.00428

Fertonani, A., Ferrari, C., & Miniussi, C. (2015). What do you feel if I apply transcranial electric stimulation? Safety, sensations and secondary induced effects. *Clinical Neurophysiology*, *126*(11), 2181–2188. doi:10.1016/j.clinph.2015.03.015

Feurra, M., Pasqualetti, P., Bianco, G., Santarnecchi, E., Rossi, A., & Rossi, S. (2013). State-dependent effects of transcranial oscillatory currents on the motor system: what you think matters. *The Journal of neuroscience : the official journal of the Society for Neuroscience*, *33*(44), 17483–9. doi:10.1523/JNEUROSCI.1414-13.2013

Fries, P., Nikolić, D., & Singer, W. (2007). The gamma cycle. doi:10.1016/j.tins.2007.05.005

Fröhlich, F. (2015). Experiments and models of cortical oscillations as a target for noninvasive brain stimulation. In *Progress in brain research* (Vol. 222, pp. 41–73). doi:10.1016/bs.pbr.2015.07.025

Fröhlich, F., & McCormick, D. A. (2010). Endogenous Electric Fields May Guide Neocortical Network Activity. *Neuron*, *67*(1), 129–143. doi:10.1016/j.neuron.2010.06.005

Ganis, G., & Kievit, R. (2015). A New Set of Three-Dimensional Shapes for Investigating Mental Rotation Processes: Validation Data and Stimulus Set. *Journal of Open Psychology Data*, *3*. doi:10.5334/jopd.ai

Gloor, P., Ball, G., & Schaul, N. (1977). Brain lesions that produce delta waves in the EEG. *Neurology*, *27*(4), 326–333. doi:10.1212/WNL.27.4.326

Goutagny, R., Gu, N., Cavanagh, C., Jackson, J., Chabot, J. G., Quirion, R., ... Williams, S. (2013). Alterations in hippocampal network oscillations and theta-gamma coupling arise before Aβ overproduction in a mouse model of Alzheimer's disease. *European Journal of Neuroscience*, *37*(12), 1896–1902. doi:10.1111/ejn.12233

Gray, C. M., König, P., Engel, A. K., & Singer, W. (1989). Oscillatory responses in cat visual cortex exhibit inter-columnar synchronization which reflects global stimulus properties. *Nature*, *338*(6213), 334–337. doi:10.1038/338334a0

Gross, J., Kujala, J., Hamalainen, M., Timmermann, L., Schnitzler, A., & Salmelin, R. (2001). Dynamic imaging of coherent sources: Studying neural interactions in the human brain. *Proceedings of the National Academy of Sciences*, *98*(2), 694–699. doi:10.1073/pnas.98.2.694

Grossman, N., Bono, D., Dedic, N., Kodandaramaiah, S. B., Rudenko, A., Suk, H.-J., ... Boyden, E. S. (2017). Noninvasive Deep Brain Stimulation via Temporally Interfering Electric Fields. *Cell*, *169*(6), 1029–1041.e16. doi:10.1016/j.cell.2017.05.024

Gruber, W. R., Klimesch, W., Sauseng, P., & Doppelmayr, M. (2005). Alpha phase synchronization predicts P1 end N1 latency and amplitude size. *Cerebral Cortex*, *15*(4), 371–377. doi:10.1093/cercor/bhh139

Grundey, J., Thirugnanasambandam, N., Kaminsky, K., Drees, A., Skwirba, A. C., Lang, N., … Nitsche, M. A. (2012). Rapid effect of nicotine intake on neuroplasticity in non-smoking humans. *Frontiers in Pharmacology*, *3 OCT*(October), 1–9. doi:10.3389/fphar.2012.00186

Haegens, S., Handel, B. F., & Jensen, O. (2011). Top-Down Controlled Alpha Band Activity in Somatosensory Areas Determines Behavioral Performance in a Discrimination Task. *Journal of Neuroscience*, *31*(14), 5197–5204. doi:10.1523/JNEUROSCI.5199-10.2011

Hammond, C., Bergman, H., & Brown, P. (2007). Pathological synchronization in Parkinson's disease: networks, models and treatments. doi:10.1016/j.tins.2007.05.004

Händel, B. F., Haarmeier, T., & Jensen, O. (2011). Alpha oscillations correlate with the successful inhibition of unattended stimuli. *Journal of cognitive neuroscience*, *23*(9), 2494–502. doi:10.1162/jocn.2010.21557

Hanslmayr, S., Aslan, A., Staudigl, T., Klimesch, W., Herrmann, C. S., & Bäuml, K.-H. (2007). Prestimulus oscillations predict visual perception performance between and within subjects. *NeuroImage*, *37*(4), 1465–1473. doi:10.1016/j.neuroimage.2007.07.011

Hanslmayr, S., Sauseng, P., Doppelmayr, M., Schabus, M., & Klimesch, W. (2005). Increasing Individual Upper Alpha Power by Neurofeedback Improves Cognitive Performance in Human Subjects. *Applied Psychophysiology and Biofeedback*, *30*(1), 1–10. doi:10.1007/s10484-005-2169-8

Harmony, T. (2013). The functional significance of delta oscillations in cognitive processing. *Frontiers in Integrative Neuroscience*, *7*. doi:10.3389/fnint.2013.00083

Helfrich, R. F., Knepper, H., Nolte, G., Strüber, D., Rach, S., Herrmann, C. S., … Engel, A. K. (2014). Selective Modulation of Interhemispheric Functional Connectivity by HD-tACS Shapes Perception. *PLoS Biology*, *12*(12). doi:10.1371/journal.pbio.1002031

Helfrich, R. F., Schneider, T. R., Rach, S., Trautmann-Lengsfeld, S. A., Engel, A. K., & Herrmann, C. S. (2014). Entrainment of Brain Oscillations by Transcranial Alternating Current Stimulation. *Current Biology*, *24*(3), 333–339. doi:10.1016/j.cub.2013.12.041

Herning, R. I., Jones, R. T., & Bachman, J. (1983). EEG Changes During Tobacco Withdrawal. *Psychophysiology*, *20*(5), 507–512. doi:10.1111/j.1469-8986.1983.tb03004.x

Herrmann, C. S., & Demiralp, T. (2005). Human EEG gamma oscillations in neuropsychiatric disorders. *Clinical neurophysiology : official journal of the International Federation of Clinical Neurophysiology*, *116*(12), 2719–33. doi:10.1016/j.clinph.2005.07.007

Herrmann, C. S. (2001). Human EEG responses to 1-100 Hz flicker: resonance phenomena in visual cortex and their potential correlation to cognitive phenomena. *Experimental brain research*, *137*(3-4), 346–53. doi:10.1007/s002210100682

Herrmann, C. S., Fründ, I., & Lenz, D. (2010). Human gamma-band activity: A review on cognitive and behavioral correlates and network models. doi:10.1016/j.neubiorev.2009.09.001

Herrmann, C. S., Murray, M. M., Ionta, S., Hutt, A., & Lefebvre, J. (2016). Shaping Intrinsic Neural Oscillations with Periodic Stimulation. *The Journal of Neuroscience*, *36*(19), 5328–5337. doi:10.1523/JNEUROSCI.0236-16.2016

Herrmann, C. S., Rach, S., Neuling, T., & Strüber, D. (2013). Transcranial alternating current stimulation: a review of the underlying mechanisms and modulation of cognitive processes. *Frontiers in Human Neuroscience*, *7*(June), 1–13. doi:10.3389/fnhum.2013.00279

Herrmann, C. S., Strüber, D., Helfrich, R. F., & Engel, A. K. (2016). EEG oscillations: From correlation to causality. *International journal of psychophysiology : official journal of the International Organization of Psychophysiology*, *103*, 12–21. doi:10.1016/j.ijpsycho.2015.02.003

Herrmann, C. S., Grigutsch, M., & Busch, N. a. (2004). EEG oscillations and wavelet analysis. In *Eventrelated potentials a methods handbook* (Chap. 11, Vol. 12, pp. 1–39). doi:261589

Hoy, K. E., Bailey, N., Arnold, S., Windsor, K., John, J., Daskalakis, Z. J., & Fitzgerald, P. B. (2015). The effect of γ-tACS on working memory performance in healthy controls. *Brain and Cognition*, *101*, 51–56. doi:10.1016/j.bandc.2015.11.002

Huang, Y., Datta, A., Bikson, M., & Parra, L. C. (2017). Realistic vOlumetric-Approach to Simulate Transcranial Electric Stimulation – ROAST – a fully automated open-source pipeline. *bioRxiv*. doi:10.1101/217331

Ilmoniemi, R. J., & Kičić, D. (2010). Methodology for combined TMS and EEG. *Brain Topography*, *22*(4), 233–248. doi:10.1007/s10548-009-0123-4

Jefferys, J. G. (1981). Influence of electric fields on the excitability of granule cells in guinea-pig hippocampal slices. *The Journal of physiology*, *319*, 143–52. Retrieved from http://www.ncbi.nlm.nih.gov/pubmed/7320909%20http://www.pubmedcentral.nih.gov/articlerender.fcgi?artid=PMC1243827

Jensen, O., & Mazaheri, A. (2010). Shaping functional architecture by oscillatory alpha activity: gating by inhibition. *Frontiers in human neuroscience*, *4*(November), 186. doi:10.3389/fnhum.2010.00186

Johnson, W., & Bouchard, T. J. (2005). The structure of human intelligence: It is verbal, perceptual, and image rotation (VPR), not fluid and crystallized. *Intelligence*, *33*(4), 393–416. doi:10.1016/j.intell.2004.12.002

Kanai, R., Chaieb, L., Antal, A., Walsh, V., & Paulus, W. (2008). Frequency-Dependent Electrical Stimulation of the Visual Cortex. *Current Biology*, *18*(23), 1839–1843. doi:10.1016/j.cub.2008.10.027

Kar, K., & Krekelberg, B. (2014). Transcranial Alternating Current Stimulation Attenuates Visual Motion Adaptation. *Journal of Neuroscience*, *34*(21), 7334–7340. doi:10.1523/JNEUROSCI.5248-13.2014

Kar, K. (2015). Commentary: On the possible role of stimulation duration for after-effects of transcranial alternating current stimulation. *Frontiers in Systems Neuroscience*, *9*(6), 311. doi:10.3389/fnsys.2015.00148

Kar, K., Duijnhouwer, J., & Krekelberg, B. (2017). Transcranial Alternating Current Stimulation Attenuates Neuronal Adaptation. *The Journal of Neuroscience*, *37*(9), 2325–2335. doi:10.1523/JNEUROSCI.2266-16.2016

Kasten, F. H., Dowsett, J., & Herrmann, C. S. (2016). Sustained Aftereffect of α-tACS Lasts Up to 70 min after Stimulation. *Frontiers in Human Neuroscience*, *10*(3), 245. doi:10.3389/fnhum.2016.00245

Kasten, F. H., & Herrmann, C. S. (2017). Transcranial Alternating Current Stimulation (tACS) Enhances Mental Rotation Performance during and after Stimulation. *Frontiers in Human Neuroscience*, *11*(2), 1–16. doi:10.3389/fnhum.2017.00002

Kasten, F. H., Negahbani, E., Fröhlich, F., & Herrmann, C. S. (2018). Non-linear transfer characteristics of stimulation and recording hardware account for spurious low-frequency artifacts during amplitude modulated transcranial alternating current stimulation (AM-tACS). *NeuroImage*, *179*(Oktober), 134–143. doi:10.1016/j.neuroimage.2018.05.068

Kleiner, M., Brainard, D. H., Pelli, D. G., Broussard, C., Wolf, T., & Niehorster, D. (2007). What's new in Psychtoolbox-3? *Perception*, *36*, S14. doi:10.1068/v070821

Kleinert, M.-L., Szymanski, C., & Müller, V. (2017). Frequency-Unspecific Effects of θ-tACS Related to a Visuospatial Working Memory Task. *Frontiers in Human Neuroscience*, *11*(July), 1–16. doi:10.3389/fnhum.2017.00367

Klimesch, W. (1999). EEG alpha and theta oscillations reflect cognitive and memory performance: A review and analysis. *Brain Research Reviews*, *29*(2-3), 169–195. doi:10.1016/S0165-0173(98)00056-3

Klimesch, W., Hanslmayr, S., Sauseng, P., Gruber, W. R., & Doppelmayr, M. (2007). P1 and traveling alpha waves: evidence for evoked oscillations. *Journal of neurophysiology*, *97*(2), 1311–8. doi:10.1152/jn.00876.2006

Klimesch, W., Sauseng, P., & Gerloff, C. (2003). Enhancing cognitive performance with repetitive transcranial magnetic stimulation at human individual alpha frequency. *European Journal of Neuroscience*, *17*(5), 1129–1133. doi:10.1046/j.1460-9568.2003.02517.x

Klimesch, W., Sauseng, P., & Hanslmayr, S. (2007). EEG alpha oscillations: The inhibition-timing hypothesis. *Brain Research Reviews*, *53*(1), 63–88. doi:10.1016/j.brainresrev.2006.06.003

Knyazev, G. G. (2012). EEG delta oscillations as a correlate of basic homeostatic and motivational processes. *Neuroscience and Biobehavioral Reviews*, *36*(1), 677–695. doi:10.1016/j.neubiorev.2011.10.002

Kohli, S., & Casson, A. J. (2015). Removal of Transcranial a.c. Current Stimulation artifact from simultaneous EEG recordings by superposition of moving averages. *Conference proceedings : ... Annual International Conference of the IEEE Engineering in Medicine and Biology Society. IEEE Engineering in Medicine and Biology Society. Annual Conference*, *2015*, 3436–9. doi:10.1109/EMBC.2015.7319131

Krause, B., & Cohen Kadosh, R. (2014). Not all brains are created equal: the relevance of individual differences in responsiveness to transcranial electrical stimulation. *Frontiers in systems neuroscience*, *8*(February), 25. doi:10.3389/fnsys.2014.00025

Laakso, I., Tanaka, S., Koyama, S., De Santis, V., & Hirata, A. (2015). Inter-subject variability in electric fields of motor cortical tDCS. *Brain Stimulation*, *8*(5), 906–913. doi:10.1016/j.brs.2015.05.002

Laczó, B., Antal, A., Niebergall, R., Treue, S., & Paulus, W. (2012). Transcranial alternating stimulation in a high gamma frequency range applied over V1 improves contrast perception but does not modulate spatial attention. *Brain Stimulation*, *5*(4), 484–491. doi:10.1016/j.brs.2011.08.008

Linn, M. C., & Petersen, A. C. (1985). Emergence and Characterization of Sex Differences in Spatial Ability: A Meta-Analysis. *Child Development*, *56*(6), 1479. doi:10.2307/1130467

Lisman, J. E., & Idiart, M. A. (1995). Storage of 7 $\pm$ 2 short-term memories in oscillatory subcycles. *Science*, *267*(5203), 1512–1515. doi:10.1126/science.7878473

Lisman, J. E., & Jensen, O. (2013). The Theta-Gamma Neural Code. doi:10.1016/j.neuron.2013.03.007. arXiv: NIHMS150003

Luscher, C., & Malenka, R. C. (2012). NMDA Receptor-Dependent Long-Term Potentiation and Long-Term Depression (LTP/LTD). *Cold Spring Harbor Perspectives in Biology*, *4*(6), a005710–a005710. doi:10.1101/cshperspect.a005710

Lustenberger, C., Boyle, M. R., Foulser, A. A., Mellin, J. M., & Fröhlich, F. (2015). Functional role of frontal alpha oscillations in creativity. *Cortex*, *67*, 74–82. doi:10.1016/j.cortex.2015.03.012

Maas, S. A. (2003). *Nonlinear Microwave and RF Circuits* (2nd). Boston: Artec House.

Mäkelä, N., Sarvas, J., & Ilmoniemi, R. J. (2017). Proceedings #17. A simple reason why beamformer may (not) remove the tACS-induced artifact in MEG. *Brain Stimulation*, *10*(4), e66–e67. doi:10.1016/j.brs.2017.04.110

Marshall, L., Helgadóttir, H., Mölle, M., & Born, J. (2006). Boosting slow oscillations during sleep potentiates memory. *Nature*, *444*(7119), 610–613. doi:10.1038/nature05278

Mathewson, K. E., Gratton, G., Fabiani, M., Beck, D. M., & Ro, T. (2009). To See or Not to See: Prestimulus Phase Predicts Visual Awareness. *Journal of Neuroscience*, *29*(9), 2725–2732. doi:10.1523/JNEUROSCI.3963-08.2009

McCarthy, M. M., Moore-Kochlacs, C., Gu, X., Boyden, E. S., Han, X., & Kopell, N. (2011). Striatal origin of the pathologic beta oscillations in Parkinson's disease. *Proceedings of the National Academy of Sciences*, *108*(28), 11620–11625. doi:10.1073/pnas.1107748108

McFarland, D. J., Miner, L. A., Vaughan, T. M., & Wolpaw, J. R. (2000). Mu and beta rhythm topographies during motor imagery and actual movements. *Brain Topography*, *12*(3), 177–186. doi:10.1023/A:1023437823106

Mellin, J. M., Alagapan, S., Lustenberger, C., Lugo, C. E., Alexander, M. L., Gilmore, J. H., … Fröhlich, F. (2018). Randomized trial of transcranial alternating current stimulation for treatment of auditory hallucinations in schizophrenia. *European Psychiatry*, *51*, 25–33. doi:10.1016/j.eurpsy.2018.01.004

Michel, C. M., Kaufman, L., & Williamson, S. J. (1994). Duration of EEG and MEG α Suppression Increases with Angle in a Mental Rotation Task. *Journal of cognitive neuroscience*, *6*(2), 139–50. doi:10.1162/jocn.1994.6.2.139

Minami, S., & Amano, K. (2017). Illusory Jitter Perceived at the Frequency of Alpha Oscillations. *Current Biology*, *27*(15), 2344–2351.e4. doi:10.1016/j.cub.2017.06.033

Miranda, P. C., Lomarev, M., & Hallett, M. (2006). Modeling the current distribution during transcranial direct current stimulation. *Clinical Neurophysiology*, *117*(7), 1623–1629. doi:10.1016/j.clinph.2006.04.009

Montez, T., Poil, S.-S., Jones, B. F., Manshanden, I., Verbunt, J. P. A., van Dijk, B. W., ... Linkenkaer-Hansen, K. (2009). Altered temporal correlations in parietal alpha and prefrontal theta oscillations in early-stage Alzheimer disease. *Proceedings of the National Academy of Sciences*, *106*(5), 1614–1619. doi:10.1073/pnas.0811699106

Negahbani, E., Kasten, F. H., Herrmann, C. S., & Frohlich, F. (2018). Targeting alpha-band oscillations in a cortical model with amplitude-modulated high-frequency transcranial electric stimulation. *NeuroImage*, *173*(January), 3–12. doi:10.1016/j.neuroimage.2018.02.005

Neubauer, A. C., Bergner, S., & Schatz, M. (2010). Two- vs. three-dimensional presentation of mental rotation tasks: Sex differences and effects of training on performance and brain activation. *Intelligence*, *38*(5), 529–539. doi:10.1016/j.intell.2010.06.001

Neubauer, A., Freudenthaler, H. H., & Pfurtscheller, G. (1995). Intelligence and spatiotemporal patterns of event-related desynchronization (ERD). *Intelligence*, *20*(3), 249–266. doi:10.1016/0160-2896(95)90010-1

Neuling, T., Rach, S., Wagner, S., Wolters, C. H., & Herrmann, C. S. (2012). Good vibrations: Oscillatory phase shapes perception. *NeuroImage*, *63*(2), 771–778. doi:10.1016/j.neuroimage.2012.07.024

Neuling, T., Rach, S., & Herrmann, C. S. (2013). Orchestrating neuronal networks: sustained after-effects of transcranial alternating current stimulation depend upon brain states. *Frontiers in human neuroscience*, *7*(April), 161. doi:10.3389/fnhum.2013.00161

Neuling, T., Ruhnau, P., Fuscà, M., Demarchi, G., Herrmann, C. S., & Weisz, N. (2015). Friends, not foes: Magnetoencephalography as a tool to uncover brain dynamics during transcranial alternating current stimulation. *NeuroImage*, *118*, 406–413. doi:10.1016/j.neuroimage.2015.06.026

Neuling, T., Ruhnau, P., Weisz, N., Herrmann, C. S., & Demarchi, G. (2017). Faith and oscillations recovered: On analyzing EEG/MEG signals during tACS. *NeuroImage*, *147*(November 2016), 960–963. doi:10.1016/j.neuroimage.2016.11.022

Neuling, T., Wagner, S., Wolters, C. H., Zaehle, T., & Herrmann, C. S. (2012). Finite-element model predicts current density distribution for clinical applications of tDCS and tACS. *Frontiers in Psychiatry*, *3*(SEP), 1–10. doi:10.3389/fpsyt.2012.00083

Nitsche, M. a., Fricke, K., Henschke, U., Schlitterlau, A., Liebetanz, D., Lang, N., ... Paulus, W. (2003). Pharmacological modulation of cortical excitability shifts induced by transcranial direct current stimulation in humans. *The Journal of physiology*, *553*(1), 293–301. doi:10.1113/jphysiol.2003.049916

Nitsche, M. a., & Paulus, W. (2001). Sustained excitability elevations induced by transcranial DC motor cortex stimulation in humans. *Neurology*, *57*(10), 1899–1901. doi:10.1212/WNL.57.10.1899

Nitsche, M. A., Nitsche, M. S., Klein, C. C., Tergau, F., Rothwell, J. C., & Paulus, W. (2003). Level of action of cathodal DC polarisation induced inhibition of the human motor cortex. *Clinical Neurophysiology*, *114*(4), 600–604. doi:10.1016/S1388-2457(02)00412-1

Nitsche, M. a., & Paulus, W. (2000). Excitability changes induced in the human motor cortex by weak transcranial direct current stimulation. *The Journal of physiology*, *527 Pt 3*, 633–9. doi:PHY_1055[pii]. arXiv: arXiv:1011.1669v3

Nolte, G. (2003). The magnetic lead field theorem in the quasi-static approximation and its use for magnetoencephalography forward calculation in realistic volume conductors. *Physics in Medicine and Biology*, *48*(22), 3637–3652. doi:10.1088/0031-9155/48/22/002

Notbohm, A., & Herrmann, C. S. (2016). Flicker Regularity Is Crucial for Entrainment of Alpha Oscillations. *Frontiers in Human Neuroscience*, *10*(October), 503. doi:10.3389/fnhum.2016.00503

Notbohm, A., Kurths, J., & Herrmann, C. S. (2016). Modification of Brain Oscillations via Rhythmic Light Stimulation Provides Evidence for Entrainment but Not for Superposition of Event-Related Responses. *Frontiers in human neuroscience*, *10*(February), 10. doi:10.3389/fnhum.2016.00010

Noury, N., Hipp, J. F., & Siegel, M. (2016). Physiological processes non-linearly affect electrophysiological recordings during transcranial electric stimulation. *NeuroImage*, *140*, 99–109. doi:10.1016/j.neuroimage.2016.03.065

Noury, N., & Siegel, M. (2017). Phase properties of transcranial electrical stimulation artifacts in electrophysiological recordings. *NeuroImage*, *158*, 406–416. doi:10.1016/j.neuroimage.2017.07.010

Noury, N., & Siegel, M. (2018). Analyzing EEG and MEG signals recorded during tES, a reply. *NeuroImage*, *167*(August 2017), 53–61. doi:10.1016/j.neuroimage.2017.11.023

Okazaki, Y. O., De Weerd, P., Haegens, S., & Jensen, O. (2014). Hemispheric lateralization of posterior alpha reduces distracter interference during face matching. *Brain Research*, *1590*(1), 56–64. doi:10.1016/j.brainres.2014.09.058

Oken, B., Salinsky, M., & Elsas, S. (2006). Vigilance, alertness, or sustained attention: physiological basis and measurement. *Clinical Neurophysiology*, *117*(9), 1885–1901. doi:10.1016/j.clinph.2006.01.017. arXiv: NIHMS150003

Oldfield, R. C. (1971). The assessment and analysis of handedness: The Edinburgh inventory. doi:10.1016/0028-3932(71)90067-4

Oostenveld, R., Fries, P., Maris, E., & Schoffelen, J. M. (2011). FieldTrip: Open source software for advanced analysis of MEG, EEG, and invasive electrophysiological data. *Computational Intelligence and Neuroscience*, *2011*, 1–9. doi:10.1155/2011/156869. arXiv: 156869

Opitz, A., Falchier, A., Yan, C. G., Yeagle, E. M., Linn, G. S., Megevand, P., ... Schroeder, C. E. (2016). Spatiotemporal structure of intracranial electric fields induced by transcranial electric stimulation in humans and nonhuman primates. *Scientific Reports*, *6*(August), 1–11. doi:10.1038/srep31236

Oshino, S., Kato, A., Wakayama, A., Taniguchi, M., Hirata, M., & Yoshimine, T. (2007). Magnetoencephalographic analysis of cortical oscillatory activity in patients with brain tumors: Synthetic aperture magnetometry (SAM) functional imaging of delta band activity. *NeuroImage*, *34*(3), 957–964. doi:10.1016/j.neuroimage.2006.08.054

Ozen, S., Sirota, A., Belluscio, M. A., Anastassiou, C. A., Stark, E., Koch, C., & Buzsaki, G. (2010). Transcranial Electric Stimulation Entrains Cortical Neuronal Populations in Rats. *Journal of Neuroscience*, *30*(34), 11476–11485. doi:10.1523/JNEUROSCI.5252-09.2010

Palomba, D., Angrilli, A., & Mini, A. (1997). Visual evoked potentials, heart rate responses and memory to emotional pictorial stimuli. *International Journal of Psychophysiology*, *27*(1), 55–67. doi:10.1016/S0167-8760(97)00751-4

Palva, J. M. (2005). Phase Synchrony among Neuronal Oscillations in the Human Cortex. *Journal of Neuroscience*, *25*(15), 3962–3972. doi:10.1523/JNEUROSCI.4250-04.2005

Pfurtscheller, G., & Lopes Da Silva, F. H. (1999). Event-related EEG/MEG synchronization and desynchronization: Basic principles. *Clinical Neurophysiology*, *110*(11), 1842–1857. doi:10.1016/S1388-2457(99)00141-8

Pfurtscheller, G., Neuper, C., Brunner, C., & Lopes Da Silva, F. (2005). Beta rebound after different types of motor imagery in man. *Neuroscience Letters*, *378*(3), 156–159. doi:10.1016/j.neulet.2004.12.034

Pfurtscheller, G., & Neuper, C. (1997). Motor imagery activates primary sensorimotor area in humans. *Neuroscience Letters*, *239*(2-3), 65–68. doi:10.1016/S0304-3940(97)00889-6

Pikovsky, A., Rosenblum, M., & Kurths, J. (2003). *Synchronization: A Universal Concept in Nonlinear Sciences*. doi:10.1063/1.1554136. arXiv: arXiv:1011.1669v3

Pollatos, O., Herbert, B. M., Matthias, E., & Schandry, R. (2007). Heart rate response after emotional picture presentation is modulated by interoceptive awareness. *International Journal of Psychophysiology*, *63*(1), 117–124. doi:10.1016/j.ijpsycho.2006.09.003

Ravden, D., & Polich, J. (1998). Habituation of P300 from visual stimuli. *International Journal of Psychophysiology*, *30*(3), 359–365. doi:10.1016/S0167-8760(98)00039-7

Reato, D., Rahman, A., Bikson, M., & Parra, L. C. (2010). Low-Intensity Electrical Stimulation Affects Network Dynamics by Modulating Population Rate and Spike Timing. *Journal of Neuroscience*, *30*(45), 15067–15079. doi:10.1523/JNEUROSCI.2059-10.2010. arXiv: NIHMS150003

Reato, D., Rahman, A., Bikson, M., & Parra, L. C. (2013). Effects of weak transcranial alternating current stimulation on brain activity-a review of known mechanisms from animal studies. *Frontiers in human neuroscience*, *7*(October), 687. doi:10.3389/fnhum.2013.00687

Ridding, M. C., & Ziemann, U. (2010). Determinants of the induction of cortical plasticity by non-invasive brain stimulation in healthy subjects. *The Journal of physiology*, *588*(Pt 13), 2291–304. doi:10.1113/jphysiol.2010.190314

Romero, R., & Polich, J. (1996). P3(00) habituation from auditory and visual stimuli. *Physiology & behavior*, *59*(3), 517–22. doi:10.1016/0031-9384(95)02099-3

Rossi, S., Hallett, M., Rossini, P. M., Pascual-Leone, A., Avanzini, G., Bestmann, S., ... Ziemann, U. (2009). Safety, ethical considerations, and application guidelines for the use of transcranial magnetic stimulation in clinical practice and research. *Clinical Neurophysiology*, *120*(12), 2008–2039. doi:10.1016/j.clinph.2009.08.016. arXiv: arXiv:1011.1669v3

Ruhnau, P., Keitel, C., Lithari, C., Weisz, N., & Neuling, T. (2016). Flicker-Driven Responses in Visual Cortex Change during Matched-Frequency Transcranial Alternating Current Stimulation. *Frontiers in Human Neuroscience*, *10*(April), 184. doi:10.3389/fnhum.2016.00184

Salmelin, R., & Hari, R. (1994). Spatiotemporal characteristics of sensorimotor neuromagnetic rhythms related to thumb movement. *Neuroscience*, *60*(2), 537–550. doi:10.1016/0306-4522(94)90263-1

Schutter, D. J. L. G. (2016). Cutaneous retinal activation and neural entrainment in transcranial alternating current stimulation: A systematic review. *NeuroImage*, *140*, 83–88. doi:10.1016/j.neuroimage.2015.09.067

Schutter, D. J. L. G., & Wischnewski, M. (2016). A meta-analytic study of exogenous oscillatory electric potentials in neuroenhancement. *Neuropsychologia*, *86*, 110–118. doi:10.1016/j.neuropsychologia.2016.04.011

Sela, T., Kilim, A., & Lavidor, M. (2012). Transcranial alternating current stimulation increases risk-taking behavior in the Balloon Analog Risk Task. *Frontiers in Neuroscience*, *6*(FEB), 1–11. doi:10.3389/fnins.2012.00022

Shepard, R. N., & Metzler, J. (1971). Mental rotation of three-dimensional objects. *Science (New York, N.Y.) 171*(3972), 701–3. doi:10.1126/science.171.3972.701

Silvanto, J., Muggleton, N., & Walsh, V. (2008). State-dependency in brain stimulation studies of perception and cognition. *Trends in Cognitive Sciences*, *12*(12), 447–454. doi:10.1016/j.tics.2008.09.004

Simon, M., Schmidt, E. A., Kincses, W. E., Fritzsche, M., Bruns, A., Aufmuth, C., ... Schrauf, M. (2011). Eeg alpha spindle measures as indicators of driver fatigue under real traffic conditions. *Clinical Neurophysiology*, *122*(6), 1168–1178. doi:10.1016/j.clinph.2010.10.044

Soekadar, S. R., Witkowski, M., Cossio, E. G., Birbaumer, N., Robinson, S. E., & Cohen, L. G. (2013). In vivo assessment of human brain oscillations during application of transcranial electric currents. *Nature communications*, *4*(May), 2032. doi:10.1038/ncomms3032

Stecher, H. I., & Herrmann, C. S. (2018). Absence of Alpha-tACS Aftereffects in Darkness Reveals Importance of Taking Derivations of Stimulation Frequency and Individual Alpha Variability Into Account. *Frontiers in Psychology*, *9*(June), 1–9. doi:10.3389/fpsyg.2018.00984

Stecher, H. I., Pollok, T. M., Strüber, D., Sobotka, F., Herrmann, C. S., & Christoph, S. (2017). Ten Minutes of α-tACS and Ambient Illumination Independently Modulate EEG α-Power. *Frontiers in Human Neuroscience*, *11*(257), 1–10. doi:10.3389/fnhum.2017.00257

Strüber, D., Rach, S., Neuling, T., & Herrmann, C. S. (2015). On the possible role of stimulation duration for after-effects of transcranial alternating current stimulation. *Frontiers in cellular neuroscience*, *9*(August), 311. doi:10.3389/fncel.2015.00311

Strüber, D., Rach, S., Trautmann-Lengsfeld, S. A., Engel, A. K., & Herrmann, C. S. (2014). Antiphasic 40 Hz oscillatory current stimulation affects bistable motion perception. *Brain Topography*, *27*(1), 158–171. doi:10.1007/s10548-013-0294-x

Taulu, S., & Simola, J. (2006). Spatiotemporal signal space separation method for rejecting nearby interference in MEG measurements. *Physics in Medicine and Biology*, *51*(7), 1759–1768. doi:10.1088/0031-9155/51/7/008

Taulu, S., Simola, J., & Kajola, M. (2005). Applications of the signal space separation method. *IEEE Transactions on Signal Processing*, *53*(9), 3359–3372. doi:10.1109/TSP.2005.853302. arXiv:arXiv:1011.1669v3

ter Huurne, N., Onnink, M., Kan, C., Franke, B., Buitelaar, J., & Jensen, O. (2013). Behavioral Consequences of Aberrant Alpha Lateralization in Attention-Deficit/Hyperactivity Disorder. *Biological Psychiatry*, *74*(3), 227–233. doi:10.1016/j.biopsych.2013.02.001

Thirugnanasambandam, N., Grundey, J., Adam, K., Drees, A., Skwirba, A. C., Lang, N., ... Nitsche, M. A. (2011). Nicotinergic impact on focal and non-focal neuroplasticity induced by non-invasive brain stimulation in non-smoking humans. *Neuropsychopharmacology*, *36*(4), 879–86. doi:10.1038/npp.2010.227

Thut, G., Schyns, P. G., & Gross, J. (2011). Entrainment of perceptually relevant brain oscillations by non-invasive rhythmic stimulation of the human brain. *Frontiers in Psychology*, *2*(JUL), 1–10. doi:10.3389/fpsyg.2011.00170

Thut, G., Veniero, D., Romei, V., Miniussi, C., Schyns, P., & Gross, J. (2011). Rhythmic TMS causes local entrainment of natural oscillatory signatures. *Current Biology*, *21*(14), 1176–1185. doi:10.1016/j.cub.2011.05.049

Tzuriel, D., & Egozi, G. (2010). Gender Differences in Spatial Ability of Young Children: The Effects of Training and Processing Strategies. *Child Development*, *81*(5), 1417–1430. doi:10.1111/j.1467-8624.2010.01482.x

Uhlhaas, P. J., & Singer, W. (2006). Neural Synchrony in Brain Disorders: Relevance for Cognitive Dysfunctions and Pathophysiology. *Neuron*, *52*(1), 155–168. doi:10.1016/j.neuron.2006.09.020

Uhlhaas, P. J., & Singer, W. (2012). Neuronal Dynamics and Neuropsychiatric Disorders: Toward a Translational Paradigm for Dysfunctional Large-Scale Networks. *Neuron*, *75*(6), 963–980. doi:10.1016/j.neuron.2012.09.004

Van Veen, B., & Buckley, K. (1988). Beamforming: a versatile approach to spatial filtering. *IEEE ASSP Magazine*, *5*(2), 4–24. doi:10.1109/53.665

Van Veen, B. D., Van Drongelen, W., Yuchtman, M., & Suzuki, A. (1997). Localization of brain electrical activity via linearly constrained minimum variance spatial filtering. *IEEE Transactions on Biomedical Engineering*, *44*(9), 867–880. doi:10.1109/10.623056. arXiv: 10.623056 [10.1109]

van Dijk, H., Schoffelen, J.-M., Oostenveld, R., & Jensen, O. (2008). Prestimulus oscillatory activity in the alpha band predicts visual discrimination ability. *The Journal of neuroscience*, *28*(8), 1816–23. doi:10.1523/JNEUROSCI.1853-07.2008

van Winsun, W., Sergeant, J., & Geuze, R. (1984). The functional significance of event-related desynchronization of alpha rhythm in attentional and activating tasks. *Electroencephalography and Clinical Neurophysiology*, *58*(6), 519–524. doi:10.1016/0013-4694(84)90042-7

Vargha, B., Schoukens, J., & Rolain, Y. (2001). Static nonlinearity testing of digital-to-analog converters. *IEEE Transactions on Instrumentation and Measurement*, *50*(5), 1283–1288. doi:10.1109/19.963198

Veniero, D., Vossen, A., Gross, J., & Thut, G. (2015). Lasting EEG/MEG Aftereffects of Rhythmic Transcranial Brain Stimulation: Level of Control Over Oscillatory Network Activity. *Frontiers in cellular neuroscience*, *9*(December), 477. doi:10.3389/fncel.2015.00477

Violante, I. R., Li, L. M., Carmichael, D. W., Lorenz, R., Leech, R., Hampshire, A., ... Sharp, D. J. (2017). Externally induced frontoparietal synchronization modulates network dynamics and enhances working memory performance. *eLife*, *6*(March). doi:10.7554/eLife.22001. arXiv: arXiv:1507.02142v2

Voss, U., Holzmann, R., Hobson, A., Paulus, W., Koppehele-Gossel, J., Klimke, A., & Nitsche, M. a. (2014). Induction of self awareness in dreams through frontal low current stimulation of gamma activity. *Nature Neuroscience*, *17*(6), 810–812. doi:10.1038/nn.3719

Vossen, A., Gross, J., & Thut, G. (2015). Alpha Power Increase After Transcranial Alternating Current Stimulation at Alpha Frequency (α-tACS) Reflects Plastic Changes Rather Than Entrainment. *Brain Stimulation*, *8*(3), 499–508. doi:10.1016/j.brs.2014.12.004

Vosskuhl, J., Huster, R. J., & Herrmann, C. S. (2015). Increase in short-term memory capacity induced by down-regulating individual theta frequency via transcranial alternating current stimulation. *Frontiers in Human Neuroscience*, *9*(May), 257. doi:10.3389/fnhum.2015.00257

Vosskuhl, J., Huster, R. J., & Herrmann, C. S. (2016). BOLD signal effects of transcranial alternating current stimulation (tACS) in the alpha range: A concurrent tACS–fMRI study. *NeuroImage*, *140*, 118–125. doi:10.1016/j.neuroimage.2015.10.003

Voyer, D., Voyer, S., & Bryden, M. P. (1995). Magnitude of sex differences in spatial abilities: A meta-analysis and consideration of critical variables. *Psychological Bulletin*, *117*(2), 250–270. doi:10.1037/0033-2909.117.2.250

Wach, C., Krause, V., Moliadze, V., Paulus, W., Schnitzler, A., & Pollok, B. (2013a). Effects of 10Hz and 20Hz transcranial alternating current stimulation (tACS) on motor functions and motor cortical excitability. *Behavioural Brain Research*, *241*(1), 1–6. doi:10.1016/j.bbr.2012.11.038. arXiv: /dx.doi.org/10.1016/j.bbr.2012.11.038 [http:]

Wach, C., Krause, V., Moliadze, V., Paulus, W., Schnitzler, A., & Pollok, B. (2013b). The effect of 10 Hz transcranial alternating current stimulation (tACS) on corticomuscular coherence. *Frontiers in Human Neuroscience*, *7*(August), 1–6. doi:10.3389/fnhum.2013.00511

Weinrich, C. A., Brittain, J.-S., Nowak, M., Salimi-Khorshidi, R., Brown, P., & Stagg, C. J. (2017). Modulation of Long-Range Connectivity Patterns via Frequency-Specific Stimulation of Human Cortex. *Current Biology*, *27*(19), 3061–3068.e3. doi:10.1016/j.cub.2017.08.075

Weisz, N., Hartmann, T., Müller, N., Lorenz, I., & Obleser, J. (2011). Alpha Rhythms in Audition: Cognitive and Clinical Perspectives. *Frontiers in Psychology*, *2*(APR). doi:10.3389/fpsyg.2011.00073. arXiv: 1401.1219

Wischnewski, M., Engelhardt, M., Salehinejad, M. A., Schutter, D. J. L. G., Kuo, M. .-.-F., & Nitsche, M. A. (2018). NMDA Receptor-Mediated Motor Cortex Plasticity After 20 Hz Transcranial Alternating Current Stimulation. *Cerebral Cortex*, (July), 1–8. doi:10.1093/cercor/bhy160

Wischnewski, M., & Schutter, D. J. (2017). After-effects of transcranial alternating current stimulation on evoked delta and theta power. *Clinical Neurophysiology*, *128*(11), 2227–2232. doi:10.1016/j.clinph.2017.08.029

Witkowski, M., Garcia-Cossio, E., Chander, B. S., Braun, C., Birbaumer, N., Robinson, S. E., & Soekadar, S. R. (2016). Mapping entrained brain oscillations during transcranial alternating current stimulation (tACS). *NeuroImage*, *140*, 89–98. doi:10.1016/j.neuroimage.2015.10.024

Zaehle, T., Rach, S., & Herrmann, C. S. (2010). Transcranial Alternating Current Stimulation Enhances Individual Alpha Activity in Human EEG. *PLoS ONE*, *5*(11), 13766. doi:10.1371/journal.pone.0013766

Zhou, G., Bourguignon, M., Parkkonen, L., & Hari, R. (2016). Neural signatures of hand kinematics in leaders vs. followers: A dual-MEG study. *NeuroImage*, *125*, 731–738. doi:10.1016/j.neuroimage.2015.11.002

Zoefel, B., Huster, R. J., & Herrmann, C. S. (2011). Neurofeedback training of the upper alpha frequency band in EEG improves cognitive performance. *NeuroImage*, *54*(2), 1427–1431. doi:10.1016/j.neuroimage.2010.08.078

Appendix

Appendix I: Supplementary Materials Study IV

Supplementary Materials: Non-linear transfer characteristics of stimulation and recording hardware account for spurious low-frequency artifacts during amplitude modulated transcranial alternating current stimulation (AM-tACS)

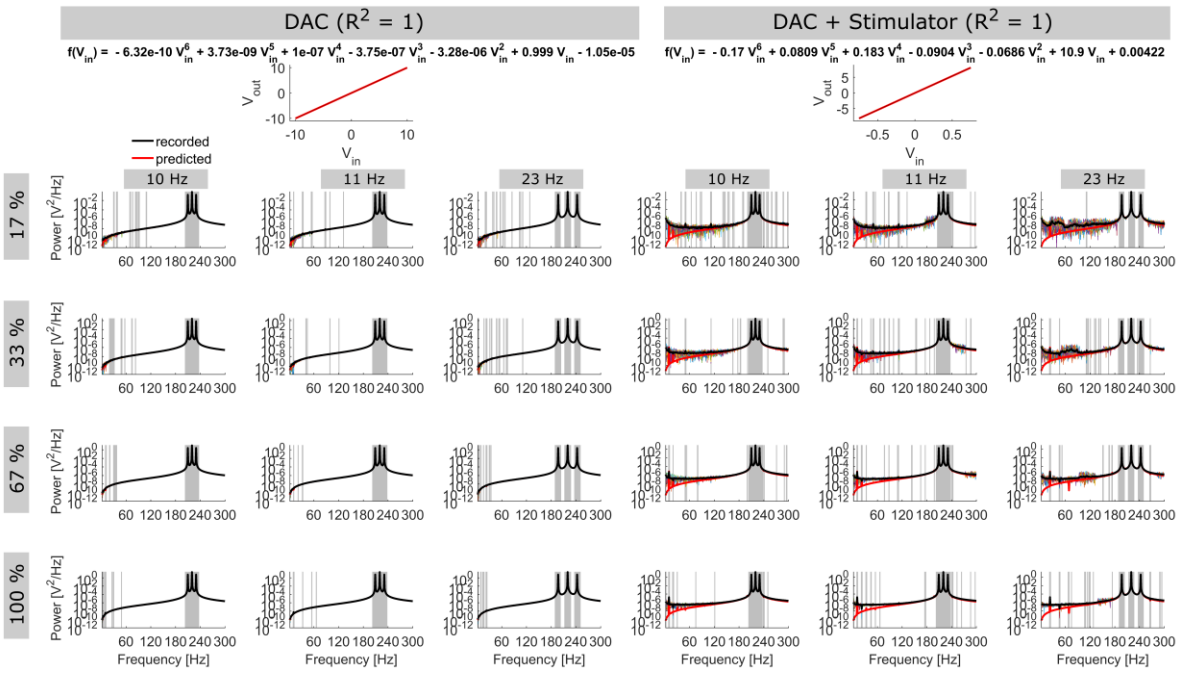

Supplementary Figure S1: Full range version of Figure 2. TFs (**top**) show recorded probe stimulus amplitudes in relation to their input amplitudes (V_{out}/V_{in}; black dots), as well as the course of the TF model (red line). The corresponding function is displayed in the title. Spectra show average power at each frequency in the different AM-recordings (black line). Thin colored lines show power spectra for each of the 60 repetitions. Red line shows the spectrum predicted by evaluating the digital AM-signal by the estimated TF of the setup. Grey areas indicate frequencies significantly differing in power compared to the two neighboring frequencies ($p < .05$, bonferroni corrected). Please note the different scaling of the power spectra.

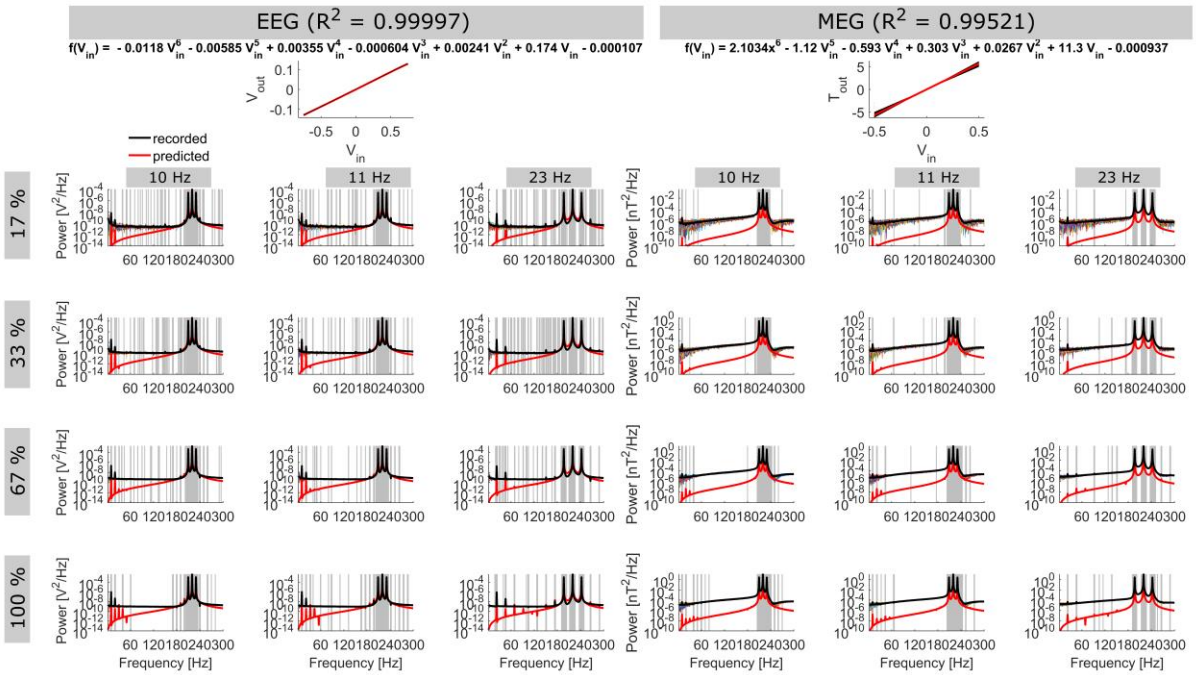

Supplementary Figure S2: Full range version of Figure 3. TFs (**top**) show recorded probe stimulus amplitudes in relation to their input amplitudes (V_{out}/V_{in}; black dots), as well as the course of the TF model (red line). The corresponding function is displayed in the title. Spectra show average power at each frequency in the different AM-recordings (black line). Thin colored lines show power spectra for each of the 60 repetitions. Red line shows the spectrum predicted by evaluating the digital AM-signal by the estimated TF of the setup. Grey areas indicate frequencies significantly differing in power compared to the two neighboring frequencies ($p < .05$, bonferroni corrected). Please note the different scaling of the power spectra.

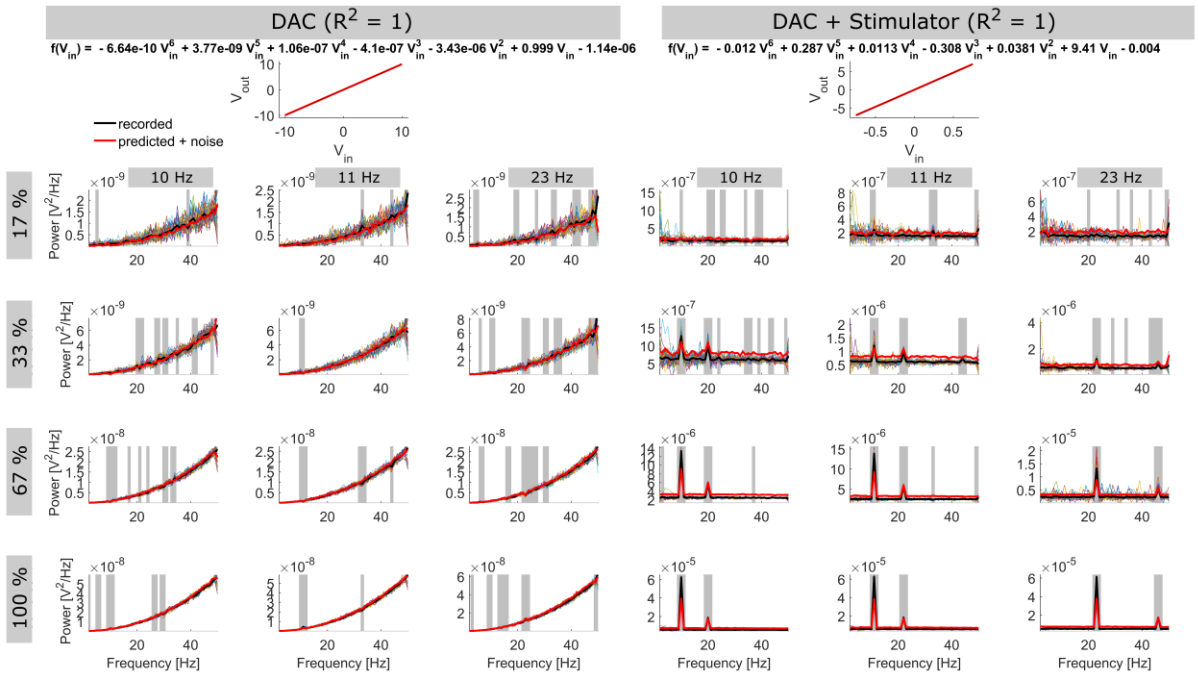

Supplementary Figure S3: Effect of noise on predicted spectra in setup 1 and 2: To investigate the effect of measurement noise on the spectra predicted by the TF models, the measurement routine was repeated for all setups. **Top row** depicts the transfer functions resulting from the new measurement. To obtain estimates of each setups' noise spectrum 10 consecutive one second recordings of a pure 300 Hz sine-wave were performed before each of the AM-tACS recording conditions. Amplitude of the 300 Hz sine was set to 50% of the subsequent AM-tACS amplitude for the setups involving the stimulator (2-4), as the noise-levels apparently depended on properties of the output signal. FFTs were computed for the obtained noise recordings, the complex Fourier coefficients were averaged for each frequency and subsequently transformed into the time-domain using inverse FFT. The resulting prototypical noise signal was added to the signal predicted by the TF models. **Bottom rows** depict spectra for the recorded AM-signals (colored thin lines represent single recordings, bold black line is the average over the 60 repetitions) and the predicted, noise incorporating signals (bold red line). Especially for the second setup (DAC+Stimulator) the noise-incorporating predicted signals resembled the averaged recorded signal relatively well. Please note the different scaling of the plots. Please also note that in contrast to the other figures in the manuscript these figures are not logarithmically scaled.

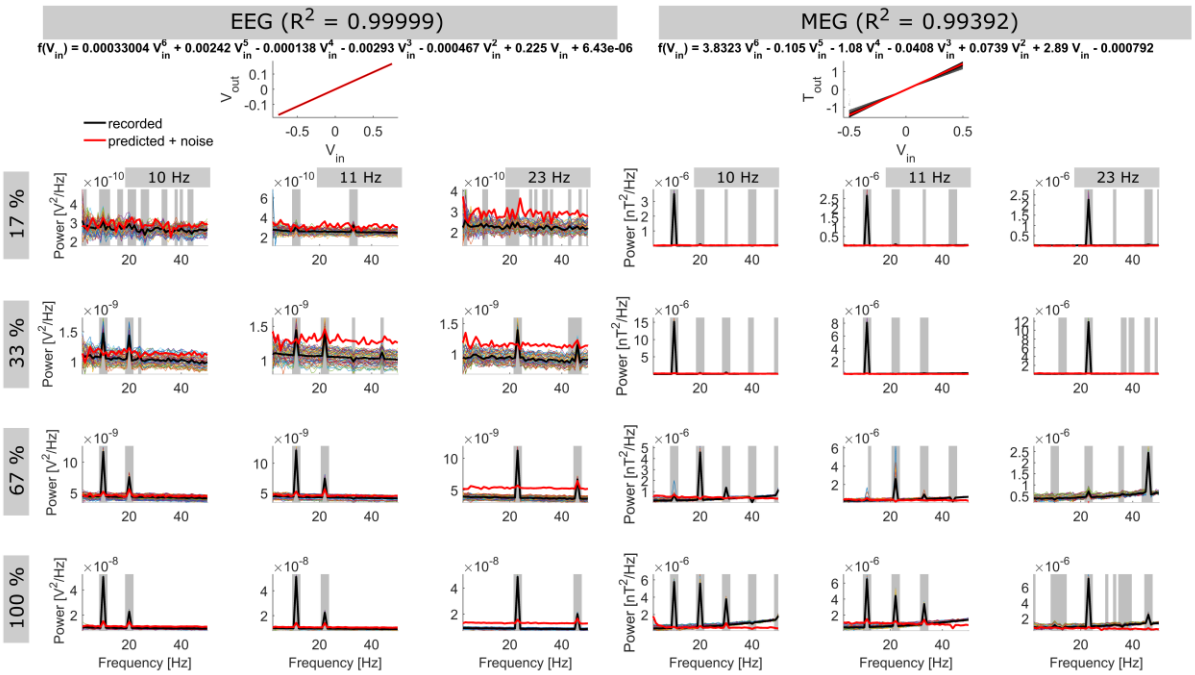

Supplementary Figure S4: Effect of noise on predicted spectra in setup 3 and 4: Top row depicts input-output transfer functions obtained for the new measurements. **Bottom rows** depict the recorded (thin colored lines represent spectra of the single recordings, bold black lines represents the average over 60 repetitions) and noise-incorporating predicted spectra (bold red line). In contrast to the previous two setups noise-incorporating models were less powerful in reconstructing the recorded signals. In general, the estimated noise spectra seem less representative for noise-levels during AM-tACS, which might indicate that the broadband noise emitted during stimulation depends on properties of the output signal (i.e. amplitude, frequency). As a consequence, the construction of a noise-incorporating model that realistically represents the recorded signals becomes highly complex, as a noise measurement signal that with matching noise levels has to be determined for each of the recording condition. In those cases were matching noise levels were obtained (i.e. 10 Hz and 11 Hz EEG), the corrected spectra, again resemble the recorded ones fairly well. Nevertheless, the artifact peaks at the modulation frequency and its harmonics were still systematically underestimated. This, however, seems not surprising as the TF models used to predict the recorded signals can only provide a noise estimate of the true underlying transfer characteristics in each setup. Please

note the different scaling of the plots. Please also note that in contrast to the other figures in the manuscript these figures are not logarithmically scaled.

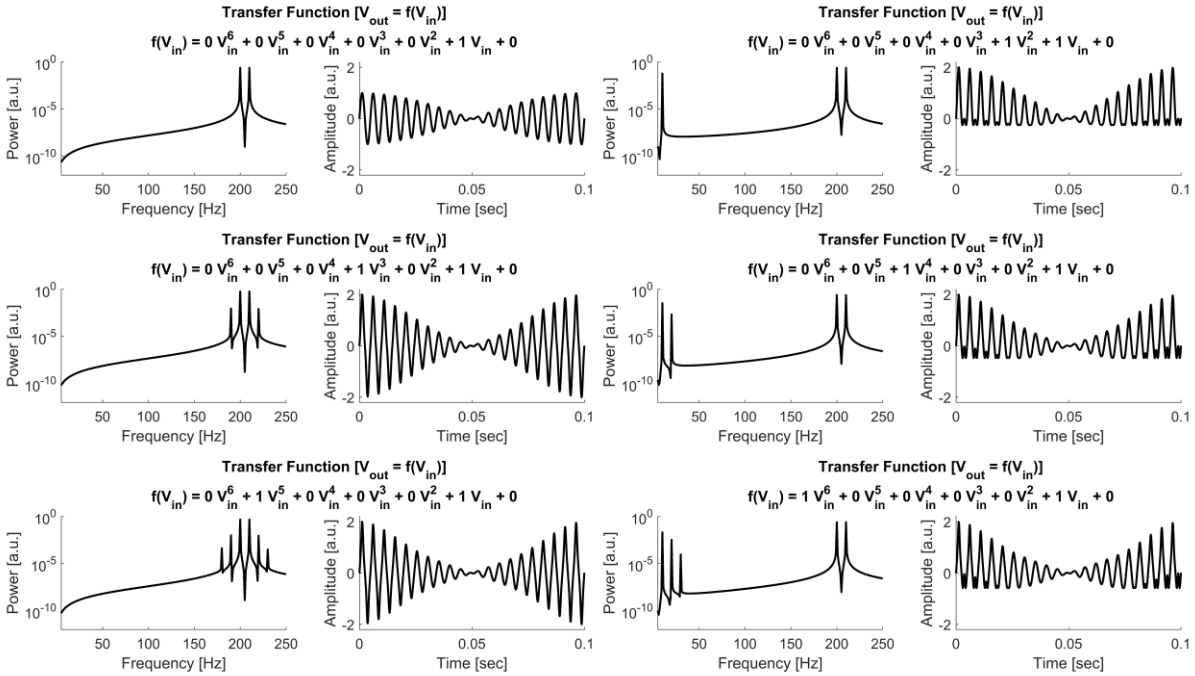

Supplementary Figure S5: Simulation of artifacts resulting from temporal interference (TI). Frequency- and time-domain representations of simulation results showing the effect of non-linear TF terms on amplitude modulated signals created by TI. Similar to the AM-waveforms, the TI signals contain no low-frequency artifact when a solely linear TF is applied (**top left**). Adding non-linear terms to the TF model results in additional side-bands around the frequencies of the two applied sine wave signals for odd-valued exponents (**1st and 2nd column**) and in low-frequency artifacts at Δf (corresponding to the modulation frequency of the AM-waveform generated by the TI signals) and its harmonics for even valued exponents of the TF model (**3rd and 4th column**).

Author Contributions

I hereby confirm, that Florian H. Kasten contributed to the aforementioned studies in chapters 2,3,4 and 5 as stated below:

Article:

Kasten, FH., Dowsett,J.,Herrmann, CS., (2016) Sustained Aftereffect of α-tACS Lasts Up to 70 min after Stimulation. *Frontiers in Human Neuroscience*., 10:245.

Author Contributions:

Designed research: FHK, JD, CSH

Perfomed Research: FHK

Analyzed Data: FHK, JD

Wrote paper: FHK, JD, CSH

Article:

Kasten, FH.,Herrmann, CS., (2017) Transcranial Alternating Current Stimulation (tACS) Enhances Mental Rotation Performance during and after Stimulation. *Frontiers in Human Neuroscience*., 11:2.

Author Contributions:

Designed research: FHK, CSH

Perfomed Research: FHK

Analyzed Data: FHK

Wrote paper: FHK, CSH

Article:

Kasten, FH., Maess, B., Herrmann, CS., (2018) Facilitated Event-Related Power-Modulations during Transcranial Alternating Current Stimulation (tACS) Revealed by Concurrent tACS-MEG. *eNeuro*., (in Press)

Author Contributions:

Designed research: FHK, BM, CSH

Perfomed Research: FHK, BM

Analyzed Data: FHK

Wrote paper: FHK, BM, CSH

Article:

Kasten, FH., Negahbani, E., Frohlich, F., Herrmann, CS., (2018) Non-linear transfer characteristics of stimulation and recording hardware account for spurious low-frequency artifacts during amplitude modulated transcranial alternating current stimulation (AM-tACS). *NeuroImage*., 179, 134-143

Author Contributions:

Designed research: FHK, EN, FF, CSH

Perfomed Research: FHK

Analyzed Data: FHK

Wrote paper: FHK, EN, FF, CSH

Prof. Dr. Christoph S. Herrmann

Declaration

I have completed the work independently and used only the indicated facilities. This dissertation is my own work. All the sources of information have been acknowledged by means of complete references.

The dissertation as a whole or in parts has not been submitted to assessment in a doctoral procedure at another university.

This dissertation has neither as a whole nor as a part been published apart from those parts where this is explicitly indicated.

I am aware of the guidelines of good scientific practice of the Carl von Ossietzky University Oldenburg and I observed them when preparing this dissertation.

I confirm that I have not availed myself of any commercial placement or consulting services in connection with my promotion procedure.

Florian H. Kasten

Curriculum Vitae

Personal Information

Florian Kasten

Born 06 June 1990 in Twistringen

Humboldtstr. 6, 26121 Oldenburg

Education

Jan 2016 - present

PhD Candidate in Psychology, Experimental Psychology Lab, Department of Psychology
Carl von Ossietzky University, Oldenburg, Germany

Okt 2013 - Dec 2015

M.Sc. Neurocognitive Psychology, Carl von Ossieztky University Oldenburg, Germany
Thesis: "*Investigating sustained physiological and behavioral after effects of transcranial alternating current!stimulation in the alpha band during mental rotation*"
Supervisor: Prof. Dr. Christoph S. Herrmann

Okt 2010 - Sep 2013

B.Sc. Psychology, University of Hildesheim, Hildesheim, Germany
Thesis: "*The role of distracter characteristics, saccadic eye movements and expectancy in distracted human time reproduction.*"
Supervisor: Prof. Dr. Kristian Folta-Schoofs

Aug 2002 - May 2009

Abitur (A-Level), Graf-Friedrich-Schule, Diepholz, Germany

Professional Experience

Jan 2016 - present

PhD Candidate in Psychology, Experimental Psychology Lab, Department of Psychology Carl von Ossietzky University, Oldenburg, Germany

Sep 2015 - Nov 2015

Intern, MEG and Cortical Networks Group, Max Planck Institute for Human Cognitive and Brain Sciences, Leipzig, Germany

Supervisor: Dr. Burkhard Maess

Aug 2012 - Okt 2012

Intern, Cognitive Neuroscience Laboratory, German Primate Center, Leibnitz Institute for Primate Research, Goettingen, Germany

Supervisor: Phillipp Schwedhelm, Prof. Dr. Stefan Treue

Publications

Kasten, F. H., Maess, B., & Herrmann, C. S. (2018). Facilitated Event-Related Power-Modulations during Transcranial Alternating Current Stimulation (tACS) Revealed by Concurrent tACS-MEG. ENeuro, ENEURO.0069-18.2018.

Kasten, F. H., Negahbani, E., Fröhlich, F., & Herrmann, C. S. (2018). Non-linear transfer characteristics of stimulation and recording hardware account for spurious low-frequency artifacts during amplitude modulated transcranial alternating current stimulation (AM-tACS). NeuroImage, 179(Oktober), 134–143.

Negahbani, E., **Kasten, F. H.**, Herrmann, C. S., Fröhlich, F., & Frohlich, F. (2018). Targeting alpha-band oscillations in a cortical model with amplitude-modulated high-frequency transcranial electric stimulation. NeuroImage, 173(January), 3–12.

Kasten, F. H., & Herrmann, C. S. (2017). Transcranial Alternating Current Stimulation (tACS) Enhances Mental Rotation Performance during and after Stimulation. Frontiers in Human Neuroscience, 11(2), 1–16.

Kasten, F. H., Dowsett, J., & Herrmann, C. S. (2016). Sustained Aftereffect of α-tACS Lasts Up to 70 min after Stimulation. Frontiers in Human Neuroscience, 10(3), 245.

Reviewer Activities

NeuroImage

PloS one

International Journal of Psychophysiology (IJP)

Experimental Brain Research

Acknowledgements

Research is rarely the sole work of a single person. I would like to take the opportunity to thank all the wonderful people I was pleased to work with during the past years. They all contributed to this work either directly as co-authors or indirectly through vivid discussions, assistance during data acquisition, by solving all the little daily problems, or simply by creating a great environment to work in:

I have to start with **Christoph**, who was a great supervisor to my work and who made all this possible. Who always gave me the freedom to develop ideas and who always supported them.

A big thank goes to my co-authors for sharing their great ideas and for all their suggestions: **James**, who helped me during my first steps into the field of tACS. **Burkhard**, who taught me so much about MEG, and who was brave enough to allow me using our stimulator inside it. **Flavio** and **Ehsan**, who dove into AM-tACS with us. They did the computer simulations, I tortured the melons.

Thanks to **Burkhard**, **Yvonne** and **Herrmann** for their hospitality, giving me a great time in Leipzig.

And of course thanks to the most amazing (current and former) colleagues in the world at the **department of hairsplitting**[1] (100% friends, 0% enemies):
Heiko, who taught me everything I know about BNC cables, LPT ports, the NiDaq ...and berries.
Fabian, my scientific room mate, teaching buddy and F-Team member. One day they will learn to tell us apart.
Joao, the master of the coffee bean and the creator of unbeanable jokes.
The A-Team : Anna, **Alina** and **Annika**.
Maryam, **Jules**, **Daniel** and **Ester**.
Sabine and **Andrea**.

[1] and nitpicking